

LANDMAN, MARILÉ

NOVEL π -HETEROARENE COMPLEXES OF CHROMIUM(0)

MSc

UP

1997

**Novel π -Heteroarene
Complexes of Chromium(0)**

by

Marilé Landman

Submitted in partial fulfilment of the degree

Magister Scientiae

in the Faculty of Science

University of Pretoria

Promoter:

Professor S. Lotz

January 1997

Acknowledgements

I would like to thank the following people for their contribution to this study:

My promoter, Prof. S. Lotz, for his guidance and interest;

Mr Eric Palmer and André Pienaar for recording all the NMR spectra;

Mr Robin Muir for all the glassware used during the practical part of this study;

Prof. P.H. van Rooyen for the crystal structure determinations;

Prof. R. Vlegaar for his assistance and support during the absence of my promoter;

Dr. Thomas Isenburg for his help during the practical stage of this study;

The Foundation for Research Development and the University of Pretoria for financial assistance;

My family and friends for their encouragement, interest and support. Thank you!

Marilé

January 1997

Table of Contents

Summary	i
Opsomming	ii
List of Compounds	iii
List of Abbreviations	vii
Chapter 1	
Introduction	
1.1 General introduction	1
1.1.1 Sandwich complexes	1
1.1.2 Half-sandwich complexes	2
1.1.3 Complexes with tilted sandwich structures	2
1.1.4 Multidecker sandwich complexes	3
1.1.5 Complexes with more than two C _n H _n ligands	3
1.2 Hydrodesulphurization	5
1.2.1 HDS of thiophene	6
1.2.2 HDS of benzothiophene	7
1.2.3 HDS of dibenzothiophene	9
1.3 Hydroprocessing of Quinoline	11
1.4 π-Pyrrole metal complexes	12
1.5 Aim of this study	13
1.6 References	14
Chapter 2	
π-Heteroarene complexes of Chromium	
2.1 Introduction	16
2.2 New π-heteroarene complexes of chromium	21
2.2.1 Thiophene derivatives	21

2.2.2 Synthesis of the nitrogen-containing π -heteroarene complexes	22
(i) Protonation of quinoline	22
(ii) Attempted synthesis of (η^6 -quinoline)tricarbonylchromium <i>via</i> silylation at the 2-position	23
(iii) Synthesis of (η^6 -phenazine)tricarbonylchromium	24
2.3 Nucleophilic addition reactions	25
2.4 Conclusion	29
2.5 Spectroscopic characterization	30
2.5.1 Infrared spectroscopy	30
2.5.2 NMR spectroscopy	34
2.5.3 Mass spectrometry	46
2.5.4 X-ray crystallography	48
2.6 References	58

Chapter 3

σ,π -Heteroarene Bimetallic complexes of Titanium and Chromium

3.1 Introduction	62
3.2 Metallation	65
3.2.1 Synthesis of ($\eta^1:\eta^6$ -benzo[<i>b</i>]thienyl-TiCp ₂ Cl)tricarbonylchromium	67
3.3 Reactions of ($\eta^1:\eta^6$-benzo[<i>b</i>]thienyl-TiCp₂Cl)tricarbonylchromium	69
3.3.1 Reaction with Thiophenol	69
3.3.2 Reaction with Water	71
3.3.3 Reaction in acetone	72
3.4 Spectroscopic characterization	72
3.4.1 Infrared spectroscopy	72
3.4.2 NMR spectroscopy	74
3.4.3 Mass spectrometry	83
3.5 References	85

Chapter 4

σ,π -Heteroarene Bimetallic complexes of Manganese, Rhenium and Chromium

4.1 Introduction	87
-------------------------	-----------

4.2 Metallation	90
4.3 Spectroscopic characterization	93
4.3.1 Infrared spectroscopy	93
4.3.2 NMR spectroscopy	96
4.3.3 Mass spectrometry	102
4.4 References	105

Chapter 5

σ, π -Heteroarene Bimetallic complexes of Platinum and Chromium

5.1 Introduction	106
5.2 Synthesis of $[\eta^1: \eta^6\text{-benzo}[b]\text{thienyl}(\text{Cr}(\text{CO})_3)_2\text{Pt}(\text{dppe})]$	109
5.3 Spectroscopic characterization	111
5.3.1 Infrared spectroscopy	111
5.3.2 NMR spectroscopy	113
5.4 References	119

Chapter 6

Experimental

6.1 Standard Operational Procedure	120
6.2 Characterization techniques	120
6.2.1 Infrared spectroscopy	120
6.2.2 Nuclear Magnetic Resonance Spectroscopy	120
6.2.3 Mass spectrometry	121
6.2.4 X-ray Crystallography	121
6.3 Preparation of Starting Compounds	121
6.4 Synthesis of Organometallic Compounds	121
6.4.1 Preparation of π -heteroarene complexes	121
6.4.2 Sulphur-containing π -heteroarene complexes	121
(a) $(\eta^6\text{-benzo}[b]\text{thiophene})\text{tricarbonylchromium}$	123
(b) $(\eta^6\text{-dibenzothiophene})\text{tricarbonylchromium}$	124
(c) $(\eta^1(\text{S}):\eta^6\text{-3,6-dimethylthieno}[3,2\text{-}b]\text{thiophene})\text{tricarbonylchromium}$	124
6.4.3 Nitrogen-containing π -heteroarene complexes	124
(a) $(\eta^6\text{-N-trimethylsilyl-2-butyl-1,2-dihydroquinoline})\text{tricarbonylchromium}$	124

(b) (η^6 -phenazine)tricarbonylchromium	125
6.4.4 Bimetallic sulphur-containing π -heteroarene complexes	125
(a) ($\eta^1:\eta^6$ -benzo[<i>b</i>]thienyl-TiCp ₂ Cl)tricarbonylchromium	126
(b) ($\eta^1:\eta^6$ -benzo[<i>b</i>]thienyl-TiCp ₂ (SPh))tricarbonylchromium	126
(c) ($\eta^1:\eta^6$ -benzo[<i>b</i>]thienyl-TiCp ₂ OH)tricarbonylchromium	127
(d) ($\eta^1:\eta^6$ -benzo[<i>b</i>]thienyl-Re(CO) ₅)tricarbonylchromium	127
(e) ($\eta^1:\eta^6$ -benzo[<i>b</i>]thienyl-Mn(CO) ₅)tricarbonylchromium	127
(f) ($\eta^1:\eta^6$ -dibenzothienyl-Re(CO) ₅)tricarbonylchromium	128
(g) [$\eta^1:\eta^6$ -benzo[<i>b</i>]thienyl(tricarbonylchromium)] ₂ Pt(dppe)	129
6.4.5 Sulphur containing σ -heteroarene complexes	129
(a) η^1 -dibenzothienyl-Re(CO) ₅	129
6.5 References	130
Appendix 1	131
Appendix 2	139

Summary

Novel π -heteroarene complexes of the type $(\eta^6\text{-arene})\text{Cr}(\text{CO})_3$ were synthesized. The reactivity of thio- and nitro-heteroarene rings towards π -coordination to a $\text{Cr}(\text{CO})_3$ -moiety were investigated. Two different synthetic routes were implemented to synthesize the π -coordinated products. It was found that the thio-heteroarene complexes were obtained in a high yield on treatment with trisammine(tricarbonyl)chromium, while higher yields were obtained for the nitro-heteroarene complexes on treatment with hexacarbonylchromium. The arene ligands under investigation were 3,6-dimethylthieno[3,2-*b*]thiophene, quinoline and phenazine. The synthesis of the $(\eta^6\text{-quinoline})\text{Cr}(\text{CO})_3$ complex has proved to be more arduous than was expected and several methods were implemented to synthesize the desired product. In the end two products were isolated, both π -coordinated to a $\text{Cr}(\text{CO})_3$ -moiety, but neither resembling the target complex. Instead, nucleophilic addition occurred at the 2-position of both products and the lone pair of the nitrogen atom was blocked by a substituent. These complexes were fully characterized and the proposed structure formulations were confirmed by single crystal X-ray determinations.

Known $(\eta^6\text{-arene})\text{Cr}(\text{CO})_3$ complexes were investigated with regard to activation and stabilization of the bridging arene ligand. The ligands benzo[*b*]thiophene and dibenzothiophene were monolithiated and treated with group IV (Ti), group VII (Mn, Re) and group X (Pt) transition metals at low temperatures to yield σ,π -bimetallic heteroarene complexes. The first σ,π -bimetallic dibenzothiophene complexes were synthesized by this method. The yields of these complexes were, however, very low. From the spectroscopic data it was clear that the activation of the dibenzothiophene $\text{Cr}(\text{CO})_3$ complex towards coordination to the second metal, i.e. the σ -bonded species, occurred on the same ring fragment as where the π -coordination took place. In an attempt to improve the yield, another synthetic route was investigated and this led to the preparation of the σ -dibenzothiophene complex, η^1 -dibenzothienyl- $\text{Re}(\text{CO})_5$. The synthetic method using this σ -complex as precursor was unfortunately unsuccessful. All the new bimetallic compounds were fully characterized by means of NMR spectroscopy, infrared spectroscopy as well as mass spectrometry.

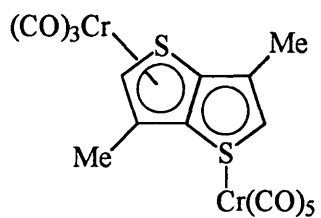
Opsomming

Die sintese van nuwe π -heterooreenkomplekse met die algemene formule $(\eta^6\text{-areen})\text{Cr}(\text{CO})_3$ is bestudeer. Die reaktiwiteit van swael- en stikstofbevattende heterooreenringe is ondersoek ten opsigte van π -koordinasie aan 'n $\text{Cr}(\text{CO})_3$ -fragment. Twee onderskeie sintese metodes is ondersoek ten einde die π -gekoördineerde produkte te berei. Daar is gevind dat die swaelbevattende heterooreen komplekse met kwantitatiewe opbrengs berei kon word deur behandeling met trisammien(trikarboniel)chrom, terwyl die stikstof-bevattende komplekse in hoër opbrengs verkry is deur dit met chromheksakarboniel te behandel. Die areenligande wat ondersoek is, was 3,6-dimetieltiëno[3,2-*b*]tiofeen, kinolien en fenasiën. Die sintese van die $(\eta^6\text{-kinolien})\text{Cr}(\text{CO})_3$ kompleks was problematies en verskeie metodes is beproef om die verlangde produk te berei. Twee produkte is geïsoleer, maar nie een van hierdie komplekse het ooreengekom met die teiken verbinding nie, alhoewel beide π -gekoördineerd aan 'n $\text{Cr}(\text{CO})_3$ -fragment was. In plaas van addisie van die verlangde trimetielsilielgroep, het nukleofiele addisie van 'n butiel groep op die 2-posisie van beide produkte plaasgevind en die alleenpaar van die stikstof is deur 'n substituent blokkeer. Hierdie komplekse is ten volle gekarakteriseer en voorgestelde strukture is bevestig deur enkel kristal X-straal analises.

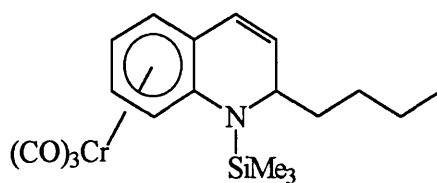
Bekende $(\eta^6\text{-heterooreen})\text{Cr}(\text{CO})_3$ komplekse is bestudeer ten opsigte van aktivering en stabilisering van die gebrugde areenligand. Die ligande benzo[*b*]tiofeen en dibensotiofeen is gemonoliteer en met groep IV (Ti), groep VII (Mn, Re) en groep X (Pt) oorgangsmetale by lae temperature behandel om die verlangde σ, π -bimetaal heterooreenkomplekse te lewer. Die eerste σ, π -bimetaal dibensotiofeen komplekse is volgens hierdie metode berei. Die opbrengs van hierdie komplekse was egtër baie laag. Spektroskopiese data het aangedui dat die aktivering van die dibensotiofeen $\text{Cr}(\text{CO})_3$ kompleks ten opsigte van koordinasie aan die tweede metaal, d.w.s die σ -gebonde spesie, op dieselfde ringfragment voorkom as waar die π -koordinering plaasvind. In 'n poging om die opbrengs te verbeter is 'n volgende sintese roete ondersoek. Dit het aanleiding gegee tot die sintese van die σ -dibensotiofeen kompleks, σ -dibensotiëniel- $\text{Re}(\text{CO})_5$. Die sintese metode waar hierdie σ -kompleks as voorloper gebruik is, was ongelukkig onsuksesvol. Die nuwe bimetaalverbinding is ten volle gekarakteriseer met behulp van KMR spektroskopie, infrarooi spektroskopie asook massa spektrometrie.

List of Compounds

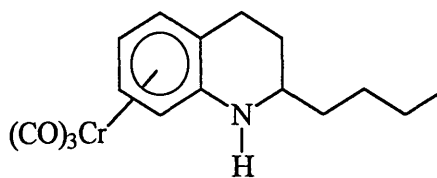
1:



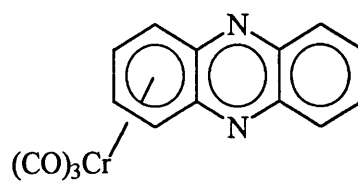
2:



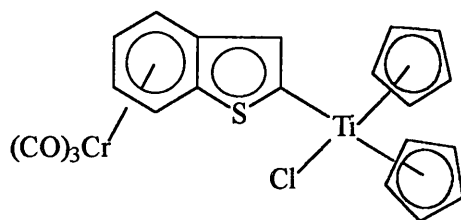
3:



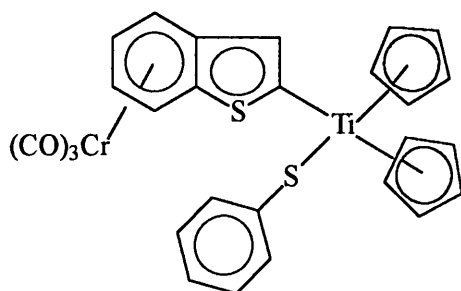
4:



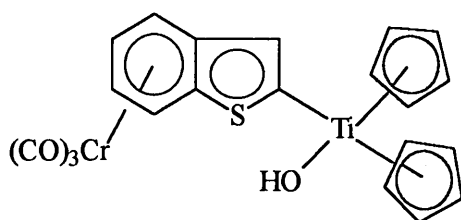
5:



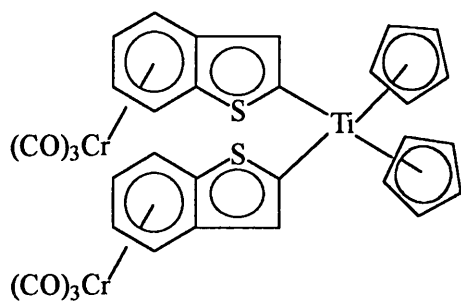
6:



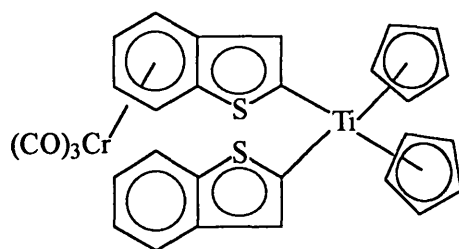
7:



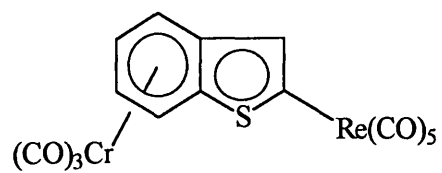
8:



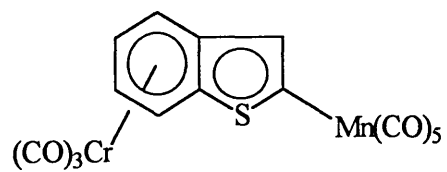
9:



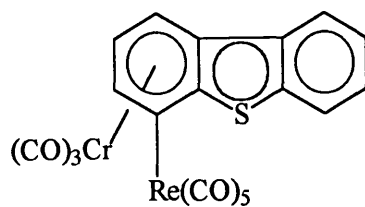
10:



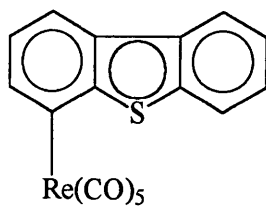
11:



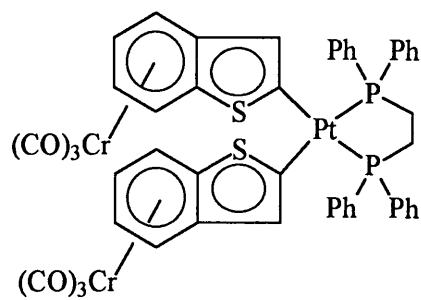
12:



13:



14:



List of Abbreviations

η^n	:	number, n, of ring atoms bonded to the metal in a π -ring fashion
Ar	:	aryl substituent
ax	:	axial
av	:	average
br	:	broad
BT	:	benzo[<i>b</i>]thiophene
CNTR	:	centre
COD	:	cyclooctadiene
Cp	:	η^5 -C ₅ H ₅
CP	:	conducting polymers
d	:	doublet
DBT	:	dibenzothiophene
DEPT	:	Distorsionless Enhancement by Polarization Transfer
DHT	:	2,3-dihydrothiophene
dppe	:	1,2-bis(diphenylphosphino)ethane
eq	:	equatorial
HDS	:	hydrodesulphurization
HETCOR	:	Heteronuclear Correlation Spectroscopy
HMO	:	Hückel molecular orbital
IR	:	Infrared Spectroscopy
m	:	medium
m	:	multiplet
MS	:	Mass Spectrometry
n.o.	:	not observed
NMR	:	Nuclear Magnetic Resonance Spectroscopy
Pet. ether	:	Petroleum ether 40-60°C
Ph	:	phenyl

ppm	:	parts per million
Q	:	quinoline
RT	:	room temperature
s	:	singlet (NMR)
s	:	strong (IR)
t	:	triplet
T	:	thiophene
THF	:	tetrahydrofuran
TLC	:	thin layer chromatography
TMEDA	:	tetramethyl ethylene diamine
TMSCI	:	chlorotrimethylsilane
vs	:	very strong
vw	:	very weak
w	:	weak
wgs	:	water-gas shift

1

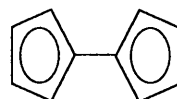
Introduction

1.1 General introduction

The first arene-transition metal complexes were prepared in the 1950s^[1]. After the discovery of ferrocene, the first sandwich complex, in 1951^[2], an increasing interest in the chemistry of arene ligands attached to transition metals was experienced. More recent studies have been extended to heterocyclic ligands. Cyclic conjugated ligands C_nH_n or heteroatom cyclic conjugated ligands C_nH_nX ($X =$ heteroatom e.g. S, N, P) are known to occur in several different classes of π -compounds.

1.1.1 Sandwich complexes

The first sandwich complex, ferrocene, was discovered accidentally, in the attempt to synthesize fulvalene.



Fulvalene

The initial structural formulation was $Fe(C_5H_4)_2$, but was soon revised and the correct sandwich structure was introduced^[3]. An enormous number of these $\eta^5-C_5H_5$ complexes are now known. Arenes such as benzene and its derivatives also have the ability to form complexes analogous to ferrocene. The first η^6 -complexes were prepared as early as 1919 when F. Hein^[4] reacted $CrCl_3$ with $PhMgBr$ to yield compounds he formulated as $[CrPh_n]^{0,+1}$ ($n = 2,3,4$). The correct disposition as η^6 -arene complexes was first recognized more than 35 years later^[5].

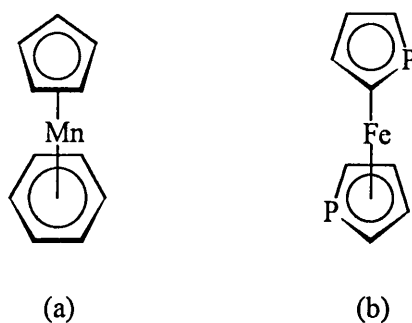


Figure 1.1 Examples of (a) arene and (b) heteroarene sandwich complexes

1.1.2 Half-sandwich complexes

Complexes containing carbocyclic or heterocyclic moieties exist where only one arene ring is π -coordinated to a transition metal, while the remainder of the coordination sites are occupied by ligands e.g. CO, NO, Cl etc. These compounds are known as half-sandwich complexes and exhibit a “piano stool” structure with the arene ring as the seat and the other ligands as the “legs”.

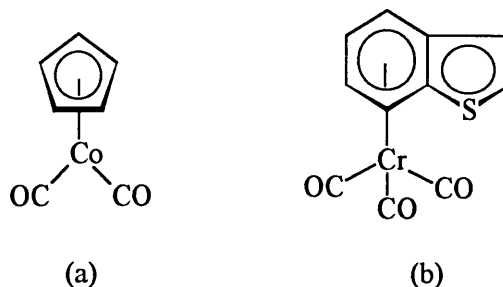


Figure 1.2 Examples of (a) arene and (b) heteroarene half-sandwich complexes

1.1.3. Complexes with tilted sandwich structures

The only true sandwich compounds with parallel rings are those of the types $(\eta^n\text{-C}_n\text{H}_n)_2\text{M}$ and $(\eta^n\text{-C}_n\text{H}_n)_2\text{M}^+$; others containing more ligands have rings at an angle, e.g. $(\eta^5\text{-C}_5\text{H}_5)_2\text{TiCl}_2$. The three types of bent sandwich compounds have one, two or three ligands.

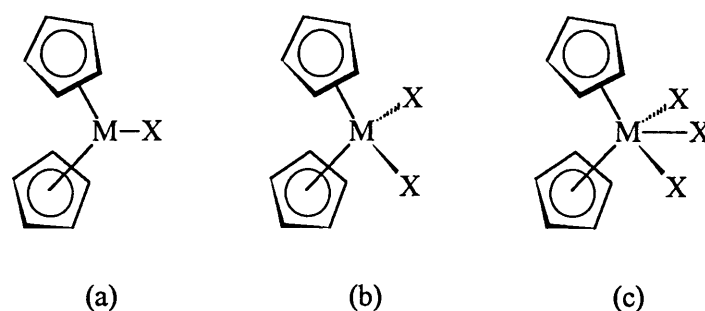


Figure 1.3 Bent sandwich complexes can have (a) one, (b) two or (c) three additional ligands

1.1.4 Complexes with more than two C_nH_n ligands

Due to size considerations as well as the accessibility of the 5f orbitals, only the actinide metals have the ability to accommodate four η^5 Cp-ligands on the same metal site. The readiness of the actinides to engage in covalent bonding also plays a significant role.

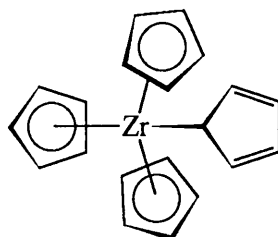


Figure 1.4 An example of a complex with four Cp-ligands, ZrCp₄

1.1.5 Multidecker sandwich complexes

The first multidecker sandwich complex was synthesized by H. Werner^[6], namely the triple-decker sandwich complex, $[Ni_2(C_3H_5)_3]^+$. Heterocyclic boron compounds have the tendency to form multidecker sandwiches with transition metals. A large variety of triple-, tetra-, penta- and hexadecker complexes are known, in which 1,3-diborolyl act as the bridging ligand. The utmost expansion of this series was the preparation of polydecker sandwich complexes. The nickel complex was found to be a semiconductor and the rhodium complex an insulator^[7].

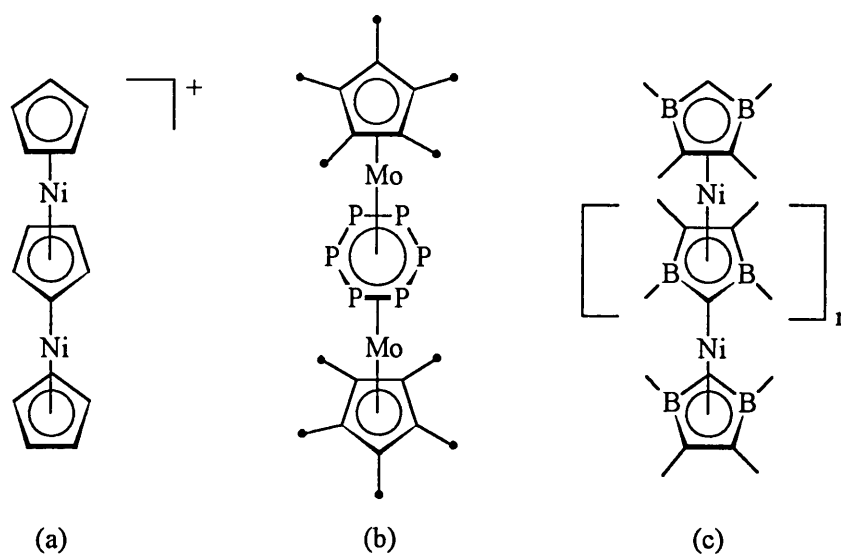


Figure 1.5 Examples of (a) a nickel triple-decker complex with Cp-rings as ligands, (b) a molybdenum triple-decker complex with hexaphosphabenzene as bridging ligand and (c) a nickel polydecker complex with 1,3-diborolyl as bridging ligand

The ability of common heteroatoms such as N, O, S etc. to form σ -complexes with transition metals is well established and can find application in various fields of analytical, biological and general chemistry. When these heteroatoms are incorporated in more complex molecules containing a π -system, e.g. pyridine, thiophene etc., the lone pair electrons of the heteroatom are still accessible for chemical reactivity. In some cases these nonbonding electrons have lower ionization potential and are therefore more available for bonding than the π -system electrons. It would thus seem that the σ -bonding mode is favoured for most heteroaromatic compounds.

There are, however, a growing number of examples of π -heteroarene complexes. The interest in these complexes are obvious for the following reasons:

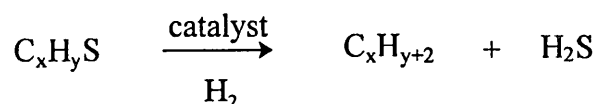
- (i) Stabilization of reactive heteroarene intermediates
- (ii) Isomerization reactions
- (iii) Biologically significant complexes
- (iv) Theoretical models of electronic structure and bonding

- (v) Modification of the chemical and physical properties of the metal centre upon coordination to the heteroarene
- (vi) Catalytic reactivity

The chemistry of thiophene (T) and thiophene derivatives in particular enjoys the most attention at this stage, since current research in the field of organometallic heteroarene chemistry is dominated by the hydrodesulphurization^[8] (HDS) of petroleum.

1.2 Hydrodesulphurization

HDS is the commercial process whereby sulphur is removed from organosulphur compounds in petroleum-based feedstocks to produce clean-burning fuels low in sulphur content. It is of prime importance in the petroleum and coal industries because of the growing need to process feedstocks of high sulphur levels with the aim of producing fuels with the smallest possible sulphur content. The volume of this process (24 million barrels of petroleum per day) entitles it to be the most important chemical process practised today. Residual sulphur in fuels is present mainly in thiophene forms and predominantly as benzo- and dibenzothiophene derivatives. Thiophenes are difficult to desulphurize due to the aromatic stabilization provided by the delocalized π -system. Benzo- and dibenzothiophenes are even more difficult to desulphurize because of their lower reactivity. The HDS reaction involves the treatment with H_2 at $400^\circ C$ over a cobalt or nickel promoted molybdenum or tungsten catalyst supported on Al_2O_3 ^[9]. Although this Co-Mo/ Al_2O_3 catalyst is the most studied because of its commercial relevance, many transition metals catalyze the HDS of thiophenes, with Ru, Os, Rh, and Ir being among the most active.



Despite the large-scale industrial application of HDS, very little is known of the mechanisms involved in this process.

1.2.1 HDS of thiophene

The proposed mechanisms for the HDS of thiophene involve either initial C-S cleavage^[10] to give butadiene that is rapidly hydrogenated to a mixture of C₄ products, or partial hydrogenation^[11] that subsequently yields the C₄ products.

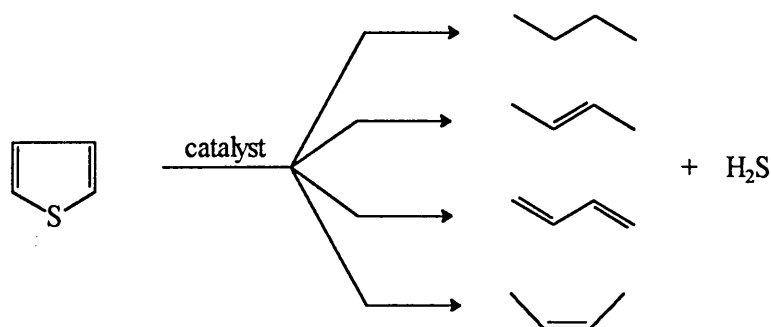


Figure 1.6 HDS of thiophene

All proposals involve the coordination of thiophene to a metal site, either through the sulphur or in a η^5 or η^2 fashion. This binding is suggested to activate the thiophene towards desulphurization participation. Considering simple reactions of thiophene in transition metal complexes, Angelici^[12] proposed a overall mechanism for thiophene HDS (figure 1.7).

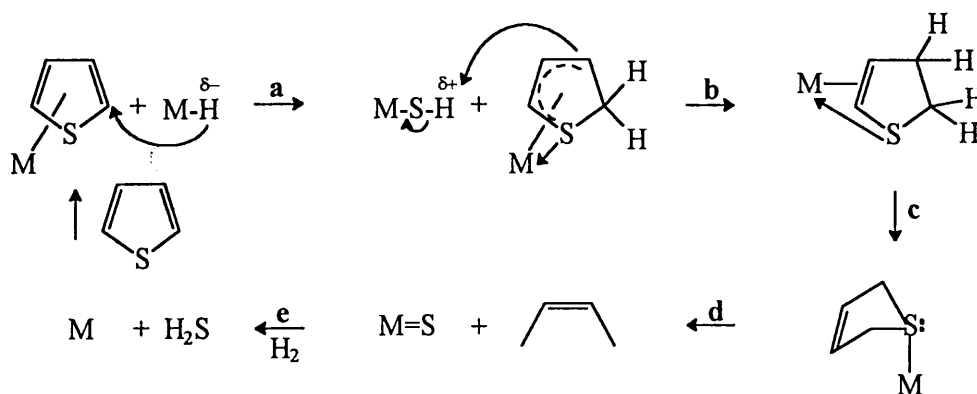


Figure 1.7 Proposed mechanism for the HDS of thiophene

The proposed mechanism entails initial η^5 -adsorption of thiophene to a metal site. This activates the thiophene to hydride attack from a nearby metal hydride (step a) at the 2-position of the thiophene, yielding the allyl sulfide intermediate. This reaction is similar to the reaction of $(\eta^5\text{-thienyl})\text{Mn}(\text{CO})_3^+$ with metal hydrides^[13]. In step b a strongly acidic proton, e.g. from a -SH group, is transferred to the 3-position of the hydrothiophene, to yield 2,3-dihydrothiophene (DHT). The isomerization of 2,3-DHT to the more stable 2,5-DHT in step c, was observed^[14] on the $\text{Re}/\text{Al}_2\text{O}_3$ catalyst at 300°C. In step d, involving the elimination of butadiene promoted by the abstraction of a sulphur atom from the η^1 -coordinated 2,5-DHT, desulphurization occurs. The C_4 products that are formed, butenes and butane, are probably the result of hydrogenation of butadiene, a reaction known to occur over HDS catalysts^[15]. A surface sulfide is converted to H_2S by reaction with H_2 , in the final step, step e.

1.2.2 HDS of benzothiophene

Since benzothiophenes contain two fused aromatic rings, π -coordination to transition metals are possible for either one or both of these rings. Several metals, identified as active HDS catalysts, e.g. Ru, Rh and Ir, were coordinated through the π -system of the benzene ring of benzo[*b*]thiophene (BT) in order to explore the reactivities of these complexes as possible models for reactions on catalysts in the HDS process. One of the most widely accepted mechanisms proposed for HDS of BT over solid catalysts involves the selective hydrogenation to 2,3-dihydrobenzo[*b*]thiophene (DHBT) prior to desulphurization to yield ethylbenzene^[16].

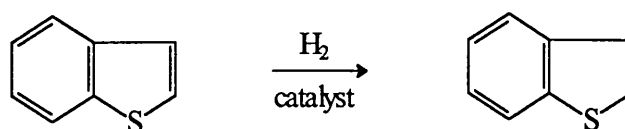


Figure 1.8 Selective hydrogenation of BT using $[\text{Rh}(\text{COD})(\text{PPh}_3)_2]^+$ as catalyst

The cleavage of the C-S bond in thiophenes is the means by which metals abstract sulphur from the hydrocarbons. An interesting reaction with $\text{Fe}_3(\text{CO})_{12}$ ^[17] that does lead to C-S bond cleavage, gives a benzothiaferrole product in which a $\text{Fe}(\text{CO})_3$ group inserts into a C-S bond. This model reaction of BT suggests an alternative reasonable first step in the HDS process.

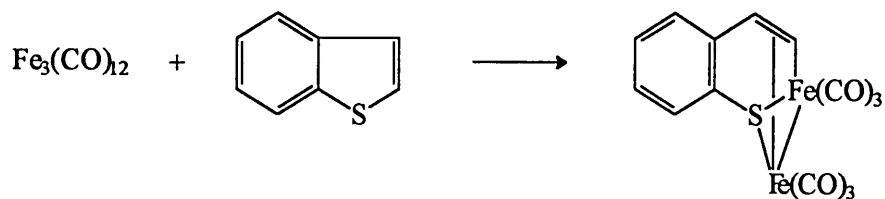


Figure 1.9 Insertion of $\text{Fe}(\text{CO})_3$ group

This benzothiaferrole product, when exposed to H_2 gas at 175°C , yields ethylbenzene (figure 1.10), the major product of BT HDS^[18]. It is however clear that the insertion of an iron atom into the C-S bond activates the heterocycle towards desulphurization.

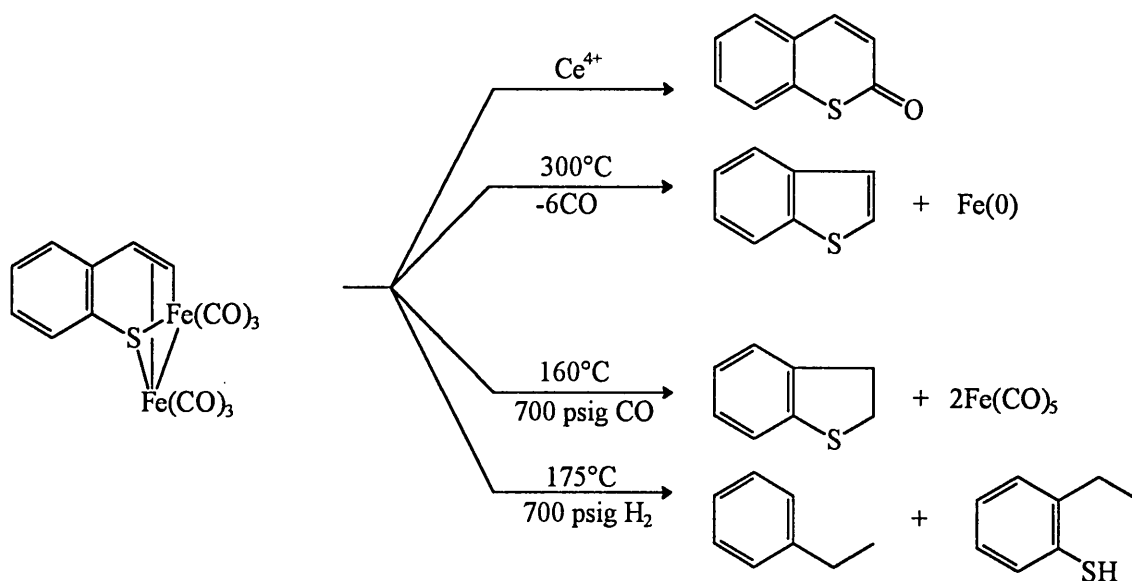


Figure 1.10 Reactions of the benzothiaferrole complex

Mechanisms for the desulphurization of benzothiophenes are not as well developed as for thiophenes. The combination of organometallic chemistry and heterogeneous reactor studies will probably yield reasonable mechanisms in the near future.

1.2.3. HDS of dibenzothiophene

Dibenzothiophene (DBT), which is present in high concentrations in heavy oils and coal-derived liquids, is 1-2 orders of magnitude less reactive than thiophene and therefore among the most difficult to desulphurize. Studies^[19] on the mechanism of DBT HDS suggest two general pathways: one involves the direct elimination to yield biphenyl and H₂S (figure 1.11, a), while the other entails the hydrogenation of a benzene ring, giving tetrahydrodibenzothiophene and hexahydrodibenzothiophene followed by subsequent desulphurization (figure 1.11, b).

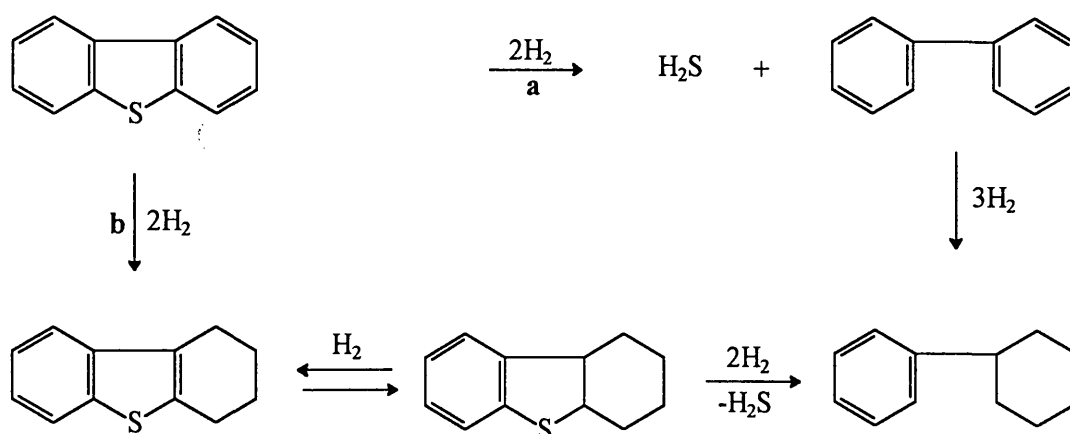


Figure 1.11 Proposed scheme for the HDS of DBT

Among the various approaches which have been developed to give information on the HDS mechanism of DBT, the study of the coordination and reactivity of DBT with soluble metal complexes has been investigated^[20]. In recent literature^[21] it has been shown that metal-activated DBT can either be desulphurized to biphenyl and H₂S or be hydrogenated to 2-phenylthiophenol. The catalyst^[22] which brings about the conversion of DBT to a mixture of these three products, is the 16-electron fragment [(triphos)IrH], [triphos = MeC(CH₂PPh₂)₃]. This fragment cleaves DBT in THF to yield the C-S metal inserted product. After hydrogenation (100°C, 5 atm of H₂), resulting in the formation of the 2-phenylthiophenolate dihydride (triphos)Ir(H)₂(SC₁₂H₉) complex, treatment of this complex (170°C, 30 atm of H₂) yields the mixture of final products (figure 1.12). This work indubitably demonstrates that (i) the energy barrier to C-S insertion of DBT is higher than those of T and BT and (ii) the DBT C-S insertion product is the most reluctant to couple a hydride ligand to the metallated carbon atom of the iridathiacycle. These

results are compatible with the observation that DBT is more difficult to desulphurize under HDS conditions than BT or T.

Other metals that have been investigated for desulphurization activity of DBT, include Ru^[23] and Fe^[24].

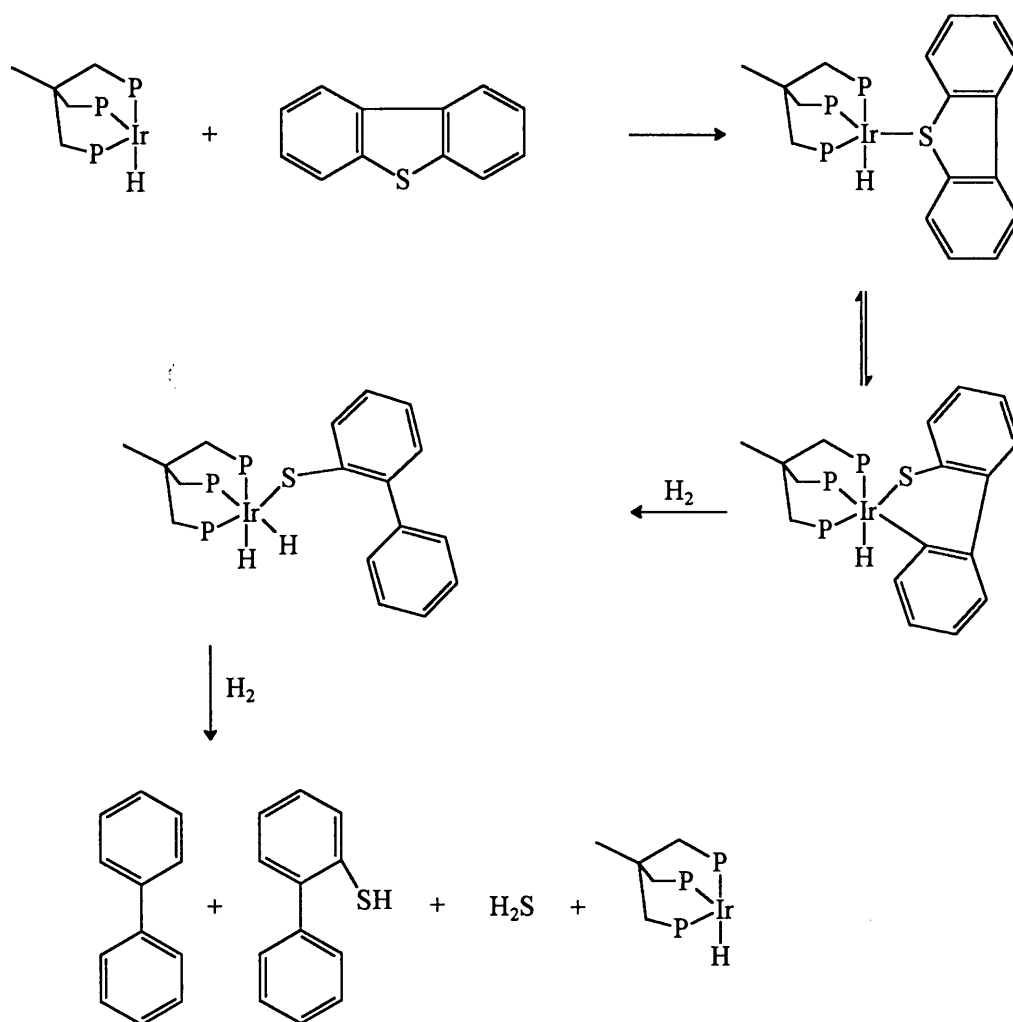


Figure 1.12 Proposed mechanism for HDS of DBT

1.3 Hydroprocessing of Quinoline

Polynuclear nitrogen heteroaromatic compounds such as quinolines and isoquinolines are present in coal and oil shale^[25]. Thus the various synthetic fuel products derived from coal or oil shale require additional hydroprocessing to minimize the nitrogen content. The selective hydrogenation of these nitrogen containing heteroarenes is essential to obtain certain key intermediates. Pettit *et al*^[26] reported the use of carbon monoxide and water as reducing agent, instead of hydrogen, in the hydroformylation of olefins and the reduction of nitroarenes. These reactions were catalyzed by transition metal carbonyl compounds. The mechanism was thought to proceed *via* the formation of transition metal carbonyl hydrides, by nucleophilic attack of water or base on coordinated carbon monoxide^[27].

Several transition metal carbonyl complexes have been investigated for potential catalytic activity towards this hydrogenation reaction. Such hydrogenations have been achieved under heterogeneous or homogeneous conditions. The transition metal carbonyl compounds were reacted with nitrogen heteroarenes under water-gas shift (CO, H₂O, base) and synthetic gas (1:1 CO:H₂) conditions and iron^[28], manganese and cobalt^[29] carbonyls were found to provide the reduced products under water-gas shift (wgs) conditions (figure 1.13). The hydrogenation is performed highly selectively. The pyridine rings are reduced to give 1,2,3,4-tetrahydroquinoline and neither 5,6,7,8-tetrahydro- nor decahydroquinoline were obtained. Murahashi *et al*^[25] extended this study to rhodium carbonyls. Generally transition metal carbonyls alone show low catalytic activity under wgs conditions and the addition of a base is required to enhance the activity. For the reaction of quinolines, however, the addition of a base is not necessary since they behave as bases. Hence the hydrogenation proceeds regioselectively and efficiently.

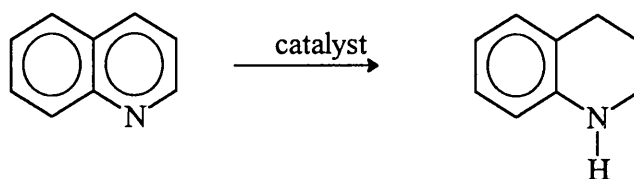


Figure 1.13 Selective hydrogenation of quinoline

These results point to the possible usefulness of these catalysts in future synthetic fuel processes concerned with removing nitrogen from the reduced nitrogen-containing ring in polynuclear heterocyclic nitrogen compounds.

1.4 π -Pyrrole metal complexes

One of the most widely studied^[30] areas of porphyrin chemistry is the ability of tetrapyrrole systems to coordinate metals. Metalloporphyrins are important natural compounds and are involved in electron transfer, respiration, photosynthesis and industrial catalysis. Four principle coordination modes are possible (figure 1.14).

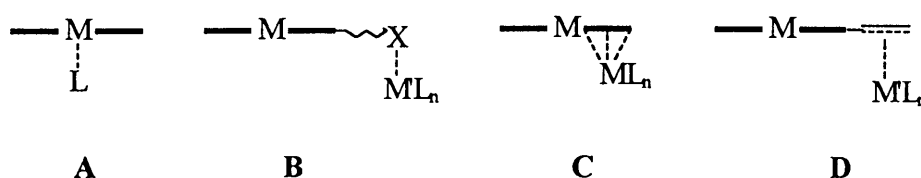


Figure 1.14 Coordination modes of metalloporphyrins

The coordination modes are: metal σ bonding by the nitrogen atom of the pyrrole (A); metal σ bonding through surrounding side chain functionalities (B); π bonding to metals by direct involvement of the aromatic porphyrin π system (C) or π bonding to metals through surrounding aromatic systems (D). Examples of coordination mode C were unknown until recently. The organometallic chemistry of pyrrole compounds has been studied more intensively. It is known that N-heterocycles prefer η^1 -coordination, *i.e.* metal-nitrogen σ bonds. However, a number of η^5 -pyrrole metal complexes are known^[31]. Most known pyrrole π complexes are obtained from the azacyclopentadienylanion. This ligand is isoelectronic to cyclopentadienyl (Cp). Sandwich complexes containing one or two^[32] η^5 -pyrrole ligands as well as tricarbonyl(η^5 -pyrrolyl)^[33] and multidecker sandwiches^[34] have been prepared. Further investigation of these and related compounds might aid in the unravelling of the mechanism of catalytic processes involving metalloporphyrin interactions.

1.5 Aim of this study

The aim of this study was two-fold:

- (a) The preparation of new π -heteroarene complexes and especially the synthesis of nitrogen-containing heteroarene complexes was studied. The different synthetic routes were critically investigated to try and obtain quantitative yields.
- (b) Activation of π -BT and π -DBT chromium complexes with σ -bonded transition metals was examined. The influence of early, middle as well as late transition metals was explored.

1.6 References

- (1) W.E. Silverthorn, *Adv. Organomet. Chem.*, **1975**, *13*, 47.
- (2) P.L. Pauson, *Nature*, **1951**, *168*, 1039.
- (3) G. Wilkinson, M. Rosenblum, M.C. Whiting, R.B. Woodward, *J. Am. Chem. Soc.*, **1952**, *74*, 2125.
- (4) F. Hein, *Chem. Ber.*, **1919**, *52*, 195.
- (5) H. Zeiss, P.J. Wheatly, H.J.S. Winkler, *Benzenoid-Metal Complexes*, Ronald Press: New York, **1966**, 101.
- (6) H. Werner, *Angew. Chem. Int. Ed.*, **1972**, *11*, 930.
- (7) W. Siebert, *Angew. Chem. Int. Ed.*, **1986**, *25*, 105.
- (8) B.C. Gates, J.R. Katzer, G.C.A. Schuit, *Chemistry of Catalytic Processes*, McGraw-Hill; New York, **1979**.
- (9) O. Weisser, S. Landa, *Sulfide Catalysts: Their properties and applications*; Pergamon: Oxford, **1973**.
- (10) S. Kolboe, *Can. J. Chem.*, **1969**, *47*, 352.
- (11) H. Kwart, G.C.A. Schuit, B.C. Gates, *J. Catal.*, **1980**, *61*, 128.
- (12) R.J. Angelici, *Acc. Chem. Res.*, **1988**, *21*, 387.
- (13) D.A. Lesch, J.W. Richardson, R.A. Jacobson, R.J. Angelici, *J. Am. Chem. Soc.*, **1984**, *106*, 2901.
- (14) E.J. Markel, G.L. Schrader, N.N. Sauer, R.J. Angelici, *J. Catal.*, **1989**, *116*, 11.
- (15) P.C.H. Mitchell, *Catalysis (London)*, **1981**, *4*, 175.
- (16) R.A. Sánchez-Delgado, V. Herrera, L. Rincón, A. Andriollo, G. Martín, *Organometallics*, **1994**, *13*, 553.
- (17) A.E. Ogilvy, M. Draganjac, T.B. Rauchfuss, S.R. Wilson, *Organometallics*, **1988**, *7*, 1171.
- (18) R. López, R. Peter, M. Zdrzil, *J. Catal.*, **1982**, *73*, 406.
- (19) G.H. Singhal, R.L. Espino, J.E. Sobel, G.A. Huff, *J. Catal.*, **1981**, *67*, 457.

- (20) C. Bianchini, M.V. Jiménez, A. Meli, S. Moneti, F. Vizza, V. Herrera, R.A. Sánchez-Delgado, *Organometallics*, **1995**, *14*, 2342.
- (21) J.J. Garcia, P.M. Maitlis, B.E. Mann, H. Adams, N.A. Bailey, *J. Am. Chem. Soc.*, **1995**, *117*, 2179.
- (22) C. Bianchini, J.A. Casares, M.V. Jiménez, A. Meli, S. Moneti, F. Vizza, V. Herrera, R.A. Sánchez-Delgado, *Organometallics*, **1995**, *14*, 4850.
- (23) T.A. Pecoraro, R.R. Chianelli, *J. Catal.*, **1981**, *67*, 430.
- (24) J.D. Goodrich, P.N. Nickias, J.P. Selegue, *Inorg. Chem.*, **1987**, *26*, 3426.
- (25) S-I. Murahashi, Y. Imada, Y. Hirai, *Tetrahedron Lett.*, **1987**, *28(1)*, 77.
- (26) T. Cole, R. Ramage, K. Cann, R. Pettit, *J. Am. Chem. Soc.*, **1980**, *102*, 6182.
- (27) N. Grice, S.C. Kao, R. Pettit, *J. Am. Chem. Soc.*, **1979**, *101*, 1627.
- (28) T.J. Lynch, M. Banah, H.D. Kaesz, C.R. Porter, *J. Org. Chem.*, **1984**, *49*, 1266.
- (29) R.H. Fish, A.D. Thormodsen, G.A. Cremer, *J. Am. Chem. Soc.*, **1982**, *104*, 5234.
- (30) M.O. Senge, *Angew. Chem. Int. Ed. Engl.*, **1996**, *35*, 1923.
- (31) K.K. Joshi, P.L. Pauson, *Proc. Chem. Soc.*, **1962**, 362.
- (32) M.-G.A. Shvekhgeimer, *Russ. Chem. Rev.*, **1996**, *65*, 41.
- (33) N. Kuhn, S. Stubenrauch, R. Boese, D. Bläser, *J. Organomet. Chem.*, **1992**, *440*, 289.
- (34) K.J. Chase, R.F. Bryan, M.K. Woode, R.N. Grimes, *Organometallics*, **1991**, *10*, 2631.

2

π -Heteroarene complexes of Chromium

2.1 Introduction

The first arene-transition metal complexes were prepared in the 1950s^[1] and the polarizability or electron deficiency of the complexes was immediately recognized to aid in the addition of nucleophiles to the arene ligand. Metal complexes containing bridged arene ligands have attracted the attention of inorganic chemists since Fischer and Hafner^[2] synthesized the compound $(\eta^6\text{-benzene})_2\text{Cr}$. Several reasons exist for the interest in arene complexes of transition elements. The arene ligand is uncharged and can donate an even number of electrons. Vacant coordination positions can be generated more easily than in the case of negatively charged ligands e.g. cyclopentadienyl. By changing the nature of additional ligands, the hapticity of the arene ligand can be varied e.g. $\eta^6 \rightarrow \eta^4 \rightarrow \eta^2$. Ring slippage is also a promoter of ligand substitution reactions. Furthermore, vacant coordination sites are created by varying the hapticity of the arene ligand and this property empowers the complexes to act as precursors for catalysts in e.g. hydrogenation or polymerization processes^[3].

One of the most important features of heteroarene metal complexes is the preferential formation of heteroatom-metal σ bonds instead of arene-metal π bonds. A possible explanation for this preference is attributed to the lower ionization energies of unbonded electron pairs of the heteroatom compared to the π -electrons of the arene ring. The unbonded electron pairs are thus more accessible for bonding than the electrons in the π -system. Another interesting trait of π -heteroarene complexes is their stability relative to their carbocyclic analogues. In general, the more electronegative atoms such as N and S form π -heteroarene complexes which tend to be air sensitive^{[4],[5]}. Modification of the chemical and physical properties of the metal centre upon coordination to the heteroarene ligand can occur.

The η^5 -heterocyclic metal carbonyls have been most thoroughly studied, e.g. η^5 -thiophene^[6] and η^5 -pyrrole^[7]. More recently the interest shifted to the benzannulated derivatives of these five membered monoheterocycles, e.g. benzo[*b*]thiophene and indole^[7], which were π -coordinated to transition metals. It is important to note that heterocycles can be classified as π -excessive or π -deficient. π -Excessive heterocycles are compounds in which the number of π -electrons in the conjugated system exceeds the number of atoms forming the cycle. The compounds pyrrole, thiophene, benzo[*b*]thiophene, indole and dibenzothiophene are classical examples of π -excessive heterocycles.

In this study the activation of the π -coordinated tricarbonylchromium complexes of benzo[*b*]thiophene and dibenzothiophene were investigated (chapters 3-5). The syntheses of these compounds are known and the complexes were fully characterized by Fischer *et al*^[8]. For both compounds the molecular orbital calculations of the localized charges for each of the carbon atoms and sulphur have been reported^[9].



Figure 2.1 Electron distribution on benzo[*b*]thiophene and dibenzothiophene

For dibenzothiophene (DBT), the highest electron densities are on the sulphur and the outer benzene carbons. Hence, it would be expected that the coordination to metal will occur either through the sulphur or as a π -complex *via* one of the benzene rings. Sulphur coordination is known in $[\text{Cp}(\text{CO})_2\text{Fe}(\text{DBT})]\text{BF}_4$ ^[10] while π -coordination is known in the complex $[\text{CpFe}(\eta^6\text{-DBT})]\text{PF}_6$ ^[11]. Benzo[*b*]thiophene (BT) is known to coordinate through the sulphur atom, as seen for $\text{Cp}(\text{CO})_2\text{Re}(\text{BT})$ ^[12], through the 2,3-double bond, e.g. $(\eta^2\text{-2,3-BT})\text{ReCp}(\text{CO})_2$ ^[13], or through π -coordination to the benzene ring.

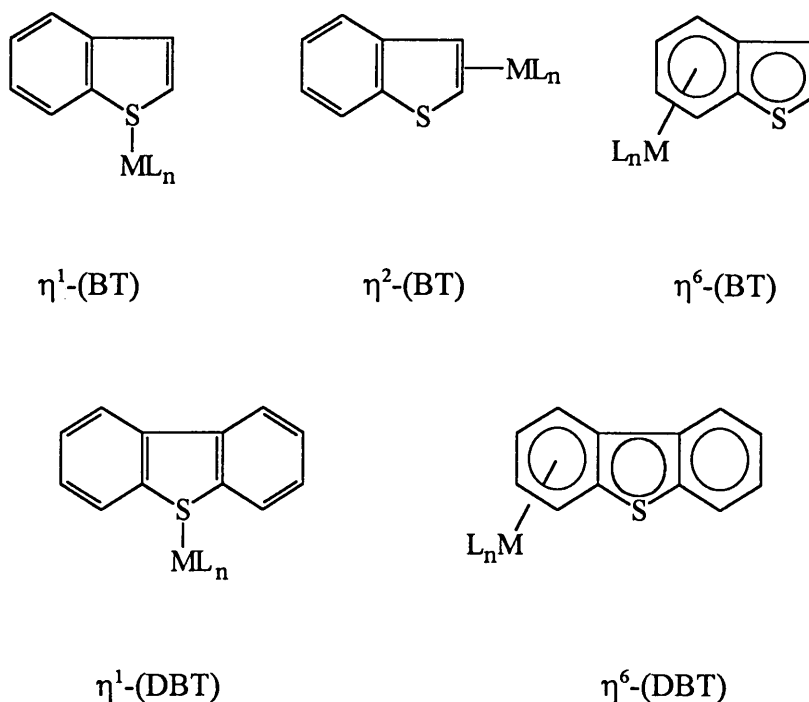


Figure 2.2 Bonding modes of benzo[*b*]thiophene and dibenzothiophene

Thiophene and its coordination to transition metals has been the subject of extensive studies the past few years. Several π -thiophene complexes have been reported^[14], although sulphur-coordinated complexes are also known^[15]. Angelici^[16] reported more diverse bonding modes in his review article.

Nitrogen containing heterocyclic compounds such as pyrrole^[17], indole^[18], phenazine, acridine^[19] and pyridine^[20] have been known to π -coordinate to transition metals such as Mn, Fe and Cr. π -Bonded indole complexes, including N-protected versions^[21], have been reported. These complexes involved η^6 -coordination of the heterocycle and were found to promote regioselective nucleophilic substitution or addition reactions or metallation at the indole six-membered ring. These reactions are of considerable interest because of their potential application in the synthesis of natural products based on the indole structure. Few syntheses of metal complexes involving π -coordination of the anionic indolyl ligand are known in literature^[22]. Chen *et al*^[23] described the deprotonation of an η^6 -indole derivative of Ir(III) which resulted in a ring shift isomerization to an η^5 -indolyl complex (figure 2.3). Reactivity studies of these complexes have not yet been done.

The η^5 -coordination of indolyl to a metal has the potential for activating the pyrrolic ring to ringopening or reduction reactions. This could be important processes in the commercial hydrodenitrogenation reactions catalyzed by heterogeneous metal catalysts^[24].

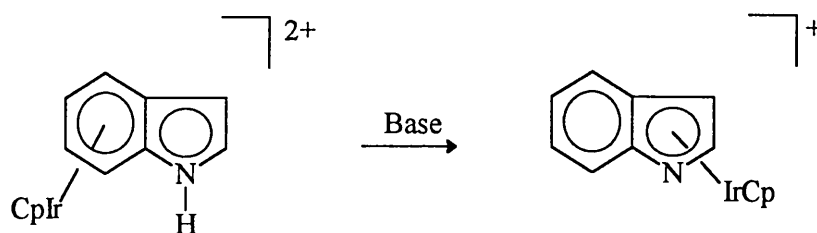


Figure 2.3 Ring shift isomerization

The synthesis and characterization of related sandwich complexes of (cymene)Ru(II) containing the indole and indolyl ligands were also reported.

The number of examples of η^6 -coordinated pyridine complexes^[25] are limited. A few substituted η^6 -pyridine^{[26],[27],[28],[29]} and 1,2-dihydropyridine tricarbonylchromium^{[30],[31],[32]} complexes have been prepared, although generally in low yield. Owing to the lack of a feasible synthetic method, η^6 -pyridinetricarbonylchromium chemistry is not well studied. The σ -coordination *via* the lone pair on the nitrogen is highly preferred over bonding which utilizes the π -electron system. Direct synthesis of η^6 -pyridine metal complexes requires the nitrogen atom to be blocked by means of substitution in the 2,6-positions^[33]. Davies^[34] proposed the synthesis of η^6 -pyridinetricarbonylchromium *via* the use of removable trimethylsilyl groups. These steric groups prevented the coordination of the chromium fragment to the nitrogen lone pair^[35]. Lithiation and subsequent nucleophilic addition of the trimethylsilyl groups occurred at the 2-position of η^6 -pyridinetricarbonylchromium.

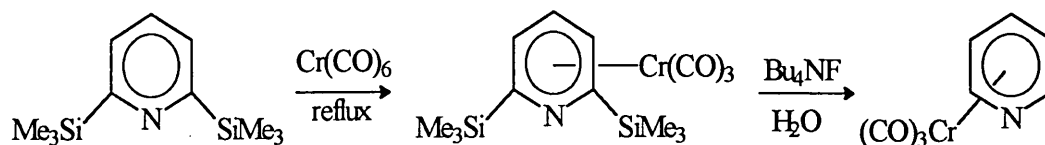
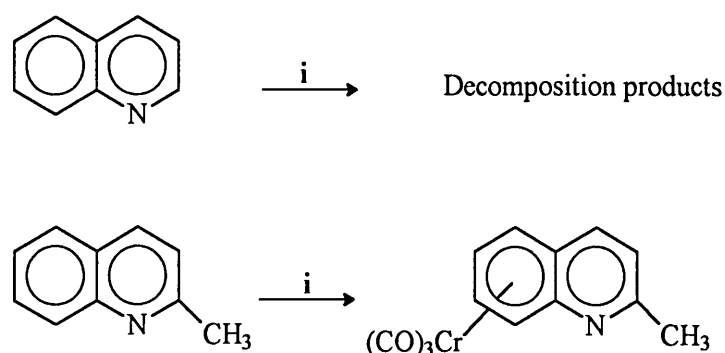


Figure 2.4 Synthesis of η^6 -pyridinetricarbonylchromium

When Fischer *et al*^[8] attempted to synthesize the π -complexes of the nitrogen heterocycles, all their efforts were unsuccessful. Only complexes containing three fused aromatic rings could be π -coordinated to a tricarbonylchromium moiety, e.g. benzoquinoline and carbazole. Öfele^[36] reported the synthesis of the π -complexes of N-methyl-dihydroquinoline and N-methyl-dihydroisoquinoline, by treating the ligands with $(\text{CH}_3\text{CN})_3\text{Cr}(\text{CO})_3$. Goti and Semmelhack^[37] examined the reaction between quinoline and $(\eta^5\text{-1-methylpyrrole})\text{tricarbonylchromium}$. The idea was to synthesize $(\eta^6\text{-quinoline})\text{tricarbonylchromium}$ by arene displacement from the methylpyrrole complex. This venture was unsuccessful. The reaction, either in ethyl acetate or dichloromethane, gave a rapid colour change from yellow to red, indicating the displacement of the ligand, but only decomposition products could be isolated. The same reaction using quinaldine, however, succeeded.



Reagent: (i) $(\eta^5\text{-1-methylpyrrole})\text{tricarbonylchromium}$

Figure 2.5 Substitution reactions of quinoline and quinaldine

In literature, the only π -coordinated phenazine compound that exists is the $(\eta^4\text{-phenazine})\text{-tricarbonyliron}(0)$ complex^[38]. The π -coordination of the tricarbonyliron fragment to the arene ring differs from arene complexes that contain tricarbonylchromium π -bonds. While the chromium complexes need six π -electrons for coordination to the arene, the iron complex accomplishes this with only four π -electrons. It was also suggested that the chromiumtricarbonyl group bonds exclusively to terminal rings, but angular annulated rings are still favoured. At the time of publication of this article, only one tricarbonylchromium complex was known, in which the metal is bonded to a linear annulated ring, *i.e.* $(\eta^6\text{-anthracene})\text{tricarbonylchromium}$. Also, no

tricarbonylchromium complex of a pyridine- or a pyrazine system was known at that stage. Quinoline was therefore chosen as ligand and the possible π -coordination to a $\text{Cr}(\text{CO})_3$ -fragment and the resulting activation of the coordinated quinoline ring was investigated.

2.2 New π -heteroarene complexes of chromium

2.2.1 Thiophene derivatives

The investigation of the synthesis and properties of thiophene oligomers^[39] promoted the study of substituted thieno[3,2-*b*]thiophenes: 3,6-Dimethylthieno[3,2-*b*]thiophene was synthesized and characterized^[40] in order to prepare oligomers of this compound. The π -coordination of this compound was envisaged and proceeded by the addition of $\text{Cr}(\text{NH}_3)_3(\text{CO})_3$, a known literature method for the π -coordination of thiophene to a chromium moiety. The σ, π -bimetallic complex, **1**, was isolated in quantitative yield, but the isolation and characterization was hampered by its instability in solution.

The π -coordination of this ligand to a $\text{Cr}(\text{CO})_3$ -moiety (figure 2.6), made the lone pair of the sulphur atom on the uncoordinated fragment accessible for σ -bonding to a second Cr-fragment, due to the disruption of the aromaticity of the coordinated ring. However, the molecule is not rigid and spectroscopic evidence seems to indicate that the π -metal fragment migrates between the two rings. When the π -bond shifts to the ring containing the σ -bonded $\text{Cr}(\text{CO})_5$ -fragment, the Cr-S bond is weakened and the pentacarbonyl-moiety is discarded. This fluxionality is probably the reason and the driving force for the instability of compound **1**. No product could be isolated with the 3,6-dimethylthieno[3,2-*b*]thiophene ligand coordinated only through the sulphur to a $\text{Cr}(\text{CO})_5$ -fragment. It was observed that, owing to the involvement of the electrons of the sulphur atom in the aromaticity of the ring, these lone pairs are not accessible for bonding to a metal fragment. This observation was made for both the 3,6-dimethylthieno[3,2-*b*]thiophene ligand as well as the thiophene ligand. However, when one of the rings of the 3,6-dimethylthieno[3,2-*b*]thiophene ligand was coordinated to a $\text{Cr}(\text{CO})_3$ -moiety, the sulphur on the second ring was σ -coordinated to a second Cr fragment. Therefore it was concluded that the π -coordination to a $\text{Cr}(\text{CO})_3$ -fragment of one of the rings is prerequisite for the coordination through the sulphur of

the second ring.

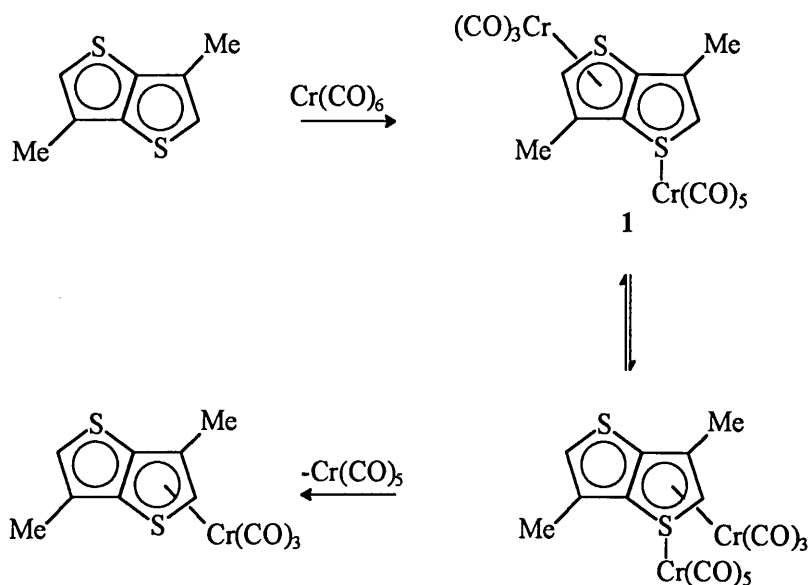


Figure 2.6 Synthesis and decomposition of compound 1

2.2.2 Synthesis of the nitrogen-containing π -heteroarene complexes

The synthesis of π -coordinated nitrogen containing arene complexes remains problematic owing to the lability of the nitrogen containing ring and the strong, competitive coordination properties of the nitrogen atom. Several routes were implemented to try and synthesize the aspired complexes.

(i) Protonation of quinoline

It was decided to protonate quinoline with the use of trifluoroacetic acid. This would result in the blocking of the accessible lone pairs of the nitrogen atom by a proton and the formation of a trifluoroacetate quinoline salt. The salt would then be used to form the π -coordinated tricarbonylchromium complex by dissolving it in a suitable solvent, adding chromiumhexacarbonyl and refluxing the mixture in dibutyl ether. The last step would involve the deprotonation of the π -coordinated quinoline salt to obtain the desired $(\eta^6\text{-quinoline})\text{Cr}(\text{CO})_3$ complex.

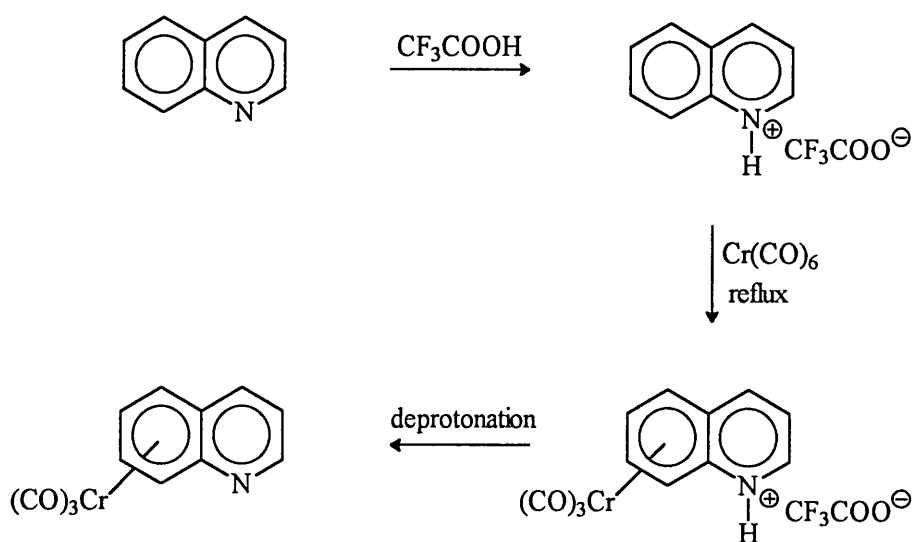


Figure 2.7 Intended synthesis of $(\eta^6\text{-quinoline})\text{Cr}(\text{CO})_3$

Quinoline was protonated using trifluoroacetic acid, according to a literature procedure proposed by Smith^[41] for the protonation of pyridine. The resulting salt was dissolved in THF, chromiumhexacarbonyl was added and the mixture was refluxed in dibutyl ether. The product was a dark-brown, viscous solid which was insoluble in water as well as hexane, but dissolved in ether. Since quinoline has a pK_b value of 9.10, it was necessary to use a stronger base to deprotonate it. Several bases were ventured, with pK_b values ranging from 2.99 (triethylamine) to 8.75 (pyridine). All attempts to deprotonate the complex were unfortunately unsuccessful in that either decomposition occurred or the strength of the base was inadequate to deprotonate the complex.

(ii) Attempted synthesis of $(\eta^6\text{-quinoline})\text{Cr}(\text{CO})_3$ *via* silylation at the 2-position

It was envisaged to synthesize $(\eta^6\text{-quinoline})\text{Cr}(\text{CO})_3$ *via* the use of a removable trimethylsilyl (TMS) group to prevent coordination to the nitrogen lone pair^[34] due to steric hinderance. After π -coordination to chromiumtricarbonyl, the TMS group could then be removed under mild conditions with aqueous tetrabutylammonium fluoride^[42] to generate the target complex $(\eta^6\text{-quinoline})\text{Cr}(\text{CO})_3$ (figure 2.8).

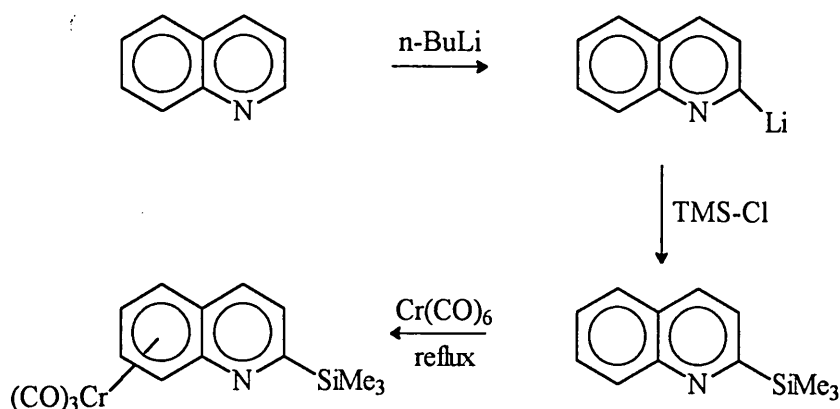


Figure 2.8 Intended synthesis of $(\eta^6\text{-2-trimethylsilylquinoline})\text{Cr(CO)}_3$

Quinoline was lithiated according to a literature method proposed by Beswick *et al.*⁴³¹ for the lithiation of indole. Chlorotrimethylsilane was added after which the reaction mixture was refluxed in dibutyl ether in the presence of chromiumhexacarbonyl. Two products, **2** and **3**, were isolated after purification of which, after characterization, neither resembled the target product, $(\eta^6\text{-2-trimethylsilylquinoline})\text{Cr(CO)}_3$. It was thus obvious that lithiation did not occur at the 2-position but that nucleophilic addition of the butyl group ensued (figure 2.9).

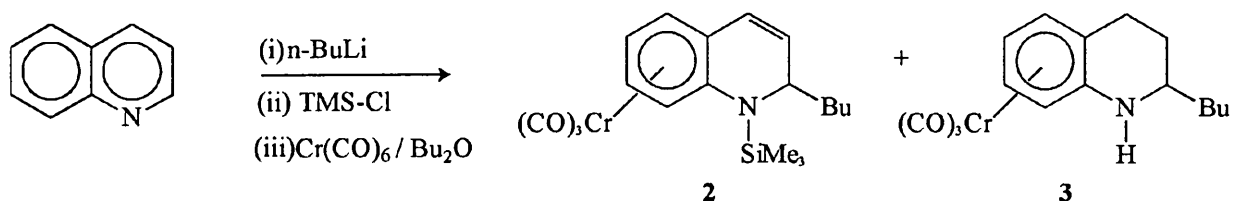


Figure 2.9 Synthesis of compounds **2** and **3**

(iii) Synthesis of $(\eta^6\text{-phenazine})\text{Cr(CO)}_3$

The attempt to synthesize the π -coordinated complex of phenazine to a Cr(CO)_3 -moiety proved to be more successful and, although the complex was obtained in a low yield, the complex was more stable than the thiophene analogue. Spectroscopic characterization revealed that only one

of the benzene rings was coordinated to a metal fragment.

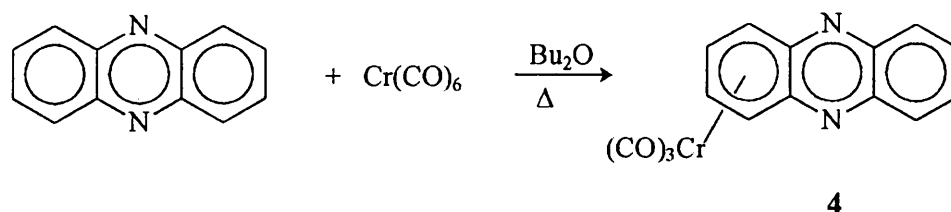
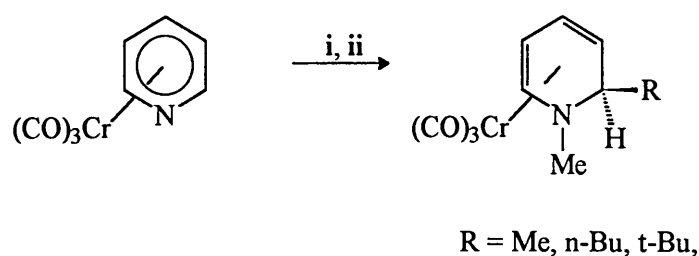


Figure 2.10 Synthesis of compound 4

2.3 Nucleophilic addition reactions

In literature several examples of pyridine complexes are known in which nucleophilic addition had occurred, but in most cases the pyridine ring was already π -coordinated to a tricarbonylchromium moiety^[34]. The metal fragment seems to play an important role in activating the arene ring. The electron withdrawing effect that the tricarbonylchromium moiety has, makes the pyridine ring susceptible to nucleophilic addition reactions^[44]. Treatment of (η^6 -pyridine)tricarbonylchromium with a range of alkyllithium reagents results in the addition of the nucleophile to the most electrophilic carbon and, after subsequent quenching with methyl iodide, the formation of (N-methyl *exo*-2-alkyl-1,2-dihydropyridine)tricarbonylchromium.



Reagents and conditions: i. RLi, THF, -78°C
 ii. MeI

Figure 2.11 Nucleophilic addition to (η^6 -pyridine)tricarbonylchromium

In 1931 Ziegler and Zeiser^[45] reported the reaction between n-butyllithium and pyridine, where n-butyllithium adds to pyridine with subsequent elimination of lithium hydride to yield 2-

butylpyridine. Consequently several reactions of this type between aromatic heterocyclic compounds and organometallic reagents of e.g. lithium and magnesium^[46] were reported.

Nucleophilic substitution of hydrogen in pyridines may proceed *via* an addition-elimination mechanism in which σ -complexes are formed. Ziegler and Zeiser noticed that a precipitate was formed when pyridine was heated together with alkyl or aryl lithium compounds. This precipitate was identified as lithium hydride, while the major product formed was the corresponding 2-substituted alkyl or aryl-pyridine. The intermediate was suggested to exhibit the structure shown in figure 2.12, where R = alkyl or aryl.

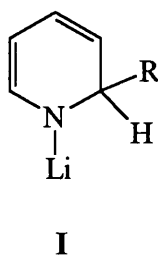


Figure 2.12 Suggested intermediate structure

This structure was supported by the observation that the addition of water to the intermediate **I** yielded the corresponding 1,2-dihydropyridine. This nucleophilic addition reaction was also employed using quinoline, isoquinoline and acridine, obtaining similar results^[48].

In all cases surveyed, it was interesting to note that addition occurred only at the 2-position. This was also the case for quinoline. In 1971 Otsuji *et al*^[47] suggested that the 2-substitution of quinolines by organolithium reagents proceeds by initial C(4) addition followed by sigmatropic rearrangement of the substituent to C(2). Scopes and Joule^[48] invalidated this proposal. Considering the π -electron densities of quinoline, obtained through HMO calculations^[49], it is obvious that the 2- and 4-positions are favoured for nucleophilic attack. Alkyl lithium, Grignard compounds, hydroxide ion and borohydride ion all react to form 2-substituted products. However, other nucleophiles including cyanide ion and hydride ion yield 4-substituted products.

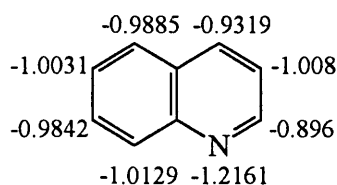


Figure 2.13 π -Electron densities of quinoline

The formation of compound **2** can be explained by examining analogous cases known in literature. Fraenkel and Cooper^[50] described the hydrolysis of the intermediate **I** with degassed D_2O to yield 1-deutero-2-butyldihydropyridine. Compound **II** could be a possible byproduct, formed during the reaction to yield **2**. After the addition of chlorotrimethylsilane and the formation of **2**, the unreacted quinoline analogue of intermediate **I** formed lithium hydride and the 2-substituted quinoline, **II**, could have resulted upon heating. This reaction is comparable with the results Ziegler *et al*^[45] obtained in the reaction of pyridine with a lithium compound. The mechanism for the synthesis of compounds **2** and **II** is set out in figure 2.14. Compound **II** was, unfortunately, not formed during the reaction, but instead compound **3**, a tetrahydroquinoline complex, was isolated. The structure of both compounds **2** and **3** were confirmed with X-ray diffraction studies.

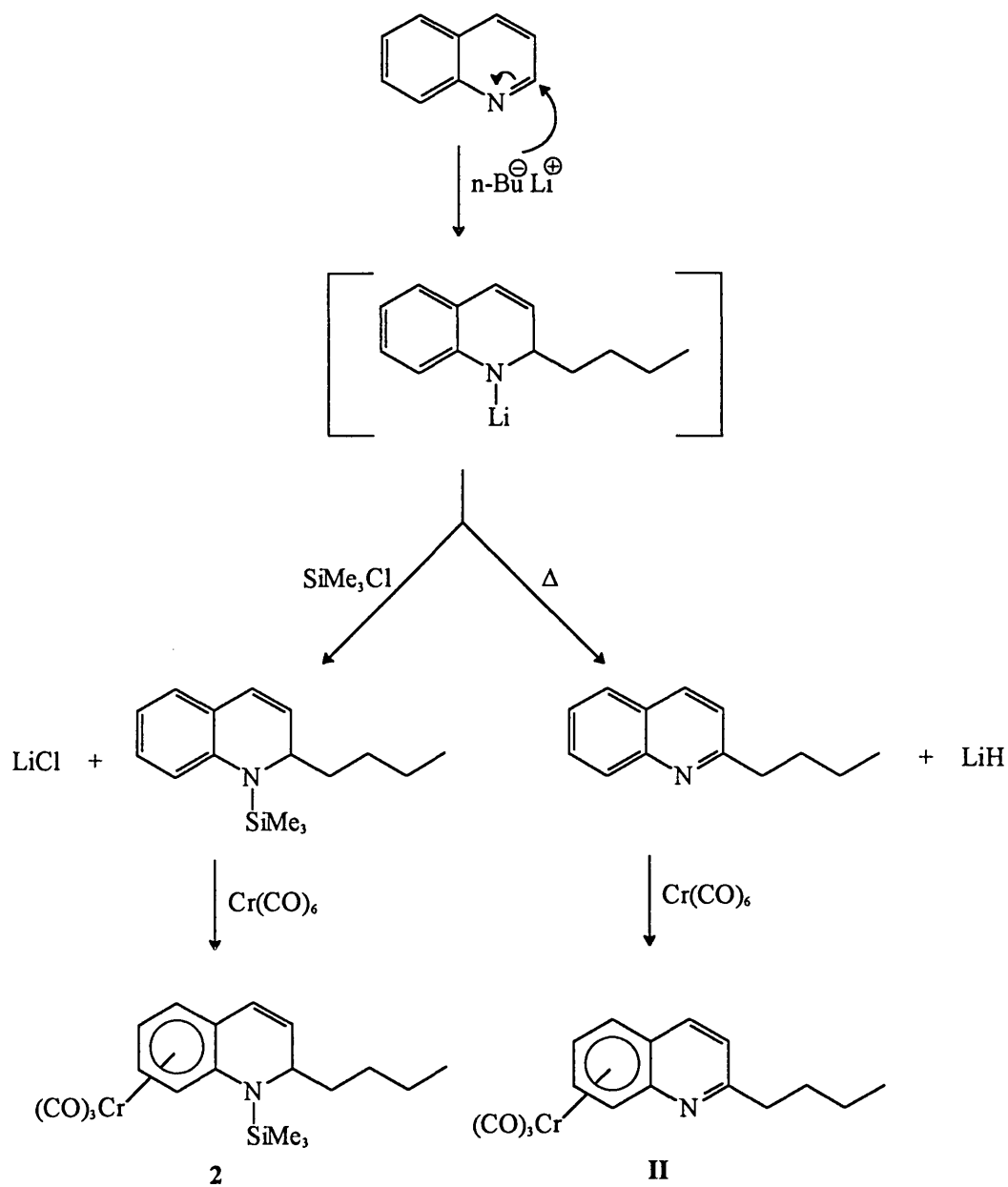


Figure 2.14 Synthesis of compounds **2** and **II**

It is anticipated that compound **2** will react with H_2O or silica gel to displace the TMS-fragment during column chromatography to afford **III** (figure 2.15).

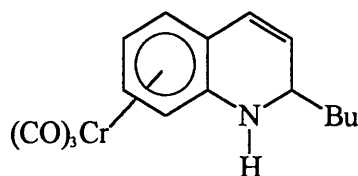


Figure 2.15 Compound III

However, the reason for the saturation of the double bond between C(3) and C(4) in compound 3 as well as the source of hydrogen atoms are still unclear. A literature survey was performed to try and explain the role the Cr metal fragment plays as well as the observed reactivity of the olefinic moiety under the recounted reaction conditions. Relevant studies have been performed by Murahashi *et al*^[51] where quinolines were selectively hydrogenated to yield 1,2,3,4-tetrahydroquinolines, using transition metal carbonyl compounds as catalysts for the reaction. Their reaction conditions, however, differed radically from the procedure employed in this study. The reaction was performed in a CO atmosphere in the presence of water.

2.4 Conclusion

From the results obtained, certain deductions can be made. Theoretically the protonation of quinoline is a novel synthetic route. However, the insolubility of the protonated product causes practical problems. It seems as if this method is not the solution to the coordination of quinoline to a metal fragment. Synthesis *via* the use of a steric group proved to be equally unsuccessful. The observed nucleophilic addition during the reaction with the blocking reagent, TMS-Cl, complicates the situation unnecessarily. The products obtained, although π -coordinated to a metal moiety, are no longer aromatic. Perhaps the use of a different base, e.g. NaH, in stead of *n*-butyllithium could improve matters.

For further studies on this system the following synthetic route is suggested: (a) Addition of a steric group, e.g. TMS-Cl, at the nitrogen atom to block the accessible lone pairs, (b) π -coordination to a metal fragment, (c) removal of the steric group with the use of

tetrabutylammoniumfluoride or even column chromatography on silica gel (figure 2.16).

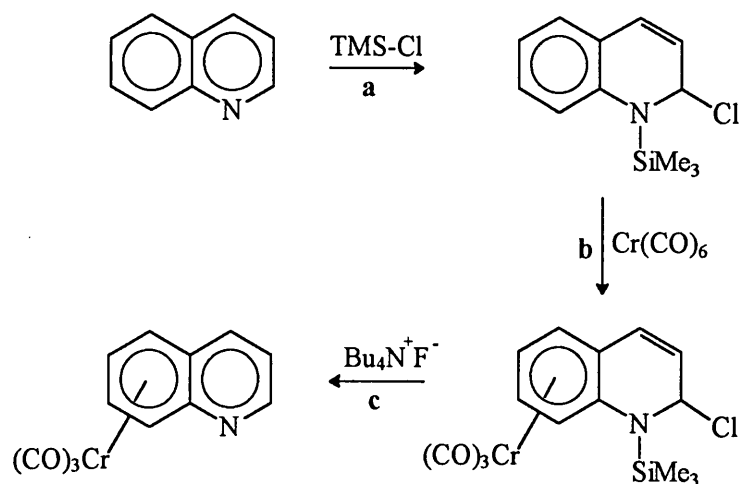


Figure 2.16 Suggested synthesis of $(\eta^6\text{-quinoline})\text{Cr}(\text{CO})_3$

2.5 Spectroscopic characterization

2.5.1 Infrared Spectroscopy

When a carbonyl is coordinated to a transition metal, the molecule undergoes certain electronic changes. The transition metal-CO bond of a terminal carbonyl ligand is described as a resonance hybrid and the bond orders for the M-C bond and the C-O bond are determined by the electronic properties of the metal and other ligands in the compound. As shown in figure 2.17, it is clear that the bond order for the M-C bond can be either 1 (a) or 2 (b) and the bond order for the C-O bond varies accordingly from 2 (b) to 3 (a).

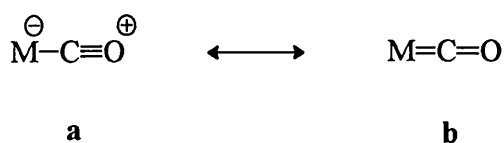


Figure 2.17 Resonance structures for the M-CO bond

A synergic bonding effect is observed when carbonyls coordinate to transition metals. The carbonyl ligand donates electron density to the metal *via* a σ -donor interaction. The metal, in return, can donate electron density to the carbonyl *via* π -interaction (backbonding). The magnitude of the backbonding depends on the nature of the transition metal. It is obvious that backbonding will play a decisive role where late transition metals are concerned, since the electron density on these metals are considerably higher than for early transition metals. A correlation between CO stretching vibrational frequencies and the bond order of the C-O bond can be made^[52], since C-O stretching vibrational frequencies can be regarded as being independent from other vibrations in the molecule.

As backbonding from the metal to the carbonyl ligand increases, the M-C bond becomes stronger and thus shorter. The C-O bond weakens accordingly and the C-O bond length increases. This increase in bond order of the M-C bond should prompt the carbonyl stretching frequency to shift to a lower wavenumber on the IR spectrum. Thus, a decrease in wavenumbers in the carbonyl region on replacing one arene ligand for another in $(\pi\text{-arene})\text{Cr}(\text{CO})_3$ complexes will correspond to an increase in electron density on the arene ring.

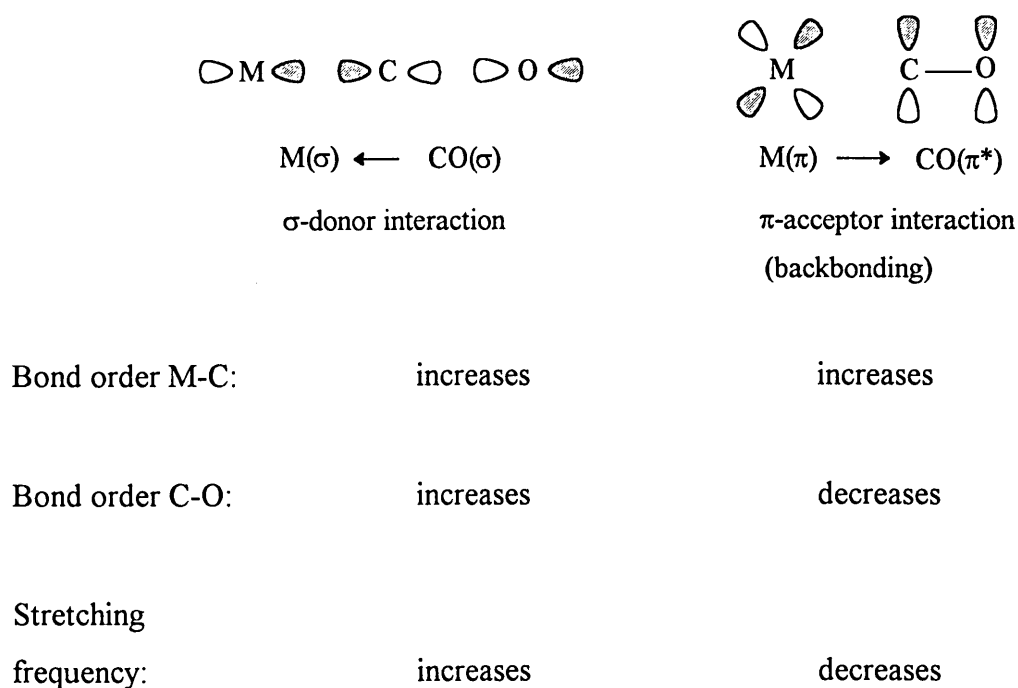


Figure 2.18 Synergic bonding effect of carbonyl ligands

The number and intensities of carbonyl stretching frequencies are dependent on the local symmetry of the carbonyl ligands around the central atom. Since complexes of the general composition $ML_3(CO)_3$ belong to the symmetry group C_{3v} , two IR-active bands are observed on the spectrum, the A_1 and the E vibrational bands. The first, sharp A_1 band is observed at higher wavenumbers than the stronger E band and is associated with the symmetrical stretching vibrations while the E band, at lower wavenumbers, is associated with the unsymmetrical stretching vibrations in the molecule. Aspects related to the pentacarbonyl fragment will be discussed in Chapter 4.

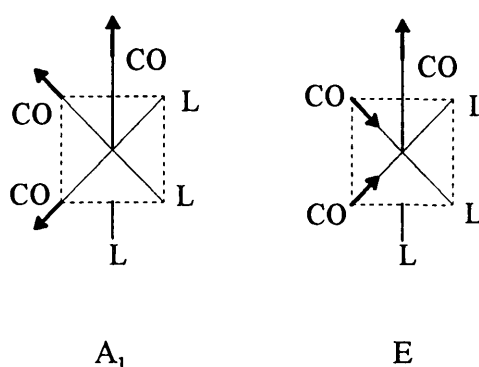


Figure 2.19 Stretching vibrations of $M(CO)_3L_3$

All IR spectra were recorded in dichloromethane, unless stated otherwise. The spectrum of compound **3** is represented in figure 2.20. The A_1 and the E bands can be easily distinguished on the spectrum.

The wavenumbers of the carbonyl bands for compounds **1-4** lie between 1863 and 2080 cm^{-1} , which indicates the presence of terminal carbonyl groups only. The stretching frequencies and the pattern of absorption show that a $Cr(CO)_5$ -moiety is present in compound **1**, while all four compounds contain a $Cr(CO)_3$ -fragment. Because of overlap of the pentacarbonyl- and the tricarbonyl moieties in compound **1**, it was impossible to unambiguously allocate a specific wavenumber to the $A_1^{(2)}$ band of the $Cr(CO)_3$ -fragment. Another problem experienced during the recording of the spectra is the low solubility of some of the compounds in hexane. An interesting observation in the spectrum of compound **2** is that the degeneracy of the E band (A' , A'') is lifted and two separate bands can be distinguished. This phenomenon can possibly be ascribed to the

nature of the quinoline ring and the presence of the heteroatom, which influences the backbonding to the carbonyls to such an extent that it leads to the splitting of the E band.

Table 2.1 IR-data of compounds 1, 2, 3 and 4

π -Arene complex	Carbonyl vibrating frequencies (cm^{-1} , CH_2Cl_2)				
	$\text{Cr}(\text{CO})_3$		$\text{Cr}(\text{CO})_5$		
	A_1	E	$A_1^{(1)}$	E	$A_1^{(2)}$
1	1949s	1885s	2067w	1970vs	1949s ^b
2	1952s 1965s ^a	1870s 1899s ^a , 1890s ^a	-	-	-
3	1950s 1963s ^a	1862s 1889s ^a	-	-	-
4	1951s	1867s	-	-	-

^a Spectra recorded in hexane

^b Observed as a shoulder

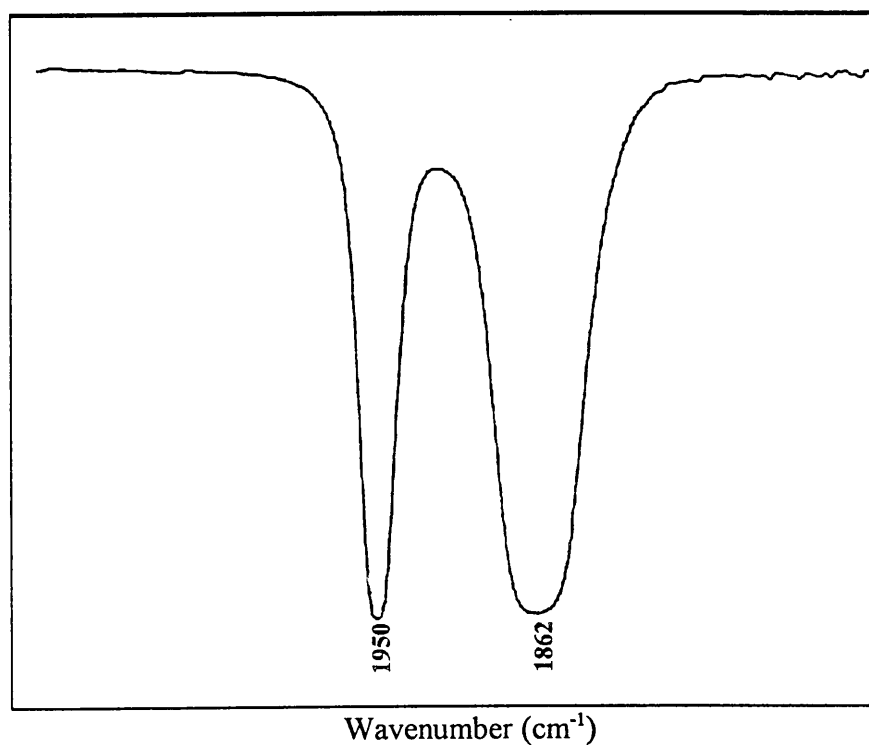


Figure 2.20. Carbonyl region on the infrared spectrum of compound 3

Within experimental error, the A_1 bands of complexes 1-4 are the same, but the complexes with nitrogen-containing arene ligands are observed at slightly lower wavenumbers than that of the coordinated thiophene ring. Coordination *via* a sulphur atom of the adjacent thiophene ring and the different types of arene ligands i.e. benzene vs thiophene, account for this small difference.

2.5.2 NMR Spectroscopy

Coordination of an organic substrate to a metal moiety affects the resonances of the nuclei in a characteristic way and valuable information is obtained concerning composition, structure and chemical environment of the ligand in the complex. π -Coordination of an arene ring to a $\text{Cr}(\text{CO})_3$ fragment leads to the localization of the double bonds and the disruption of the aromaticity of the ring. The ring current, the induced magnetic lines of force that result from the flow of charge, is destroyed and the result is an upfield chemical shift on the NMR spectrum. π -Electron density is withdrawn from the ring, enhancing shielding of the ring protons, thus explaining the upfield chemical shift. The reactivity and aromaticity of heteroaromatic compounds can be studied by nuclear resonance spectroscopy by measuring the chemical shifts and coupling constants of the arene protons and carbons.

All NMR spectra were recorded in CDCl_3 , unless stated otherwise. The ^{13}C spectra were recorded at -20°C in order to improve the resolution and to delay decomposition of the complexes. The spectra of compound 1 was recorded at -40°C because of the low stability of this complex. The following system of numbering the protons and carbon atoms of the individual compounds will be used throughout the whole discussion.

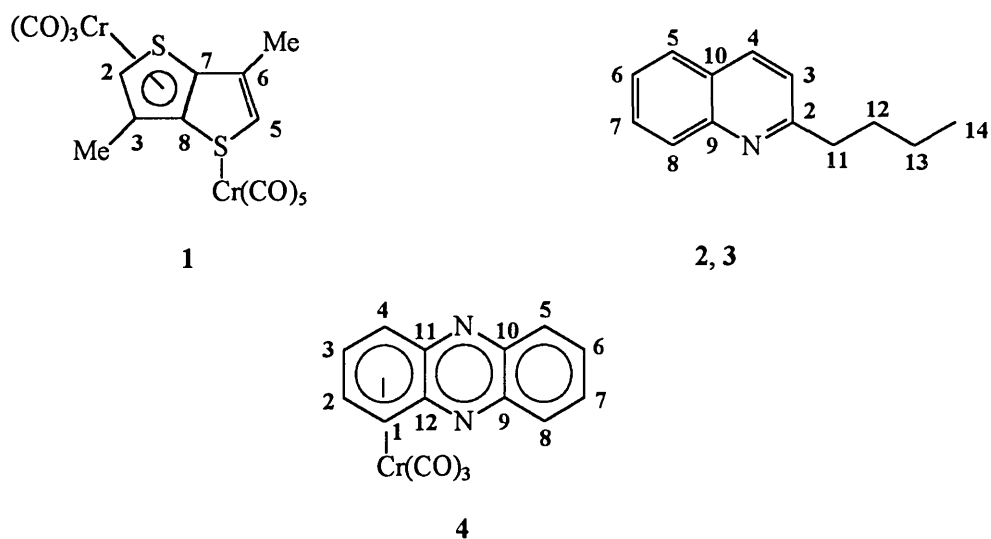


Figure 2.21 Atom labelling in the individual complexes

^1H NMR Spectroscopy

The ^1H NMR data of complexes 1, 2, 3 and 4 are summarized in table 2.3, while the data of the uncoordinated ligands are summarized in table 2.2, for comparison.

Table 2.2 ^1H NMR data of the uncoordinated ligands^a

Assignment	Ligands					
	Chemical shifts (δ , ppm) and coupling constants (J, Hz)					
	3,6-Dimethylthieno[3,2- <i>b</i>]thiophene		Quinoline ^b		Phenazine ^b	
Proton	δ	$^3J_{\text{H-H}}$	δ	$^3J_{\text{H-H}}$	δ	$^3J_{\text{H-H}}$
H1	-	-	-	-	8.23 (m)	8.9
H2	6.92 (m)	-	8.90 (dd)	4.2	7.93 (m)	6.7 8.9
H3	-	-	7.47 (dd)	8.3 4.2	7.93 (m)	6.7 8.9
H4	-	-	8.28 (dd)	8.2	8.23 (m)	8.9
H5	6.92 (m)	-	8.07 (d)	8.2	8.23 (m)	8.9
H6	-	-	7.74 (ddd)	8.5 7.0	7.93 (m)	6.7 8.9
H7	-	-	7.57 (ddd)	8.2 6.8	7.93 (m)	6.7 8.9
H8	-	-	7.92 (dd)	8.2	8.23 (m)	8.9
C-Me	2.33 (s)	-	-	-	-	-

^a Assignment based on literature values: 3,6-dimethylthieno[3,2-*b*]thiophene^[40], quinoline^[53], phenazine^[19]

^b Spectrum was recorded in deuterated acetone as solvent

Table 2.3 ^1H NMR data of complexes 1, 2, 3 and 4

Assignment	Complexes							
	Chemical shifts (δ , ppm) and coupling constants (J, Hz)							
	1		2		3		4 ^a	
Proton	δ	$^3J_{\text{H-H}}$	δ	$^3J_{\text{H-H}}$	δ	$^3J_{\text{H-H}}$	δ	$^3J_{\text{H-H}}$
H1	-	-	-	-	3.50 (s)	-	5.06 (m)	-
H2	5.36 (s)	-	3.85 (dt)	9.7 5.4	3.12 (m)	-	5.01 (m)	-
H3	-	-	5.94 (dd)	9.8 9.8	H _{ax} 12.4 1.72 4.3 (dddd) 12.4 H _{eq} 1.98 (dddd)		5.01 (m)	-
H4	-	-	6.05 (d)	9.9	H _{ax} 11.8 2.65 4.5 (ddd) H _{eq} 3.7 2.42 3.7 (ddd)		5.06 (m)	-
H5	7.24 (s)	-	5.21 (m)	-	4.68 (d)	6.8	6.53 (m)	-
H6	-	-	5.01 (dd)	6.8 6.6	4.72 (t)	6.2	6.30 (m)	-
H7	-	-	5.01 (dd)	6.8 6.6	5.42 (t)	6.4	6.30 (m)	-
H8	-	-	5.21 (m)	-	5.53 (d)	6.2	6.53 (m)	-

Assignment	Complexes							
	Chemical shifts (δ , ppm) and coupling constants (J, Hz)							
	1		2		3		4 ^a	
Proton	δ	$^3J_{\text{H-H}}$	δ	$^3J_{\text{H-H}}$	δ	$^3J_{\text{H-H}}$	δ	$^3J_{\text{H-H}}$
C-Me	2.33 (m)	-	-	-	-	-	-	-
H11	-	-	1.25 -	-	1.24 -	-	-	-
H12			1.45		1.53			
H13			(m)		(m)			
H14	-	-	0.91 (t)	7.0	0.91 (t)	7.0	-	-
SiMe ₃	-	-	0.34 (s)	-	-	-	-	-

^a Spectrum was recorded in deuterated acetone as solvent

Comparing the data of the uncoordinated compounds (table 2.2) with the data of the compounds containing a π -bonded $\text{Cr}(\text{CO})_3$ -moiety, it is evident that the π -coordination of an arene ligand to a transition metal, has a significant influence on the ring protons. Complex formation leads to shielding of the ring protons of about 2-3 ppm. This effect is reflected in the profound difference in chemical shift values. The chemical shifts of the protons on rings that contain a $\text{Cr}(\text{CO})_3$ -fragment are observed at lower ppm values than the corresponding protons in uncoordinated complexes. The π -coordination of the ligands to $\text{Cr}(\text{CO})_3$ leads to the localization of the double bonds and a loss of aromaticity and ring current of the arene ligand.

On the spectrum of compound 1, two singlets are distinguished for the ring protons. It is obvious that one of the rings is π -coordinated, while the other one remains uncoordinated. This deduction can be made on comparing the chemical shift values with those of the uncoordinated ligand. The upfield shift of the one proton is the result of the π -coordination to a $\text{Cr}(\text{CO})_3$ -moiety, while the downfield shift arises from the σ -coordination to a $\text{Cr}(\text{CO})_5$ -fragment. The methyl protons are observed as a multiplet at 2.33 ppm. Since the spectrum was recorded at -40°C , the restricted rotation around the C-Me bond results in line broadening and a multiplet signal is observed.

On the ^1H NMR spectrum of compound **3**, the axial and equatorial protons on C(3) and C(4) can be clearly distinguished. In the case of cyclohexane^[54] the difference in chemical shift between the axial and equatorial protons is about 0.5 ppm, and is measured at low temperatures where the rate of chair-chair interconversion is slow. The axial protons are more strongly shielded than the equatorial protons because of magnetic anisotropy. This result can be graphically represented by anisotropic shielding cones (figure 2.22).



Figure 2.22 Anisotropic cone shielding in cyclohexane

Compound **3**, however, does not resemble the cyclohexane structure entirely. Because of the π -coordinated benzene ring and the butyl group which prefers the equatorial position, this molecule is not likely to interconvert as is the case for cyclohexane. The two protons on C(3) protons exhibit a doublet of doublet of doublet of doublet splitting pattern. This splitting pattern is the result of a geminal coupling and three vicinal couplings, one to the equatorial neighbour proton (H4) and two to the axial neighbour protons (H2 and H4). The two protons on C4 exhibit a doublet of doublet of doublet splitting pattern. It is interesting to note here that the equatorial proton is observed at a higher field than the axial proton, which is contradictory to the normal trend, observed in cyclohexanes. The assignments of these protons were based on the different splitting patterns and the coupling constants. It is possible to distinguish between the axial and the equatorial protons on each carbon by considering the magnitude of the coupling constants. Coupling constants to the various protons differ considerably. Usually coupling of one axial proton to another axial proton (J_{aa}) varies from 8 to 13 Hz, while coupling to an equatorial proton (J_{ae}) differs from 2 to 4 Hz. The coupling constant for two equatorial protons (J_{ee}) is smaller, it usually varies from 1 to 3 Hz. The values obtained experimentally were very similar to these literature values. The values of the geminal coupling constants were 12.4 Hz for H3 and 15.9 Hz for H4. It is therefore obvious that an equatorial proton can have only one large coupling, which will be the geminal coupling. All other couplings to an equatorial proton will be much smaller.

Figure 2.23 depicts part of the proton spectrum of compound **3**, illustrating the axial and equatorial protons of H3 and H4.

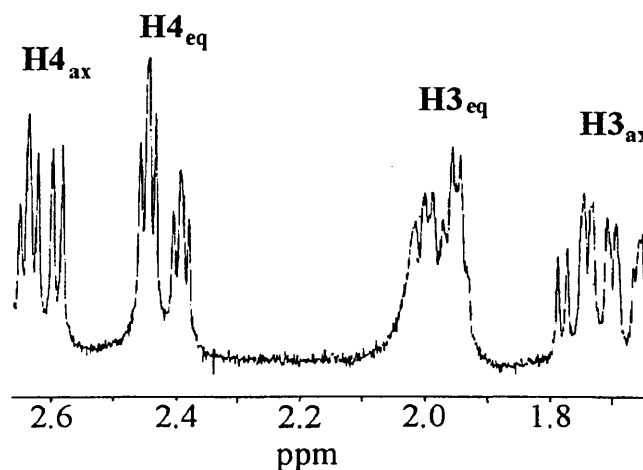


Figure 2.23 Part of the ¹H NMR spectrum of compound **3**

On comparing the chemical shift values of the protons on C(3) and C(4) of compounds **2** and **3**, it is obvious that the two carbon atoms are both sp^2 hybridized in compound **2**, while sp^3 carbons are under discussion in compound **3**. This was also confirmed by conducting a DEPT experiment.

Four multiplet signals are present on the spectrum of compound **4**. The four protons on the π -coordinated benzene ring are observed more upfield than the four protons on the uncoordinated ring. The two upfield signals, representing protons H(1), H(4) and H(2), H(3) respectively, overlap, causing second order effects.

On comparing the chemical shift values of the protons on the coordinated benzene ring of compounds **2**, **3** and **4**, it is observed that the proton closest to the nitrogen atom experiences deshielding and shifts more downfield than the rest of the protons.

^{13}C NMR Spectroscopy

The ^{13}C NMR data of complexes **1**, **2**, **3** and **4** are summarized in table 2.5, while the data of the uncoordinated ligands are given in table 2.4. The chemical shift values of the starting material as well as the information gained from the HETCOR experiment were used to assign the signals.

Table 2.4 ^{13}C NMR data of the uncoordinated ligands^a

Assignment	Ligands		
	Chemical shifts (δ , ppm)		
	3,6-Dimethylthieno[3,2- <i>b</i>]thiophene	Quinoline	Phenazine
Carbon	δ	δ	δ
C1	-	-	130.3
C2	121.8	150.2	129.6
C3	140.0	120.9	129.6
C4	-	135.7	130.3
C5	121.8	127.6	130.3
C6	140.0	126.4	129.6
C7	130.1	129.2	129.6
C8	130.1	129.4	130.3
C9	-	148.3	143.5
C10	-	128.2	143.5
C11	-	-	143.5
C12	-	-	143.5
C-Me	14.6	-	-

^a Assignments based on literature values: 3,6-dimethylthieno[3,2-*b*]thiophene^[40], quinoline^[55], phenazine^[56]

Table 2.5 ^{13}C NMR data of complexes 1, 2, 3 and 4

Assignment	Complexes			
	Chemical shifts (δ , ppm)			
	1	2	3	4
Carbon	δ	δ	δ	δ
C1	-	-	-	89.0
C2	77.2	53.9	51.9	79.9
C3	93.0	122.1	27.4	79.9
C4	-	132.2	26.4	89.0
C5	121.7	91.5	82.3	123.1
C6	128.2	84.6	75.3	114.4
C7	149.4	91.5	95.7	114.4
C8	149.9	92.7	97.9	123.1
C9	-	n.o.	130.6	n.o.
C10	-	n.o.	91.5	n.o.
C11	-	32.6	35.8	n.o.
C12	-	29.7	27.7	n.o.
C13	-	27.4	22.6	-
C14	-	14	13.9	-
CO	233.1	235.2	235.4	237.0
C-Me	22.7 (C3) 14.3 (C6)	-	-	-
SiMe ₃	-	1.2	-	-

Notable differences are observed when comparing the ^{13}C NMR chemical shift values of the uncoordinated ligands with those of the π -coordinated ligands. It is obvious that the benzene ring, where the π -coordination occurs, is more affected than the pyridine or uncoordinated benzene ring fragment, in compounds 2, 3 and 4.

In the spectra of all four compounds the Cr-CO signal is depicted as a singlet, indicating

equivalence of the CO-ligands and signifying free rotation of the $\text{Cr}(\text{CO})_3$ -moiety around the Cr-arene axis. It is also conspicuous to note that the chemical shift of the Cr-CO carbon is very comparable for the different complexes and varies from 231 to 237 ppm.

HETCOR Experiment

To assign the spectra of compounds **3** and **4** unambiguously, a heteronuclear correlated 2D experiment (HETCOR) proved useful. In this experiment one-bond ^1H - ^{13}C couplings are used to show directly which protons are attached to which carbon atoms. In figures 2.24 and 2.25 the HETCOR spectra of these two compounds are represented. The chemical shifts of H (δ_{H}) are stipulated on the y-axis, while the chemical shifts of C (δ_{C}) are introduced on the x-axis.

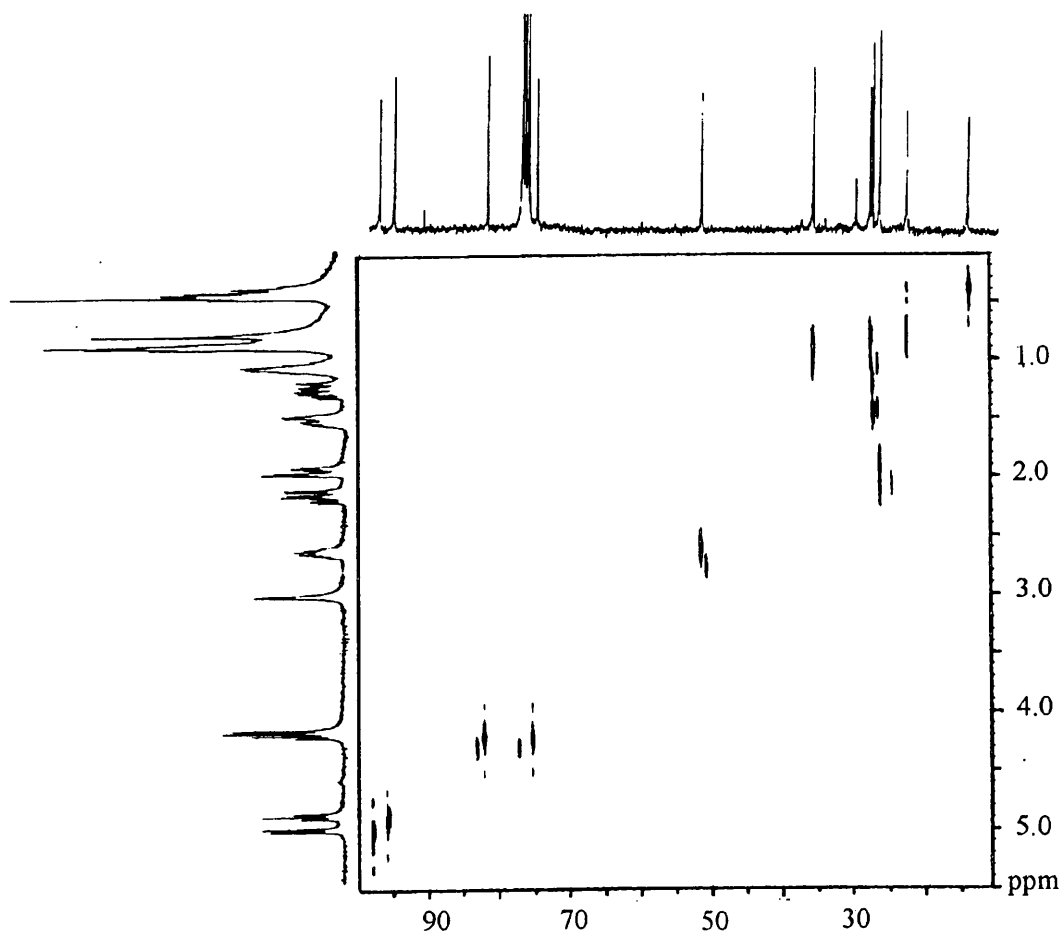


Figure 2.24 HETCOR spectrum of compound **3**

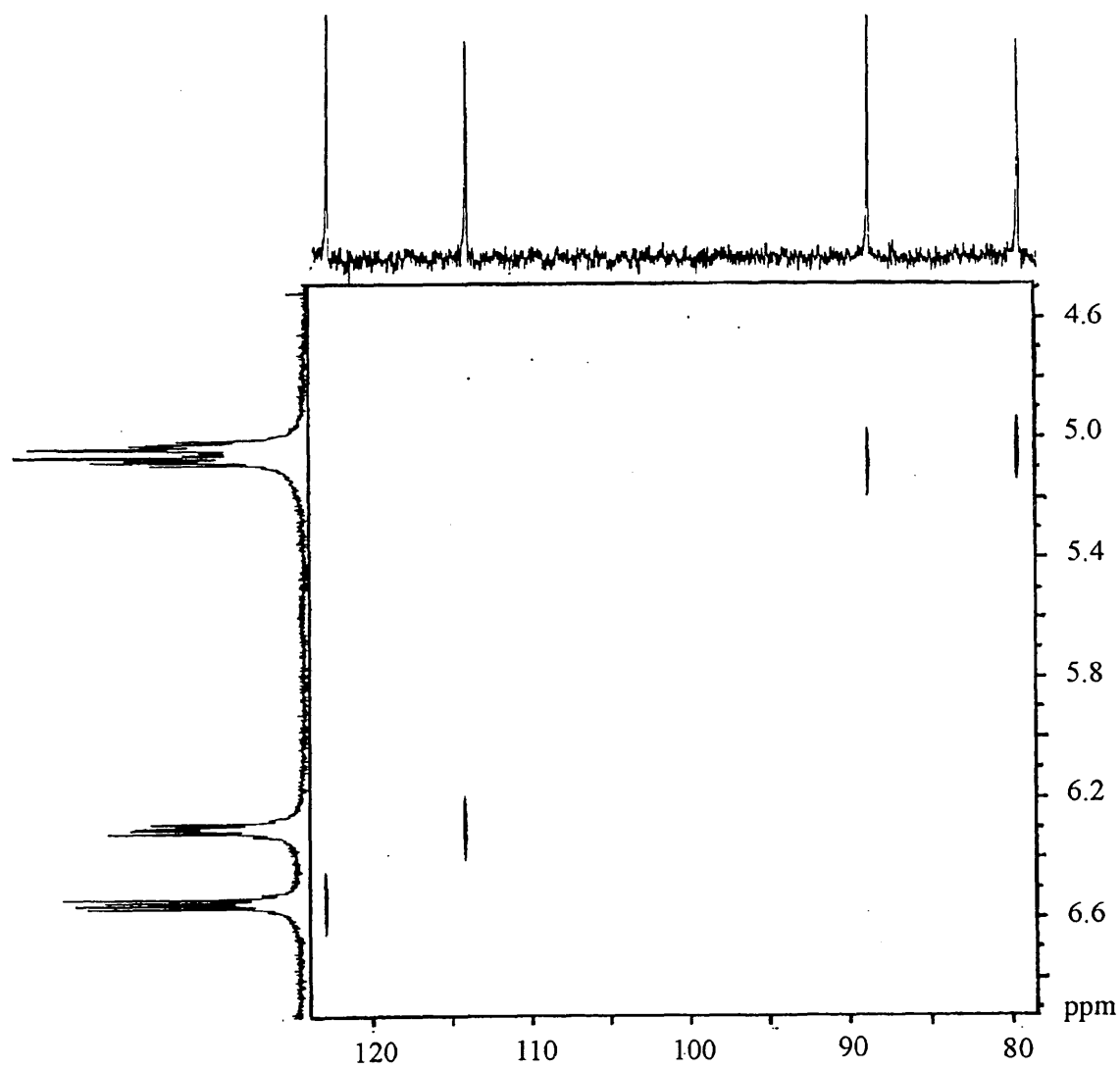


Figure 2.25 HETCOR spectrum of compound 4

DEPT Experiment

In interpreting ^{13}C NMR spectra it is useful to know which signals belong to quaternary, CH, CH_2 and CH_3 carbon nuclei. To distinguish between the different carbon nuclei in the DEPT experiment, the pulse angle can be varied. By recording the spectrum with the variable pulse angle, θ , set to 135° , negative signals are assigned to carbon nuclei in CH and CH_3 groups and positive signals to those in CH_2 groups. Figure 2.26 portrays the DEPT spectrum of compound **3**. It was uncertain if the two carbon atoms C(3) and C(4) were sp^3 or sp^2 hybridized, but by conducting a DEPT experiment this question was answered.

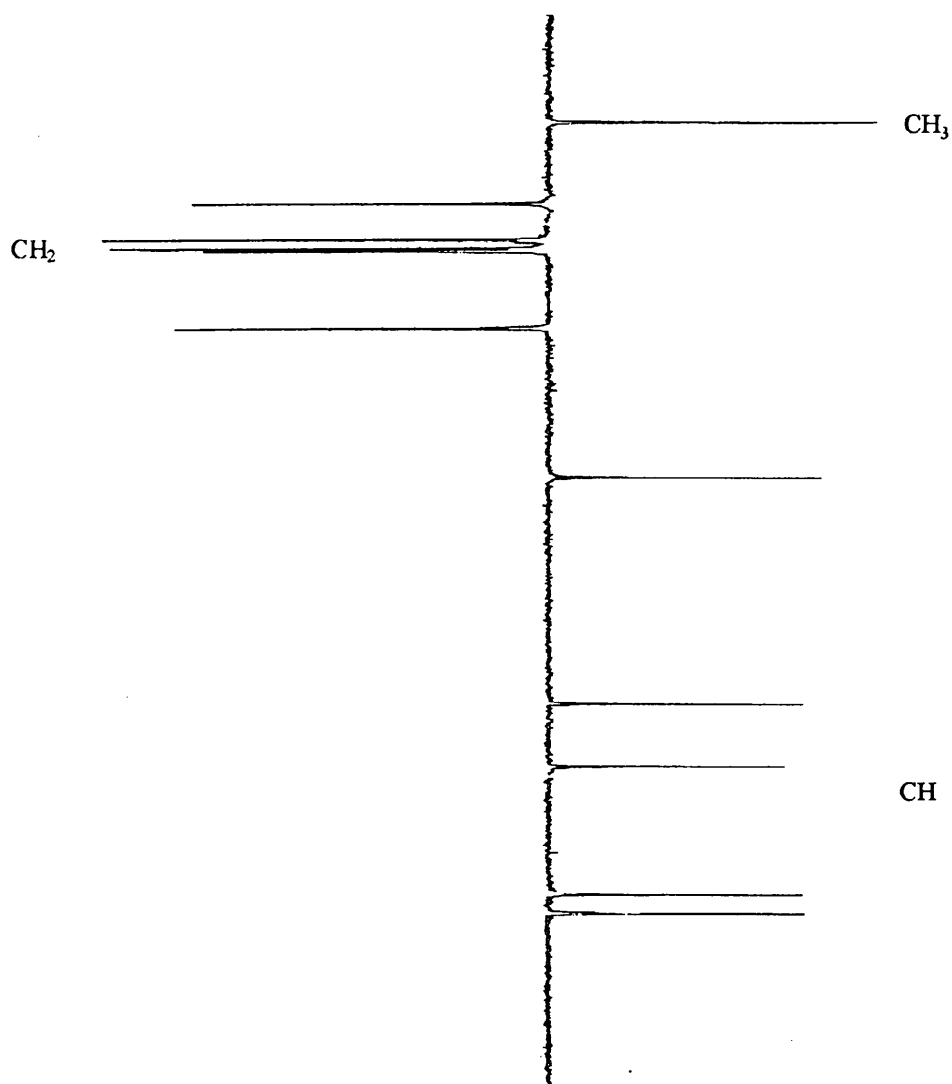


Figure 2.26 DEPT spectrum of compound **3**

2.5.3 Mass Spectrometry

The molecular ion peak was observed for compounds **2**, **3** and **4**. The m/z -values of M^+ and the most important fragment ions are shown in table 2.6. Figure 2.27 represent the mass spectrum of compound **3**.

Table 2.6 Mass spectra data of compounds **2**, **3** and **4**

Complex	Mass peaks, m/z (I, %)
2	395 (20) [M^+], 339 (6) [$M^+ - 2CO$], 311 (100) [$M^+ - 3CO$], 258 (12) [$M^+ - 3CO - Cr$], 202 (53) [$C_{12}H_{16}NSi^+$], 156 (2) [$C_9H_7NSi^+$], 130 (3) [$C_9H_7N^+$]
3	325 (16) [M^+], 269 (10) [$M^+ - 2CO$], 241 (100) [$M^+ - 3CO$], 188 (43) [$M^+ - 3CO - Cr$], 132 (18) [$C_9H_9N^+$], 129 (1) [Quinoline $^+$]
4	318 (19) [M^+], 290 (0) [$M^+ - CO$], 262 (14) [$M^+ - 2 CO$], 234 (53) [$M^+ - 3 CO$], 182 (100) [Phenazine $^+$]

A general fragmentation pattern can be recognized. These molecules show an initial fragmentation of three carbonyls, followed by the loss of the chromium metal. For compounds **2** and **3**, the loss of the butyl group from the nitrogen-containing heteroarene substrate succeeds the dismissal of the chromium atom. The principal ions of compounds **2** and **3** are $(\pi\text{-arene})Cr^+$ and $(\pi\text{-arene})^+$ for **4**.

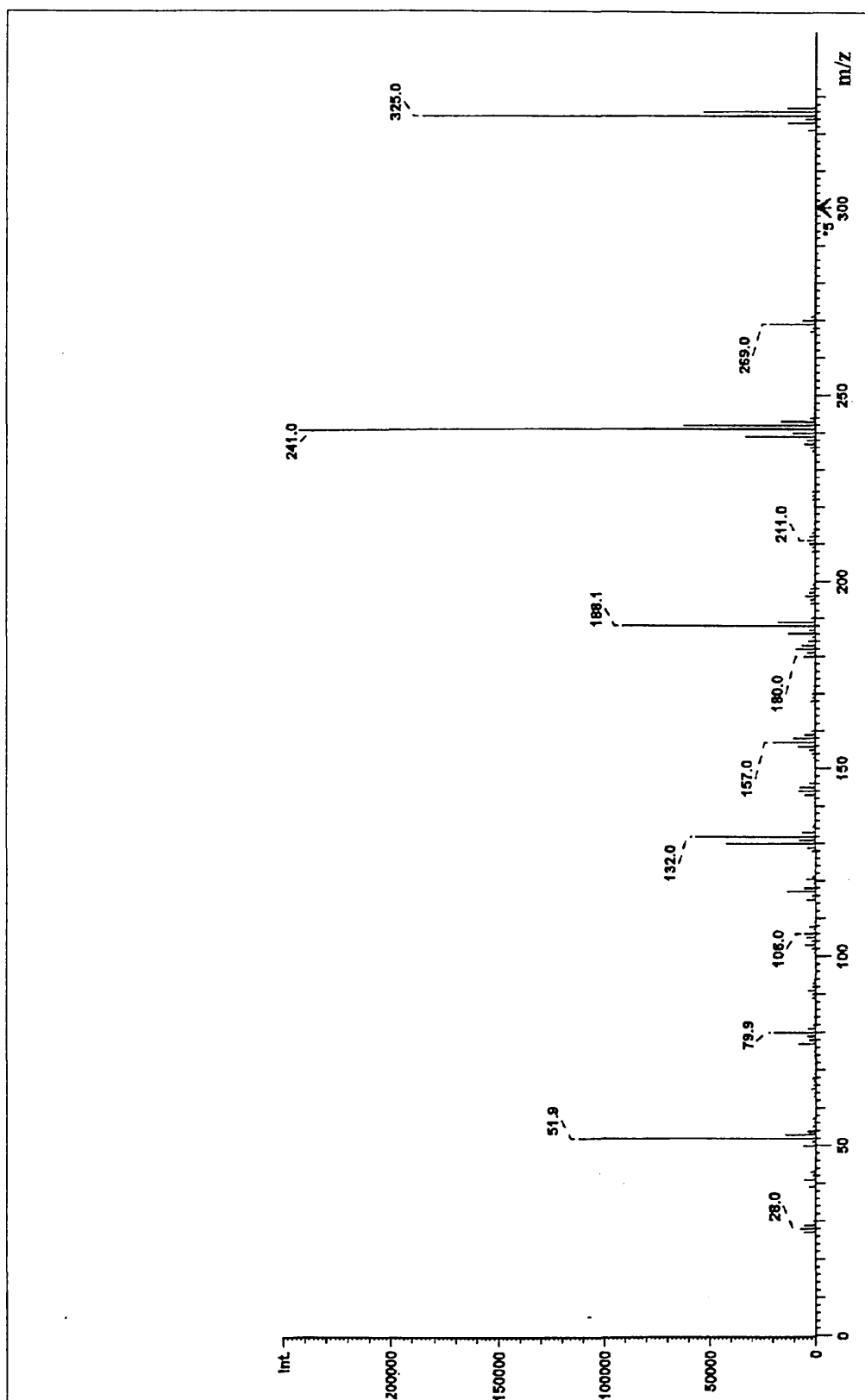


Figure 2.27 Mass spectrum of compound 3

2.5.4 X-ray Crystallography

Final confirmation of the structures of **2** and **3** was obtained with X-ray diffraction studies. In **Appendix 1** the crystallographic data of **2** is listed, while the data for structure determination of **3** is reproduced in **Appendix 2**. Figures 2.28 and 2.29 represent the ORTEP^[57] plots of the two structures. Single crystals of **2** and **3** were isolated from dichloromethane/hexane (1:1) solutions. Compound **2** crystallized in the space group $P\bar{1}$ with $a = 9.129(2)$, $b = 9.153(1)$, $c = 13.304(2)$ Å, $Z = 2$, while compound **3** crystallized in the space group $P2_1/c$ with $a = 15.961(4)$, $b = 8.097(2)$, $c = 12.571(6)$ Å, $Z = 4$.

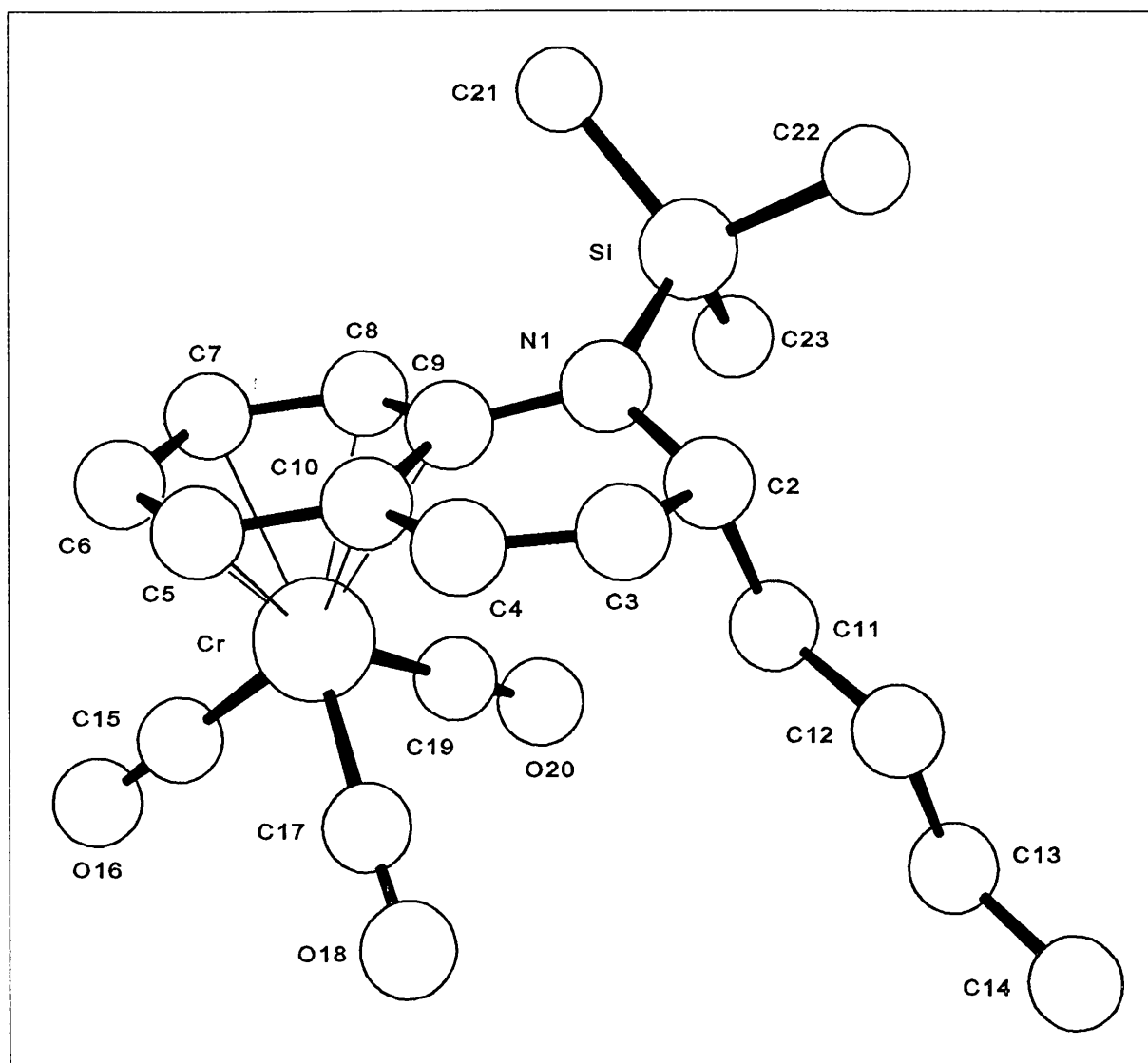


Figure 2.28 ORTEP drawing of compound **2**

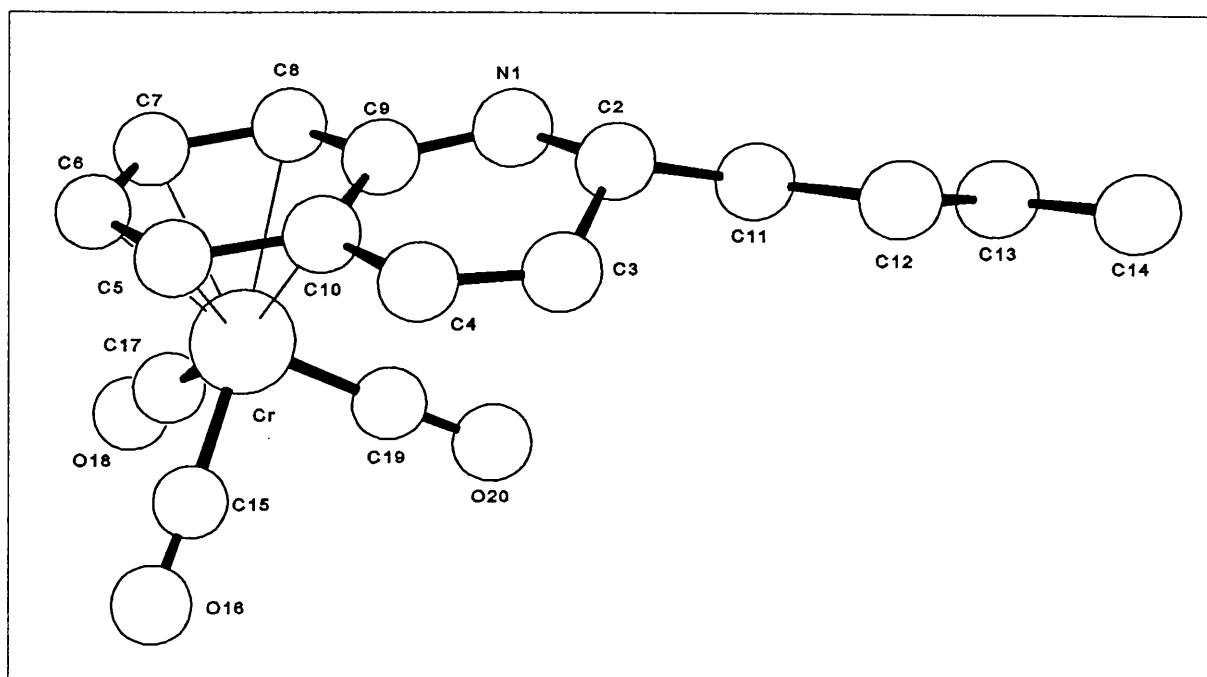


Figure 2.29 ORTEP drawing of compound **3**

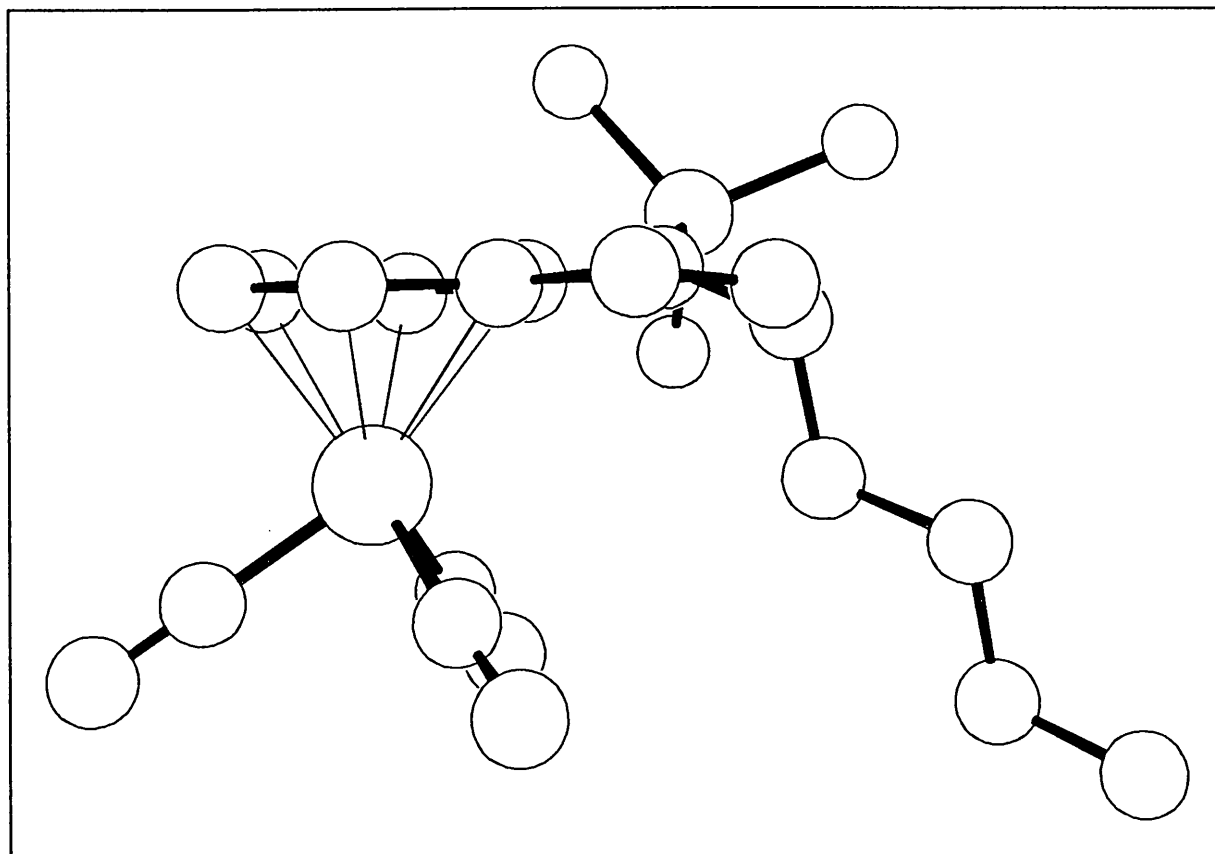
Bond lengths and bond angles

From the ORTEP plots of the two structures represented in figures 2.30 and 2.31 it is observed that the benzene ring fragment, π -coordinated to the $\text{Cr}(\text{CO})_3$ -moiety, is planar for both compounds **2** and **3**. The distances between the ring carbon atoms and the chromium metal for the two compounds are remarkably similar and an average value was calculated as 2.247 Å for **2** and 2.252 Å for **3**. Boutonnet *et al*^[58] reported these interatomic Cr-C distances to be 2.257 Å (av) for the complex $(\eta^6\text{-N-methylindole})\text{Cr}(\text{CO})_3$, while the literature values for the complexes $(\eta^6\text{-benzene})\text{Cr}(\text{CO})_3$ ^[59] and $(\eta^6\text{-naphthalene})\text{Cr}(\text{CO})_3$ ^[60] were stated to be 2.233 Å (av) and 2.26 Å (av) respectively. The N-containing ring fragments, on the other hand, are not planar. Although the two atoms N and C(4) are still in the plane of the benzene ring fragment, it is clear that carbons C(2) and C(3) are not in the plane. In table 2.7 the torsion angles are given for the distortions out of the plane for C(2) and C(3). The plane is defined as N(1)-C(9)-C(10)-C(4). From the data in the table it is noted that the distortion of C(2) is more distinct for **2**, while C(3) is more distorted out of the plane in **3**.

Table 2.7 Torsion angles for the distortion of C(2) and C(3)

Atom	Torsion angle ($^{\circ}$) (Compound 2)	Torsion angle ($^{\circ}$) (Compound 3)
C(2)-N(1)-C(9)-C(10)	25.28	4.19
C(3)-C(4)-C(10)-C(9)	9.90	14.99

The reason for the large torsion angle for C(2)-N(1)-C(9)-C(10) in **2** is probably the orientation of the butyl group. Steric reasons prevent the butyl group from occupying an equatorial position, since the presence of the trimethylsilyl group on the neighbouring N atom forces the butyl group to inhabit an axial position. The torsion angle for C(9)-N(1)-C(2)-C(11) is 89° . For compound **3** the torsion angle is -151° , indicating a more equatorial position for the butyl substituent. The absence of a large steric group allows the butyl group to occupy the equatorial position, since the neighbouring N atom is only bonded to a proton.

**Figure 2.30** A side-view ORTEP plot of **2**

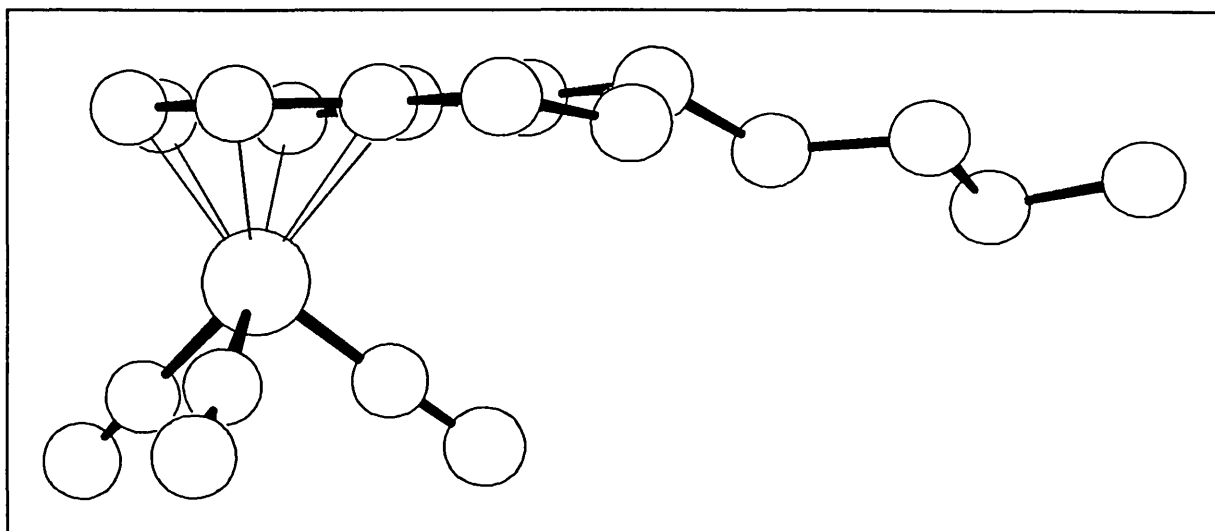


Figure 2.31 A side-view ORTEP plot of **3**

The bond lengths of the carbons present in the ring system are illustrated in figure 2.32.

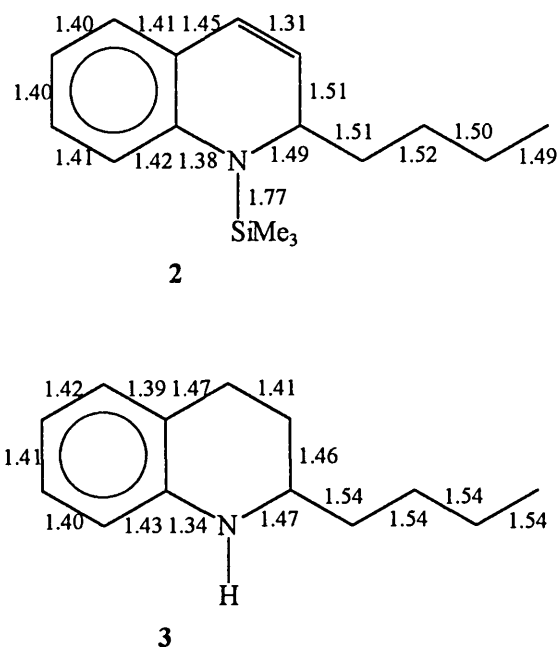


Figure 2.32 Bond lengths in the ring systems of **2** and **3**

The average bond length of the C-C bonds of the benzene ring fragment was calculated as 1.41 Å (av) for both compounds. The literature value reported for $(\eta^6\text{-benzene})\text{Cr}(\text{CO})_3$ ^[59] is 1.42 Å (av), while the values for $(\eta^6\text{-naphthalene})\text{Cr}(\text{CO})_3$ ^[60] and $(\eta^6\text{-N-methylindole})\text{Cr}(\text{CO})_3$ ^[58] were

stated to be 1.41 Å (av) and 1.40 Å (av) respectively. Distinguishing between 2- and 3-substituted products hinged on the assignment of the nitrogen atom position. In both complexes **2** and **3** a significantly shorter bond length is associated with the C-N bond, i.e. the N-C(9) bond, compared to that of the opposite C-C bond, i.e. the C(4)-C(10) bond, thus unambiguously confirming the assignment. In literature the distance of this C-N bond was reported to be 1.38 Å for 4-(trimethylsilyl)indole^[61]. Comparing the bond lengths of the C(3)-C(4) bond for compounds **2** and **3**, a distinct difference is observed. The bond distance in compound **2** is 0.1 Å shorter than the bond length in compound **3**, confirming saturation of the bond for compound **3**.

In structural studies of many silylamines, wide variations have been observed, but Si-N distances have been remarkably constant. Electron diffraction studies calculate the Si-N distance in N(SiMe₃)₃ to be 1.76 Å^[62]. The Si-Me bond lengths vary from 1.85 to 1.87 Å for the complex 4-(trimethylsilyl)indole^[61] and for N(SiMe₃)₃ the value was reported^[62] as 1.88 Å. For complex **2** the value obtained was 1.86 Å.

Bond angles of the atoms in the ring system are represented in figure 2.33.

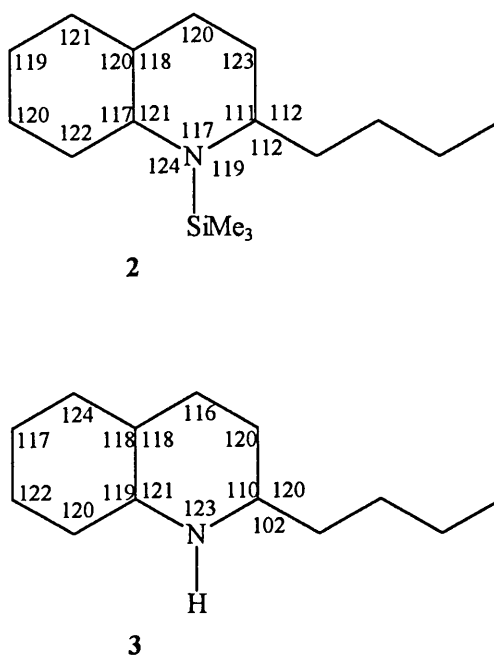


Figure 2.33 Bond angles in the ring systems of **2** and **3**

The bond angles in the complex $(\eta^6\text{-benzene})\text{Cr}(\text{CO})_3$ ^[59] were reported to be 120° (av). The average value calculated for the bond angles of the π -coordinated benzene ring fragment was 120° (av) for both **2** and **3**, while the value determined for the N-containing ring was 118° (av). Similar to the observation made for the bond lengths of C(3)-C(4), a difference in bond angle is also observed for the angles concerning these two atoms (see figure 2.32). This difference can be ascribed to the hybridization of the respective carbon atoms. For compound **2** both atoms are sp^2 hybridized, while in compound **3** sp^3 hybridization applies. Striking is the large difference between the internal ring angles at the nitrogen atom, which is 117° for **2** and 123° for **3**. Since the electronegativities of a SiMe-group and a proton substituent are very similar, this result must be ascribed to the bulkiness of the SiMe₃-moiety.

The values determined for the angles between the Si atom and the methyl groups in compound **2** varied from 108 to 110°. Literature values^[62] obtained for the Me-Si-Me bond angles in the compound N(SiMe₃)₃ ranged from 105 to 108°.

Carbonyl ligands: Bond lengths, bond angles and conformation

One of the most interesting stereochemical features of $(\pi\text{-arene})\text{Cr}(\text{CO})_3$ compounds is the slippage of the Cr(CO)₃ fragment towards the four unsubstituted carbon atoms of the arene ring and away from the two ring junction atoms. This slippage results in the bond length of the Cr-C being shorter for the four unsubstituted ring carbons than for the ring junction carbons. A difference in bond length of approximately 0.1 Å is observed. This trend is also noted in the structures of **2** and **3**. Cr-C (unsubstituted) bond lengths range from 2.207-2.248 Å, while the Cr-C (ring junction) distances varies from 2.269 to 2.351 Å.

The average bond length for the Cr-C bond is reported in literature as 1.84 Å for $(\eta^6\text{-benzene})\text{Cr}(\text{CO})_3$ ^[59] and as 1.81 Å for $(\eta^6\text{-N-methylindole})\text{Cr}(\text{CO})_3$ ^[58]. The C-O lengths are stated as 1.16 Å for $(\eta^6\text{-N-methylindole})\text{Cr}(\text{CO})_3$ ^[58]. Figure 2.34 represents the bond lengths obtained for the Cr(CO)₃ fragment in both compounds **2** and **3**.

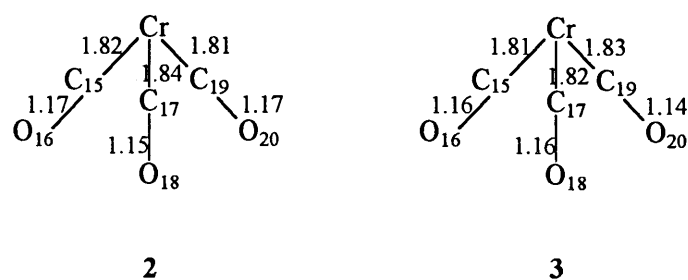


Figure 2.34 Bond lengths of the Cr-CO fragments of **2** and **3**

The bond angles for the $\text{Cr}(\text{CO})_3$ fragment are summarized in figure 2.35 for both compounds **2** and **3**. These results correspond well with literature values obtained for the $(\pi\text{-arene})\text{Cr}(\text{CO})_3$ complexes $(\eta^6\text{-benzene})\text{Cr}(\text{CO})_3$ ^[63] and $(\eta^6\text{-N-methylindole})\text{Cr}(\text{CO})_3$ ^[58]. The C-O bond angle was found to be 179° (av) for compound **2**, while a value of 180° (av) was obtained for compound **3**.

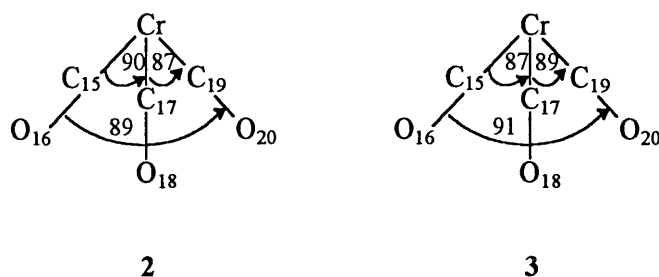


Figure 2.35 Bond angles between chromium and the carbonyl ligands for **2** and **3**

All condensed aromatic compounds can be considered to be minimally *ortho* disubstituted because of the connected ring system. Three orientations are possible for the $\text{Cr}(\text{CO})_3$ fragment (figure 2.36). The preferred orientation is usually the S orientation. The E orientation is usually detected for substituted arene complexes, e.g. $(\eta^6\text{-C}_6(\text{C}_2\text{H}_5)_6)\text{Cr}(\text{CO})_3$. Electronic considerations are the driving force for this preference in conformation^[59].

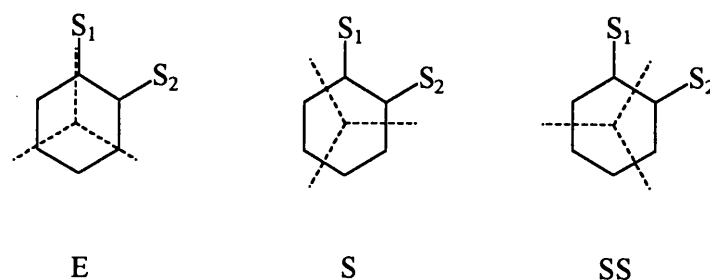


Figure 2.36 Possible orientations for ML_3 fragments

In figure 2.37 and figure 2.38 projections perpendicular to the arene ring along the Cr-CNTR axis are represented for complexes **2** and **3** and the conformations of the carbonyl ligands can be observed. The Cr-CNTR axis is defined as the line joining the chromium atom and the centre of the benzene ring fragment.

From figure 2.37 it is obvious that the carbonyl ligands adopt the S orientation in **2**, while the E orientation is observed for the carbonyl ligands of **3**. The torsion angles C(arene)-CNTR-Cr-C(CO) for the respective carbonyl ligands were determined and the results are summarized in table 2.8. No clear reason on electronic or steric grounds can explain why **3** adopts the E-orientation, but it must be kept in mind that the energy differences between these conformations are small and crystal packing can also influence the orientation of the carbonyl ligands.

Table 2.8 Torsion angles concerning the CO ligands

Atom	Torsion angle ($^{\circ}$) (Compound 2)	Torsion angle ($^{\circ}$) (Compound 3)
C(5)-CNTR-Cr-C _{CO}	42.20	1.29
C(6)-CNTR-Cr-C _{CO}	20.48	59.33
C(7)-CNTR-Cr-C _{CO}	39.12	2.47
C(8)-CNTR-Cr-C _{CO}	21.47	57.46
C(9)-CNTR-Cr-C _{CO}	38.58	0.23
C(10)-CNTR-Cr-C _{CO}	18.04	59.83

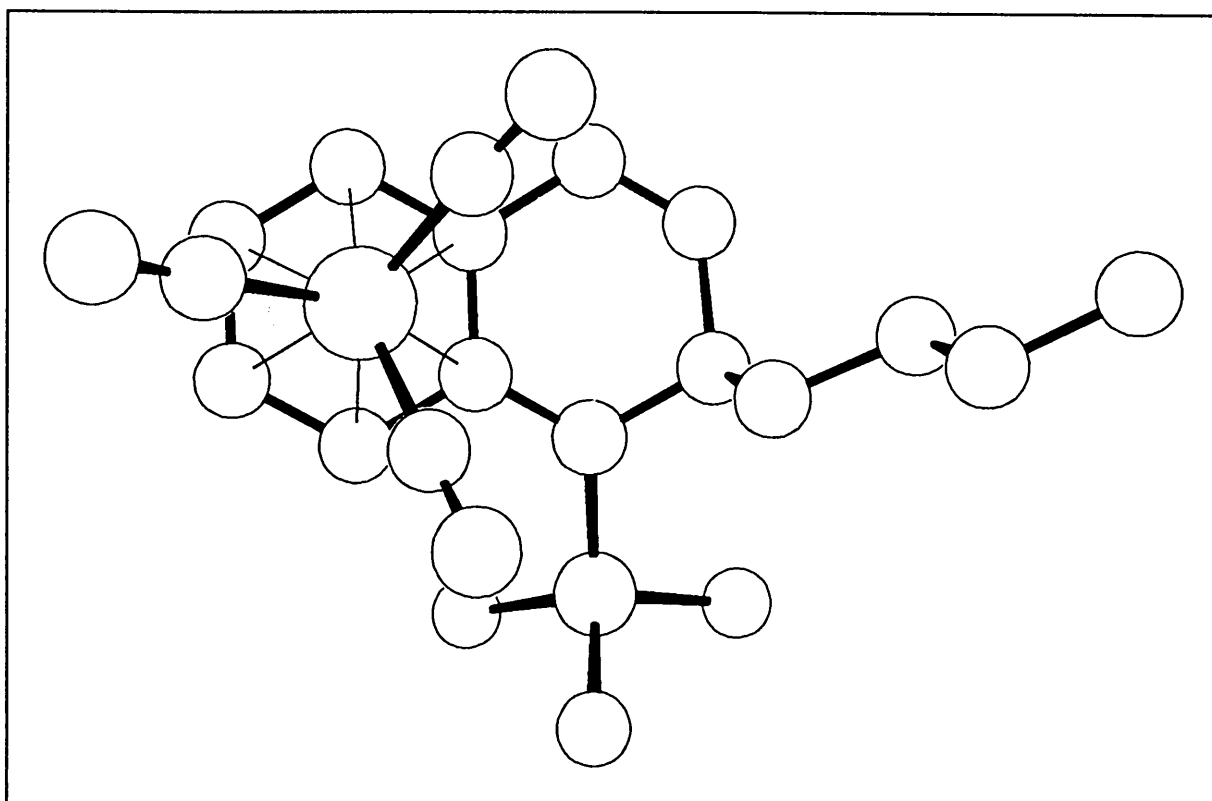


Figure 2.37 View of ORTEP plot of **2** along the Cr-Centre axis

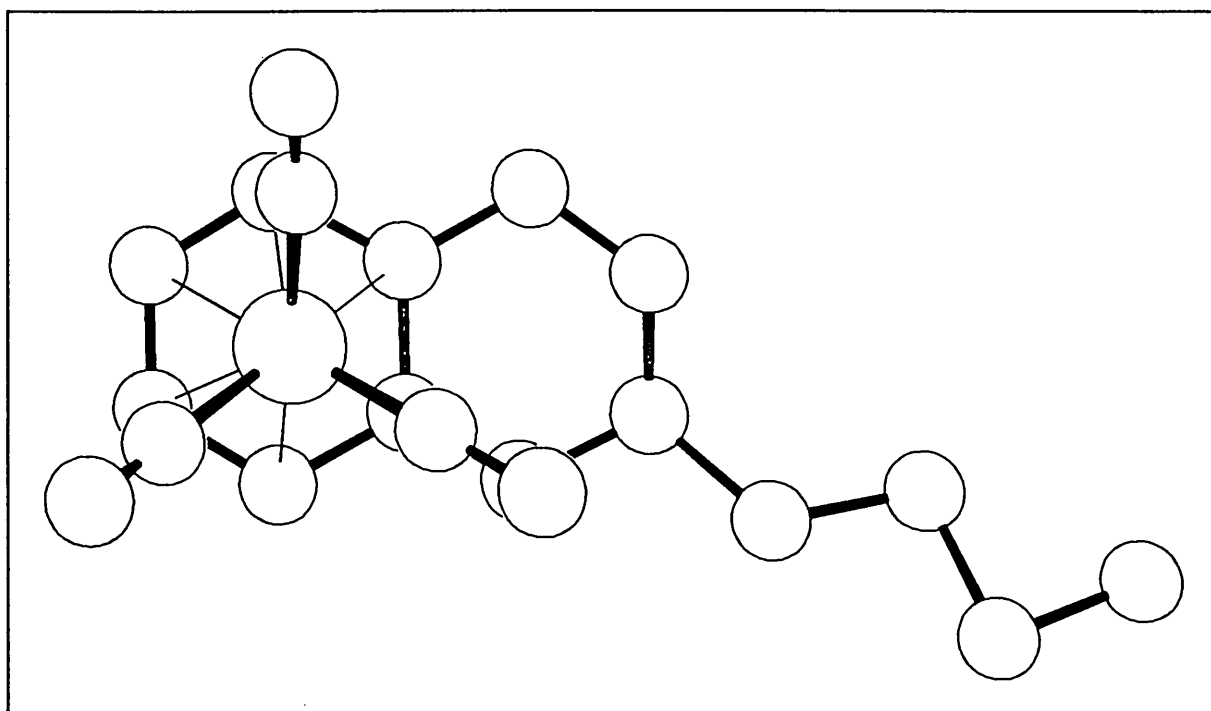


Figure 2.38 View of ORTEP plot of **3** along the Cr-Centre axis

In conclusion: This study proclaims that to eliminate the strong ligand donor properties of the nitrogen atom in quinoline, it is not only a simple matter of blocking the 2-position with a bulky substituent when π -bonding of $\text{Cr}(\text{CO})_3$ to the benzene ring fragment is considered. Factors such as nucleophilic additions at the 2-position and resulting steric and electronic activation during complexation to $\text{Cr}(\text{CO})_3$ play a decisive role in the composition of the final product.

The coordination of the uncomplexed thiophene ring through the sulphur atom to a $\text{Cr}(\text{CO})_5$ -fragment in the bimetallic 3,6-dimethylthieno[3,2-*b*]thiophene complex, was unexpected but logic in hindsight. The principle of disruption of aromaticity by π -coordination in multiple ring heteroarene ligands can be employed and exploited in the design and activation of bridging S-containing arene ligands in σ, π -bimetallic complexes.

2.5 References

- (1) H.H. Zeiss, P.J. Wheatly, H.J.S. Winkler, *Benzenoid-Metal Complexes*, Ronald Press., New York, 1966.
- (2) E.O. Fischer, W. Hafner, *Z. Naturforsch.*, 1955, 10B, 665.
- (3) a. M.Y. Darensbourg, E.L. Muetterties, *J. Am. Chem. Soc.*, 1978, 100, 7425.
b. T.W. Bell, M. Helliwell, M.G. Partridge, R.N. Perutz, *Organometallics*, 1992, 11, 1922.
c. A.M. Morken, D.P. Eyman, M.A. Wolff, S.J. Schauer, *Organometallics*, 1993, 12, 725.
d. C. Pellecchia, A. Grazzi, A. Immirzi, *J. Am. Chem. Soc.*, 1993, 115, 1160.
- (4) M. Novi, G. Giuseppe, C. Dell'Erba, *J. Heterocycl. Chem.*, 1975, 12, 1055.
- (5) G.E. Herberich, J. Hengesback, V. Kolle, W. Oschmann, *Angew. Chem. Int. Ed. Engl.*, 1977, 16, 42.
- (6) C.H. Langford, *Inorg. Chem.*, 1965, 4, 265.
- (7) K.K. Joshi, P.L. Pauson, *Proc. Chem. Soc.*, 1962, 326.
- (8) E.O. Fischer, H.A. Goodwin, C.G. Kreiter, H.D. Simmons, K. Sonogashira, S.B. Wild, *J. Organomet. Chem.*, 1968, 14, 359.
- (9) P. Geneste, A. Guicla, D. Levache, *Bull. Soc. Chim. Fr.*, 1983, 5-6, 136.
- (10) J.D. Goodrich, P.N. Nickias, J.P. Selegue, *Inorg. Chem.*, 1987, 26, 3424.
- (11) C.L. Lee, B.R. Steele, R.G. Sutherland, *J. Organomet. Chem.*, 1980, 186, 265.
- (12) K. Choi, R.J. Angelici, *Organometallics*, 1992, 11, 330.
- (13) J.A. Rudd, R.J. Angelici, *Inorg. Chim. Acta*, 1995, 240, 393.
- (14) H.J. Singer, *J. Organomet. Chem.*, 1967, 9, 135.
- (15) M. Draganjac, D.J. Ruffing, T. Rauchfuss, *Organometallics*, 1985, 4, 1909.
- (16) R.J. Angelici, *Coord. Chem. Rev.*, 1990, 105, 61.
- (17) N.J. Gogan, R. McDonald, H.J. Anderson, C.E. Loader, *Can. J. Chem.*, 1989, 67, 433.

- (18) R.B. King, A. Efraty, *J. Organomet. Chem.*, **1969**, *20*, 264.
- (19) R.A. Bauer, E.O. Fischer, C.G. Kreiter, *J. Organomet. Chem.*, **1970**, *24*, 737.
- (20) P.L. Timms, *Angew. Chem. Int. Ed. Engl.*, **1975**, *14*, 273.
- (21) M.F. Semmelhack, W. Wulff, J.L. Garcia, *J. Organomet. Chem.*, **1982**, *240*, C5.
- (22) C. White, S.J. Thompson, P.M. Maitlis, *J. Chem. Soc., Dalton Trans.*, **1977**, 1654.
- (23) S. Chen, V. Carperos, B. Noll, R.J. Swope, M.R. DuBois, *Organometallics*, **1995**, *14*, 1221.
- (24) T.C. Ho, *Catal. Rev.-Sci. Eng.*, **1988**, *30*, 117.
- (25) K.H. Pannell, B.L. Kalsotra, C. Parkanyi, *J. Heterocycl. Chem.*, **1978**, *15*, 1057.
- (26) H-G. Biedermann, K. Öfele, J. Tajtelbaum, *Z. Naturforsch.*, **1976**, *31B*, 321.
- (27) E.O. Fischer, K. Öfele, *Chem. Ber.*, **1960**, *93*, 1156.
- (28) K. Dimroth, R. Thamm, H. Kaletsch, *J. Chem. Soc., Chem. Commun.*, **1984**, *39*, 207.
- (29) R.E. Schmidt, W. Massa, *J. Chem. Soc., Chem. Commun.*, **1984**, *39*, 213.
- (30) K. Öfele, *Angew. Chem. Int. Ed. Engl.*, **1967**, *6*, 988.
- (31) K. Öfele, *J. Organomet. Chem.*, **1968**, *12*, P42.
- (32) G.S. Huttner, O.S. Mills, *Chem. Ber.*, **1972**, *105*, 3924.
- (33) J.J. Lagowski, *J. Am. Chem. Soc.*, **1976**, *98*, 1044.
- (34) S.G. Davies, M.R. Shipton, *J. Chem. Soc., Chem. Commun.*, **1989**, 995.
- (35) C. Elschenbroich, J. Koch, J. Kroker, M. Wansch, W. Massa, G. Baum, G. Stork, *Chem. Ber.*, **1988**, *121*, 1983.
- (36) K. Öfele, *Angew. Chem.*, **1967**, *79*, 1009.
- (37) A. Goti, M.F. Semmelhack, *J. Organomet. Chem.*, **1994**, *470*, C4.
- (38) R.A. Bauer, E.O. Fischer, C.G. Kreiter, *J. Organomet. Chem.*, **1970**, *24*, 725.
- (39) J. Nakayama, Y. Nakamura, S. Murabayashi, M. Hoshino, *Heterocycles*, **1987**, *26*, 939.

- (40) J. Nakayama, H. Dong, K. Sawada, A. Ishii, S. Kumakura, *Tetrahedron*, **1996**, *52*, 471.
- (41) C. Smith, W.G. Schneider, *Can. J. Chem.*, **1961**, *39*, 1158.
- (42) P.D. Baird, J. Blagg, S.G. Davies, K.H. Sutton, *Tetrahedron*, **1988**, *44*, 171.
- (43) P.J. Beswick, C.S. Greenwood, T.J. Mowlem, G. Nechvatal, D.A. Widdowson, *Tetrahedron*, **1988**, *44*, 7325.
- (44) M.F. Semmelhack, J.L. Garcia, D. Cortes, R. Farina, R. Hong, B.K. Carpenter, *Organometallics*, **1983**, *2*, 467.
- (45) K. Ziegler, H. Zeiser, *Ann.*, **1931**, *485*, 174.
- (46) N. Goetz-Luthy, *J. Am. Chem. Soc.*, **1949**, *71*, 2254.
- (47) Y. Otsuji, K. Yutani, E. Imoto, *Bull. Chem. Soc. Japan*, **1971**, *44*, 520.
- (48) D.I.C. Scope, J.A. Joule, *J. Chem. Soc. Perkin Trans. I*, **1972**, 2811.
- (49) G. Jones, *Chem. Heterocycl. Compd.*, **1977**, *32*, 3.
- (50) G. Fraenkel, J.C. Cooper, *Tetrahedron Lett.*, **1968**, *15*, 1825.
- (51) S-I Murahashi, Y. Imada, Y. Hirai, *Tetrahedron Lett.*, **1987**, *28(1)*, 77.
- (52) C. Elsenbroich, A. Salzer, *Organometallics: A Concise Introduction*, VCH Verlagsgesellschaft, Weinheim, Germany, **1992**, p. 227.
- (53) P. Hamm, W.v. Philipsborn, *Helv. Chim. Acta*, **1971**, *54*, 2363.
- (54) H. Günther, *NMR Spectroscopy, An Introduction*, Georg Thieme Verlag, Stuttgart, **1987**, p. 72.
- (55) S.R. Johns, R.I. Willing, *Aust. J. Chem.*, **1976**, *19*, 1617.
- (56) E. Breitmeier, *J. Org. Chem.*, **1976**, *41*, 2104.
- (57) C.K. Johnson, ORTEP, Report ORNL-3794, Oak Ridge National Laboratory, Oak Ridge, Tn, **1965**.
- (58) J-C. Boutonnet, J. Levisalles, E. Rose, *J. Organomet. Chem.*, **1983**, *255*, 317.
- (59) E.L. Muetterties, J.R. Bleeke, E.J. Wucherer, *Chem. Rev.*, **1982**, *82*, 499.
- (60) V. Kunz, W. Nowacki, *Helv. Chim. Acta*, **1967**, *50*, 1052.
- (61) A.G.M. Barrett, D. Dauzonne, D.J. Williams, *J. Chem. Soc., Chem. Comm.*, **1982**, 636. .

- (62) D.G. Anderson, D.W.H. Rankin, H.E. Robertson, G. Gundersen, R. Seip, *J. Chem. Soc. Dalton Trans.*, **1990**, 161.
- (63) B. Rees, P. Coppens, *Acta Crystallogr., Sect. B*, **1973**, B29, 2516.

3 σ, π -Heteroarene Bimetallic complexes of Titanium and Chromium

3.1 Introduction

Interest in organotitanium(IV) compounds developed after the discovery that certain organotitanium(IV) compounds show higher carbanion selectivity than organolithium compounds. Classical organic C-C bond formation reactions e.g. Grignard-type, Michael addition or Wittig olefination reactions are very useful reactions but have certain limitations. These reagents are basic and extremely reactive, affording wide application but low chemoselectivity and limiting the number of additional functional groups that can be used. It was discovered that titanation of carbanions using TiClX_3 leads to species with reduced basicity and reactivity^[1]. In reactions with organic compounds such as aldehydes, ketones and alkyl halides, the stereoselectivity, regioselectivity as well as chemoselectivity are increased. Stereochemical predictions can therefore be made in many C-C bond forming reactions, because the ligand X can be varied to control the electronic and steric nature of the reagents.

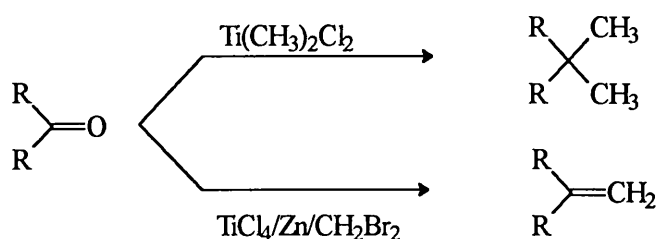


Figure 3.1 Unusual reaction types are possible when using organotitanium reagents

The arrival of Ziegler-Natta catalysts and the relevance of these compounds in organic syntheses, gave impetus to research in the field of organotitanium compounds. These heterogeneous catalysts are formed by mixing triethylaluminium and titanium tetrachloride and are used in the polymerization of ethylene, propylene and other α -olefins^[2].



Figure 3.2 Polymerization of ethylene using Ziegler-Natta catalysts

The Ziegler-Natta polymerization process and its enormous commercial applicability, led to the syntheses of various monomeric alkyl-titanium compounds, including TiCH_3Cl_3 ^[3]. A large number of η^5 -cyclopentadienyltitanium compounds have been prepared, containing either one or two Cp ligands^[4]. These Cp-groups have a strong electron donating effect and are said to have a “stabilizing” effect on titanium-alkyl bonds. This stabilizing effect can be very useful in adjusting carbanion-reactivity and selectivity. It was found that, when replacing a chlorine in compounds of the type TiRCl_3 by Cp-groups, the reactivity was reduced considerably.

New generation polymerization catalysts are homogeneous metallocene derivatives^[5] and have far-reaching implications for the development of new materials. In contrast to heterogeneous Ziegler-Natta catalysts, polymerization occurs at a single type of metal centre with a specific coordination. It is therefore possible to correlate metallocene structures with polymer properties and regio- and stereoregularities can be controlled. Of particular significance is the discovery of homogeneous isotactic polymerization of α -olefins, brought about by a catalyst generated from a chiral zirconocene halide and methyl alumoxane. The actual catalyst is thought to be the coordinatively unsaturated cation Cp_2ZrMe^+ which mimics the catalytic sites of surface-alkylated TiCl_3 of the Ziegler-Natta system by causing isotactic polymerization in a sequence of π -coordination and insertion steps.

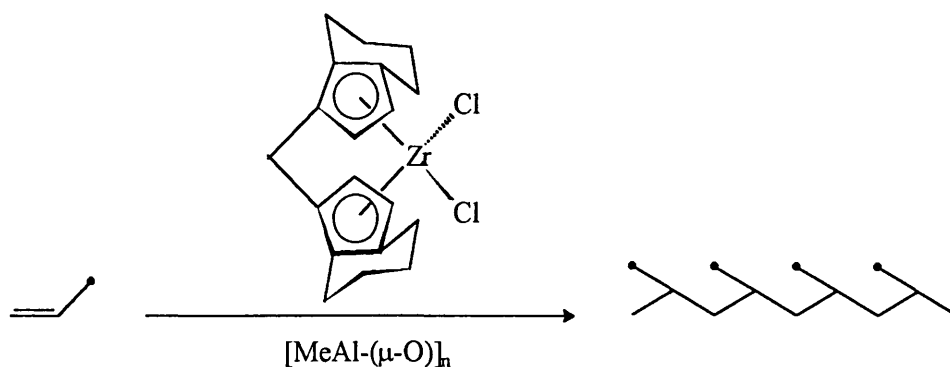


Figure 3.3 Polymerization of α -olefins using a chiral zirconocene halide and methyl alumoxane

In complexes of the form TiCp_2X_2 , e.g. where $\text{X} = \text{Cl}$, the halide moieties can easily be substituted for other ligands such as alkyl or aryl groups.

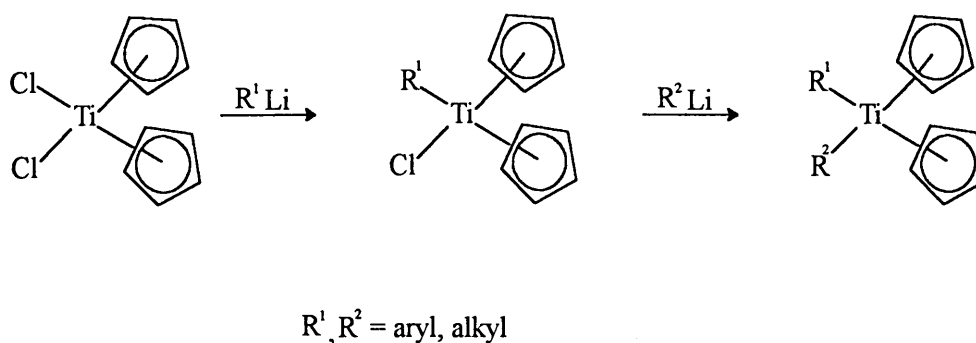


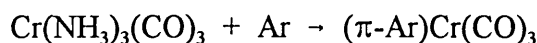
Figure 3.4 Substitution of chlorine moieties in TiCp_2Cl_2 by aryl or alkyl ligands

Growing interest in the synthesis of complexes containing organic ligands that can act as delocalized π -systems to form an electronic bridge between two dissimilar metal centres, has led to the investigation of the $\text{Cr}(0)$ - $\text{Ti}(\text{IV})$ system. Several σ, π -arene bimetallic complexes of titanium and chromium are known and have already been synthesized in our laboratories and characterized^[6]. Compounds of the form $(\eta^1:\eta^6\text{-Ar-TiCp}_2\text{X})\text{Cr}(\text{CO})_3$ were reported, where $\text{Ar} =$ benzene, substituted benzene and thiophene. These studies promoted investigation of the active sites of the different arene ligands. Two disparate metal centres are present in these compounds.

Titanium(IV) (d^0), an early transition metal, can be classified as electron-deficient. Chromium(0) (d^6), on the other hand, is a middle transition metal. In this study the investigation of the Cr(0)-Ti(IV) σ, π -bimetallic system was extended to the organic ligands benzo[*b*]thiophene and dibenzothiophene.

3.2 Metallation

The (π -arene)tricarbonylchromium(0) complexes that were used in the syntheses, were prepared according to known literature methods^[7]. The preparation involved the displacement of the ammine-ligands in the complex $\text{Cr}(\text{NH}_3)_3(\text{CO})_3$ by the organic arene ligand in the presence of boron trifluoride diethyl etherate in boiling dibutyl ether.



Ar = benzo[*b*]thiophene, dibenzothiophene

The coordination of a transition metal to an arene ligand in a π -complex modifies the reactivity of the arene ligand. A definite result is the acidification of the ring protons, which allows direct proton abstraction from the ligand. The first observation of metallation of arene ligands was reported in 1968^[8] and the first examples with chromiumtricarbonyl activation followed soon afterwards^[9].

Considering the arene complex $[\text{Cr}(\text{CO})_3(\eta^6\text{-C}_6\text{H}_6)]$, three electrophilic sites are present: the aromatic ring (figure 3.5, path a), the carbonyl ligand (path b) and the ring protons (path c). Most nucleophiles or bases will add to the ring (path a) while a few organolithium reagents are known to add to the carbonyl ligand (path b)^[10]. The acidifying effect of coordination to chromiumtricarbonyl was confirmed by equilibration measurements, suggesting that the pK_a of $[\text{Cr}(\text{CO})_3(\eta^6\text{-C}_6\text{H}_6)]$ is ~ 34 , compared to 43 for benzene. The abstraction of a ring proton (path c) is thus accomplished by the employment of a strong base, e.g. *n*-butyllithium.

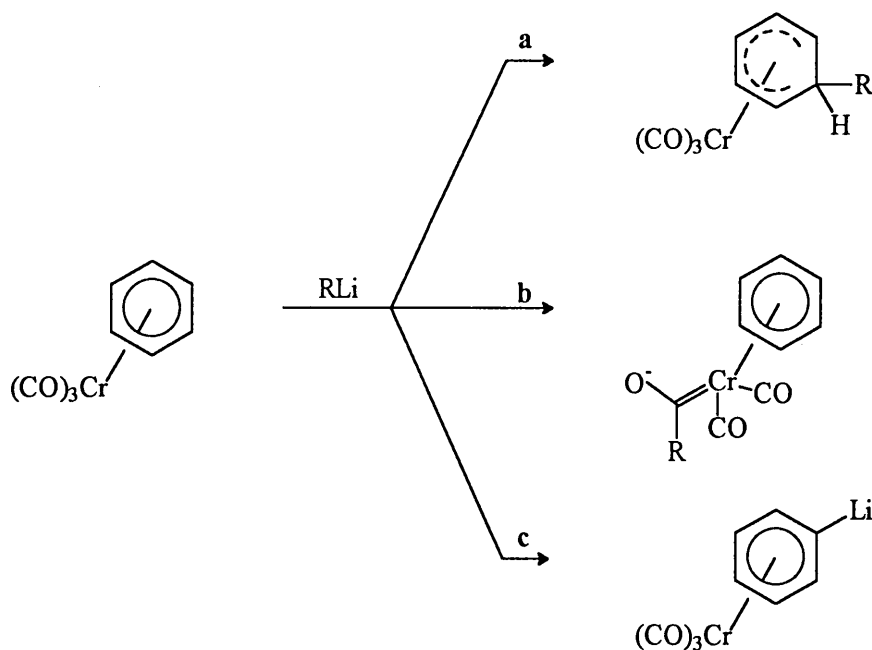
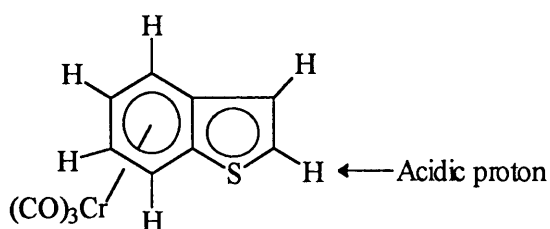


Figure 3.5 Electrophilic sites of $[\text{Cr}(\text{CO})_3(\text{C}_6\text{H}_6)]$

An important property of $(\pi\text{-arene})\text{tricarbonylchromium}$ complexes is the enhanced acidity of the arene hydrogens. Despite the fact that the tricarbonylchromium moiety is coordinated to the benzene ring in the π -complex of benzo[*b*]thiophene, the α -proton on the thiophene ring remains the most acidic^[11].



Deprotonation of the $(\pi\text{-benzo}[b]\text{thiophene})\text{tricarbonylchromium}(0)$ complex is accomplished by the use of a strong base ($\text{p}K_{\text{a}} > 20$) e.g. *n*-butyllithium. The enhanced acidity of the arene protons resulting from the π -coordination, enables hydrogen-metal exchange to occur under conditions where the uncoordinated substrate is unreactive.

3.2.1 Synthesis of $(\eta^1:\eta^6\text{-benzo}[b]\text{thienyl-TiCp}_2\text{Cl})\text{tricarbonylchromium}$

The metallated $(\pi\text{-benzo}[b]\text{thiophene})\text{tricarbonylchromium}(0)$ complex has nucleophilic properties located on the carbon in the 2-position of the thiophene ring and attacks the electron-deficient titanocene dichloride complex. According to the Green classification^[12], compounds with the formula TiL_4X_4 are 16 electron complexes and can therefore be described as electron-deficient. The nucleophilic attack affords the σ, π -bimetallic complex **5** directly. The formation of the LiCl salt is the driving force of the reaction. Even though a 1:1 ratio of reagents was used, **8** formed nevertheless, indicating an increase in the reactivity of the remaining chloro ligand of **5**.

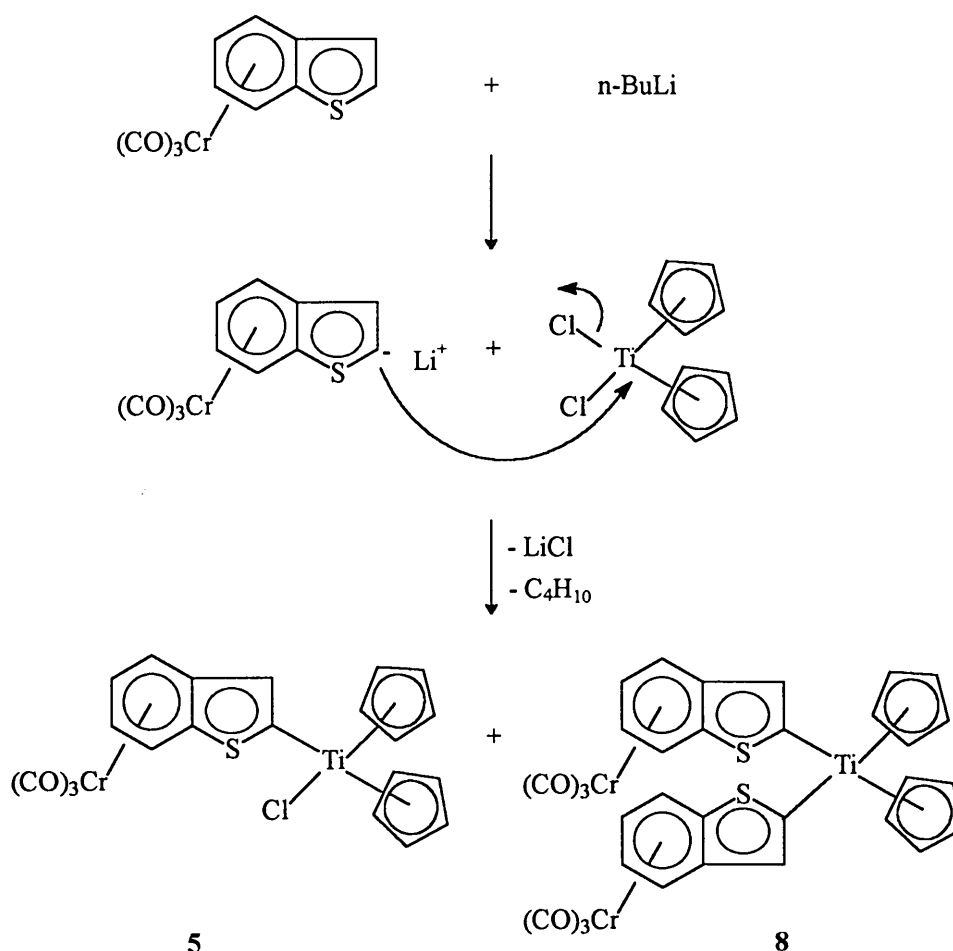


Figure 3.6 Metallation of $(\pi\text{-benzo}[b]\text{thiophene})\text{tricarbonylchromium}(0)$ and synthesis of **5** and **8**

The coordination of a titanium(IV) fragment σ to the arene substrate and a tricarbonylchromium fragment π -bonded to it, afforded the green coloured compounds, **5** and **8**. The green colour of the compounds, which is seldomly observed for arene-chromium complexes, indicates that charge is probably transferred from Cr(0), a d^6 -species, through the π -system to Ti(IV), a d^0 -species, when the electron-deficient Ti(IV) is directly bonded to the delocalized π -arene system. Since the titanium compound has empty d-orbitals, π -interactions can occur. The π -arene ring system donates electrons into these suitably orientated empty d-orbitals of the titanium. The titanium moiety can be seen as a Lewis acid, while the (π -arene)tricarbonylchromium fragment displays properties of a Lewis base.

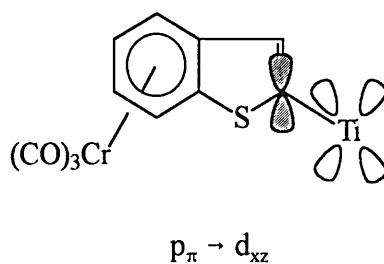


Figure 3.7 π -Electron transfer in the σ, π -bimetallic complex

After synthesizing compounds **5** and **8**, they were purified using column chromatography, using silica gel as resin. On purification, the green compound **5** reacted with the hydroxygroup of the silica gel and this reaction coloured the silica gel orange. The resulting orange compound could not be eluted from the column. The remaining chlorine ligand of the bimetallic complex was substituted by the hydroxy group of the silica gel.

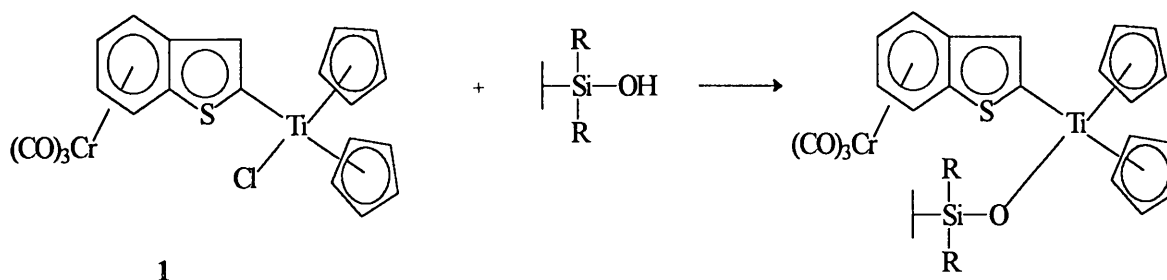


Figure 3.8 Reaction of $(\eta^1:\eta^6\text{-benzo}[b]\text{thienyl-TiCp}_2\text{Cl})\text{tricarbonylchromium}$ with the hydroxy group of the silica gel

It was attempted to synthesize $(\eta^1:\eta^6\text{-dibenzothieryl-TiCp}_2\text{R})\text{tricarboxylchromium}$ ($R = \text{Cl, SPh}$), but this was unsuccessful (figure 3.9). Metallation of the π -complex and addition of titanocene-dichloride afforded a green product that was clearly visible on a tlc plate. However, all attempts to isolate this product failed. The reason for this could be the reaction of the remaining chlorine ligand on the titanium with the OH-group of the silica gel. Treatment of the reaction mixture with thiophenol in the presence of the base TMEDA afforded an orange-red product that could also be seen on a tlc plate, but isolation of this product was impossible.

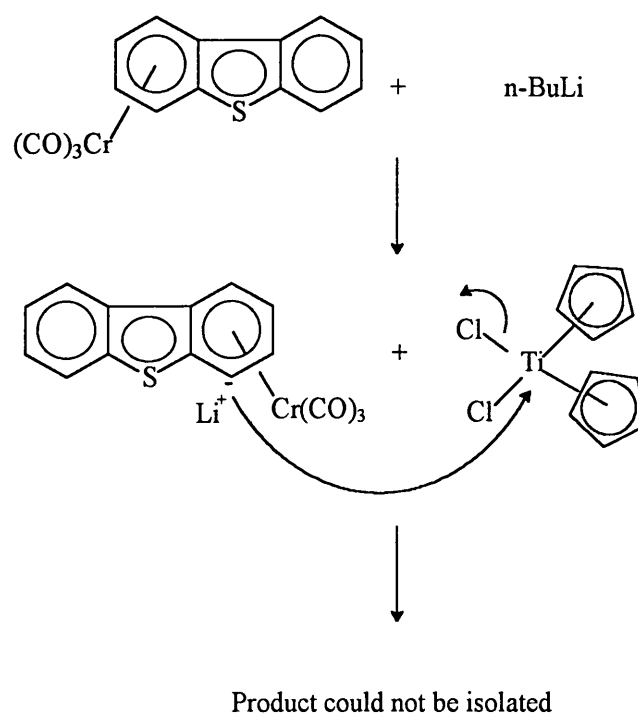


Figure 3.9 Metallation of $(\pi\text{-dibenzo}[b]\text{thiophene})\text{tricarboxylchromium}(0)$ and the reaction with TiCp_2Cl_2

3.3 Reactions of $(\eta^1:\eta^6\text{-benzo}[b]\text{thienyl-TiCp}_2\text{Cl})\text{tricarboxylchromium}$

3.3.1 Reaction with Thiophenol

Since the complex $(\eta^1:\eta^6\text{-benzo}[b]\text{thienyl-TiCp}_2\text{Cl})\text{tricarboxylchromium}$ is very reactive because

of the polarity of the Ti-Cl bond, it was attempted to exchange the chlorine ligand for another group that is less reactive and easier to isolate. Thiophenol was chosen because of the stability of the Ti-S bond. It is therefore far less reactive than the chlorine analogue. The reaction of $(\eta^1:\eta^6$ -benzo[*b*]thienyl-TiCp₂Cl)tricarbonylchromium with thiophenol in dichloromethane in the presence of the base TMEDA, afforded the orange-red target compound $(\eta^1:\eta^6$ -benzo[*b*]thienyl-TiCp₂(SPh))tricarbonylchromium, **6**, as well as the known purple titanium complex TiCp₂(SPh)₂.

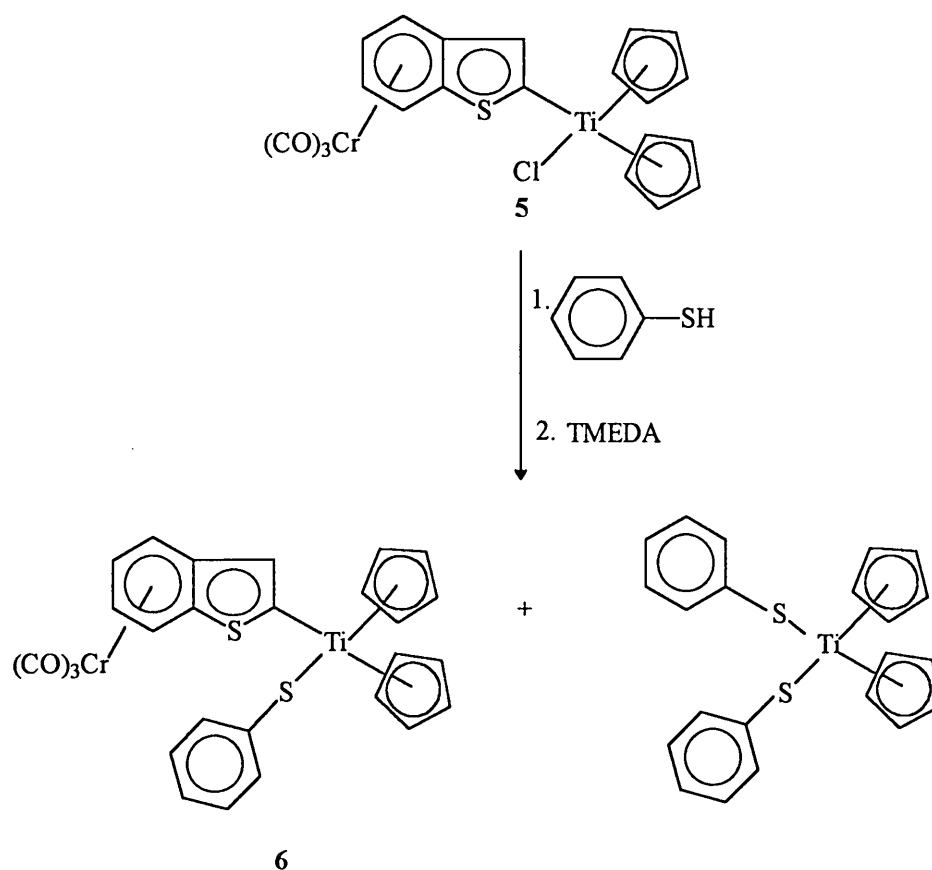


Figure 3.10 Reaction of $(\eta^1:\eta^6$ -benzo[*b*]thienyl-TiCp₂Cl)tricarbonylchromium with thiophenol

The bisphenylsulphide compound and the starting π -complex were formed by the protonation of the π -coordinated benzothienyl ligand by an excess of thiophenol (figure 3.11). The formation of these two products provides evidence of electron deficiency on the titanium.

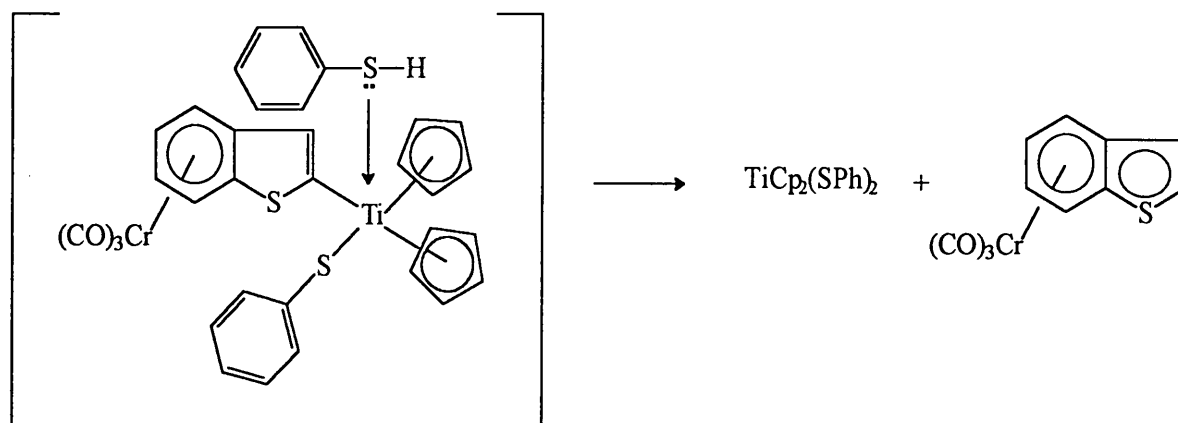


Figure 3.11 Formation of $\text{TiCp}_2(\text{SPh})_2$

3.3.2 Reaction with Water

F.G.A. Stone *et al.*^[13] was the first to synthesize and characterize compounds of the type $\text{TiCp}_2\text{R}(\text{OH})$. This was accomplished by adding a mixture of THF and water to the compound $\text{TiCp}_2(\text{C}_6\text{F}_5)\text{Cl}$ in the presence of KOH.

After the addition of water to the mixture of $(\eta^1:\eta^6\text{-benzo}[b]\text{thienyl-TiCp}_2\text{Cl})\text{tricarboxylchromium}$ in dichloromethane, the reaction solution was stirred overnight. The colour of the solution changed from green to orange-brown and afforded the product $(\eta^1:\eta^6\text{-benzo}[b]\text{thienyl-TiCp}_2\text{OH})\text{tricarboxylchromium}$, **7**.

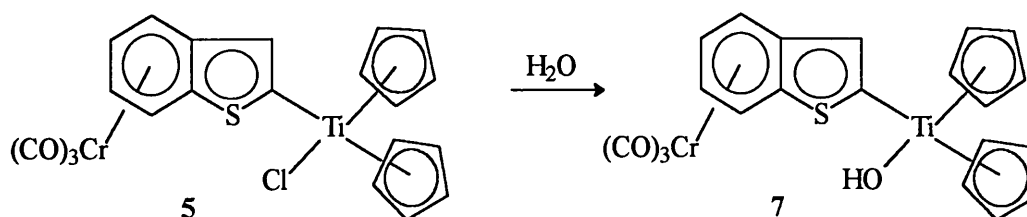


Figure 3.12 Reaction of $(\eta^1:\eta^6\text{-benzo}[b]\text{thienyl-TiCp}_2\text{Cl})\text{tricarboxylchromium}$ with water

3.3.3 Reaction in acetone

Compound **8** was dissolved in acetone, in order to record a NMR spectrum. The colour of the solution was orange, and not the expected green. In acetone the π -bond of one of the arene ligands to the $\text{Cr}(\text{CO})_3$ -moiety was broken and only the free benzo[*b*]thiophene ligand remained bonded, affording compound **9**. The acetone associated with the free $\text{Cr}(\text{CO})_3$ -moiety to form the unstable byproduct $\text{Cr}(\text{CO})_3(\text{Acetone})_3$.

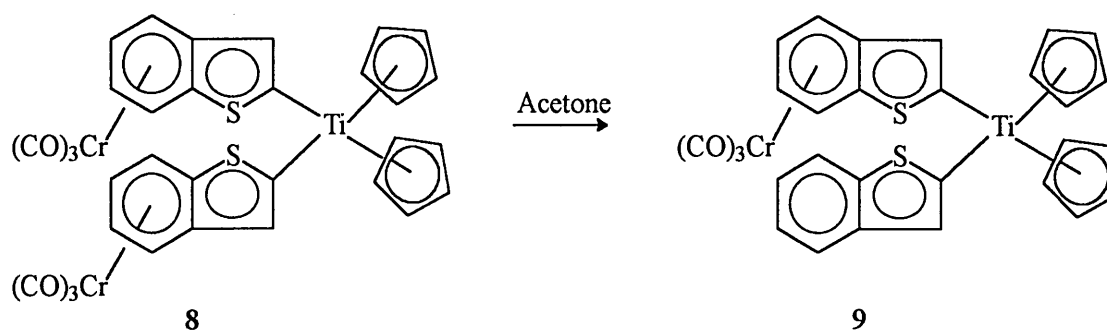


Figure 3.13 Conversion of compound **8** into **9** in acetone

3.4 Spectroscopic characterization

3.4.1 Infrared Spectroscopy

The data of the infrared spectra of compounds **5**, **6**, **7**, **8** and **9** are summarized in table 3.1, together with the data of the starting compound, (η^6 -benzo[*b*]thiophene)tricarbonylchromium. The infrared spectrum of the carbonyl region of compound **7** is represented in figure 3.14. The characteristic A_1 and E vibrational bands of a tricarbonyl complex can be clearly seen. The spectra of all the compounds were recorded in dichloromethane.

Table 3.1 IR-data of (η^6 -benzo[*b*]thiophene)tricarbonylchromium and ($\eta^1:\eta^6$ -benzo[*b*]thienyl-TiCp₂R)tricarbonylchromium

π -Arene complex	ν_{CO} (cm ⁻¹ , CH ₂ Cl ₂)	
	A ₁	E
(η^6 -benzo[<i>b</i>]thiophene)- tricarbonylchromium	1964 s	1885 vs
5 (R = Cl)	1953 s	1872 vs
6 (R = SPh)	1952 s	1870 vs
7 (R = OH)	1952 s	1870 vs
8	1954 s	1875 vs
9	1953 s	1873 vs

The replacement of a proton by a titanium moiety in (π -BT)Cr(CO)₃ complexes, has a definite effect on the electronic structure of the complex. This can be deduced from the difference in the wavenumbers of the bands in the IR-spectra of the monometallic substrate and the bimetallic products (table 3.1). The decrease in wavenumber with the addition of the titanium fragment suggests that the electron density is higher on the substituted benzothienyl ring relative to the (η^6 -benzo[*b*]thiophene)tricarbonylchromium complex. Since π -interaction is found to play an unimportant role in this case, polarization of the Ti-C bond is suggested, with δ^+ at the titanium and δ^- at the ring. The data in table 3.1 implies that the polarized Ti-C bond affects the Cr-CO bond significantly. The bond order of the Cr-CO bond increases because the polarized Ti-C bond raises the electron density on the aromatic ring. The π -backbonding from the chromium to the carbonyl ligands is enhanced. The CO bond is weakened and affords lower wavenumbers on the IR-spectra.

The influence of the different substituents (R = Cl, SPh, OH, (η^6 -benzo[*b*]thiophene)Cr(CO)₃, benzo[*b*]thiophene) of the titanium moiety is apparently negligible, since the vibrational frequencies of the complexes are approximately the same.

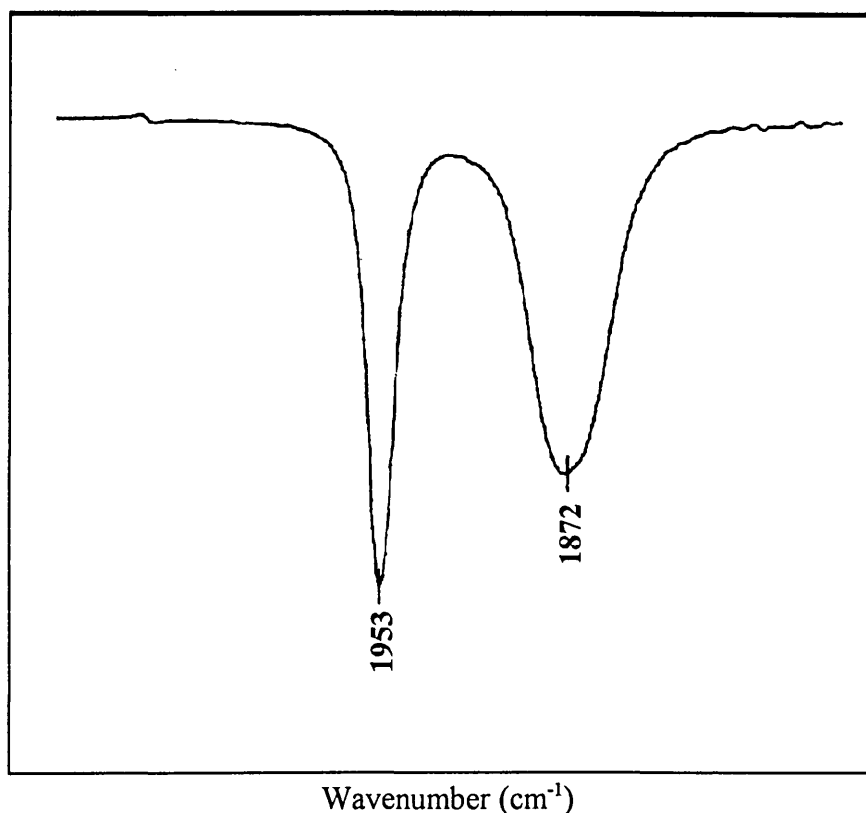


Figure 3.14 Infrared spectrum of ($\eta^1:\eta^6$ -benzo[*b*]thienyl-TiCp₂OH)-tricarbonylchromium, 7

3.4.2 NMR Spectroscopy

The resonance frequencies of ligand nuclei are affected when coordination of an organic ligand to a metal fragment occurs. The resulting coordination shift, defined as the chemical shift difference between the metal bonded ligand and the free ligand, is introduced with the symbol $\Delta\delta$.

Ultimate results are observed at metal-bonded protons. Strong shielding is experienced by protons that are directly bonded to a metal centre and a large coordination shift is detected. These protons are generally regarded as hydridic. The general trend for a group of metal atoms is that the shielding of a proton increases with an increase in the atomic number. The coordination shifts, $\Delta\delta$, of protons bonded to metal-bonded carbons are extremely smaller, while protons at non-coordinated carbon atoms display hardly any coordination shifts^[14].

All NMR spectra were recorded in CDCl_3 as deuterated solvent, unless stated otherwise. The ^{13}C spectra were recorded at -20°C in order to improve the resolution and to delay decomposition of the complexes. The following system of numbering the protons and carbon atoms of benzo[*b*]thiophene will be used throughout the whole discussion.

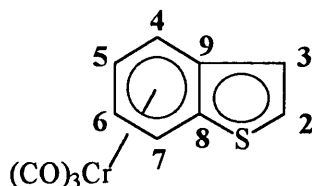


Figure 3.15 Atom labelling used for benzo[*b*]thiophene complexes

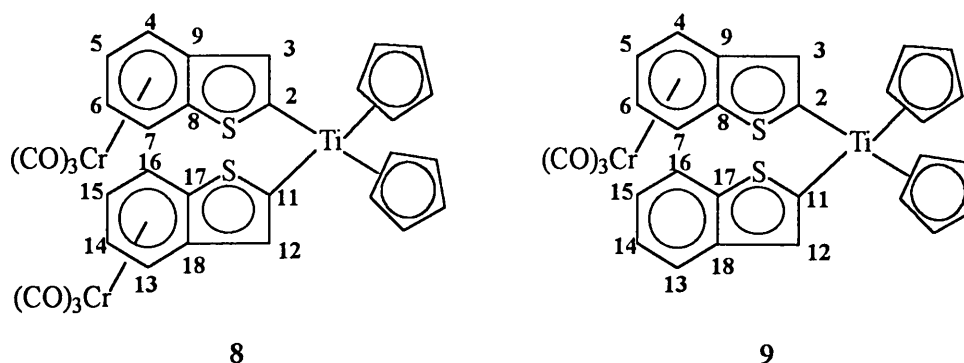


Figure 3.16 Atom labelling used for compounds **8** and **9**

^1H NMR Spectroscopy

The ^1H NMR data of the starting compound, (η^6 -benzo[*b*]thiophene)tricarbonylchromium as well as the data of complexes **5**, **6** and **7**, are summarized in Table 3.2, while the data of compounds **8** and **9** are outlined in Table 3.3.

Table 3.2 ^1H NMR data of $(\eta^6\text{-benzo}[b]\text{thiophene})\text{Cr}(\text{CO})_3$ and complexes **5**, **6** and **7**^a

Assignment	Complexes							
	Chemical shifts (δ , ppm) and coupling constants (J, Hz)							
	$(\eta^6\text{-BT})\text{-Cr}(\text{CO})_3$		5		6		7	
Proton	δ	$^3J_{\text{H-H}}$	δ	$^3J_{\text{H-H}}$	δ	$^3J_{\text{H-H}}$	δ	$^3J_{\text{H-H}}$
H2	7.42 (d)	5.6	-	-	-	-	-	-
H3	7.07 (d)	5.7	6.40 (d)	-	6.44 (s)	-	6.43 (s)	-
H4	6.19 (d)	6.5	6.08 (dd)	6.2	6.00 (d)	6.4	n.o.	-
H5	5.24 (dd)	6.5 6.1	5.21 (dd)	6.3	5.22 (dd)	7.7 6.4	5.22 (dd)	6.3 5.9
H6	5.41 (dd)	6.5 6.1	5.32 (dd)	6.7 6.3	5.22 (dd)	7.6 6.0	5.23 (dd)	6.2 6.0
H7	6.26 (d)	6.5	6.16 (d)	6.7	6.21 (d)	6.0	n.o.	-
Cp	-	-	6.43- 6.46 (m)	-	6.09 (s) 6.10 (s)	-	6.39 (s) 6.40 (s)	-
$\text{C}_6\text{H}_5\text{S}$	-	-	-	-	7.27- 7.30 (m)	-	-	-
OH	-	-	-	-	-	-	8.06 (s)	-

^a Assignments based on literature data^[15] of the starting compound

Table 3.3 ^1H NMR data of complexes 8 and 9

Assignment	Complexes			
	Chemical shifts (δ , ppm) and coupling constants (J, Hz)			
	8		9 ^a	
Proton	δ	$^3J_{\text{H-H}}$	δ	$^3J_{\text{H-H}}$
H3	6.33 (s)	-	6.49 (d)	-
H4	5.99 (dd)	6.1	6.33 (d)	6.0
H5	5.21 (dd)	5.9 5.9	5.53 (dd)	4.3 6.1
H6	5.22 (dd)	5.9 5.9	5.54 (dd)	4.3 6.1
H7	6.20 (d)	6.5	6.65 (d)	6.0
H12	6.33 (s)	-	6.55 (s)	-
H13	5.99 (dd)	6.1	7.19 (m)	-
H14	5.21 (dd)	5.9 5.9	7.19 (m)	-
H15	5.22 (dd)	5.9 5.9	7.19 (m)	-
H16	6.20 (d)	6.5	7.19 (m)	-
Cp	6.39 (s) 6.40 (s)	-	6.51 (s) 6.60 (s)	-

^a Recorded in deuterated acetone as solvent

Comparing the ^1H NMR data of the uncoordinated benzo[*b*]thiophene with the data of the starting compound (η^6 -benzo[*b*]thiophene)tricarbonylchromium, it is obvious that the aromaticity of the ring is disrupted by π -coordination of the $\text{Cr}(\text{CO})_3$ moiety. The chemical shifts (ppm) of the protons of uncoordinated benzo[*b*]thiophene^[15] are: 7.40 (H2), 7.18 (H3), 7.67-7.92 (H4, H7) and 7.30 (H5, H6). Since the π -coordination of the chromium fragment occurs at the benzene ring, the chemical shift of H2 remains unaffected for the starting compound. With the addition of the second metal, the chemical shift of H3 is drastically altered. A change in shifts of ~ 0.7 ppm is observed. Since the electronegativity of C (~ 2.5) is higher than for Ti (~ 1.3), the carbon-titanium σ -bond can be seen as a polarized covalent bond, compared to a carbon-hydrogen bond, where the difference in electronegativities is much smaller. The electron density is therefore higher at the arene ring than on the titanium and induces shielding of the arene protons, affording an upfield chemical shift for H3.

Two singlets were observed for the two Cp-ring protons on the spectra of all the compounds. The two Cp-rings are bonded to a prochiral titanium atom and are therefore not equivalent but diastereotopic. The anisotropic effect of the carbonyl-ligands causes deshielding of one of the Cp-rings, while the other Cp-ring experiences shielding from the π -arene ring. The non-equivalence of the Cp-rings is the reason for the observation of two signals instead of only one. The chemical shifts of the protons of the Cp-rings were different for compound 6, than for compounds 5 and 7. In compound 6 a sulphur atom is bonded to the titanium atom. The donor atom, sulphur, is a stronger nucleophile than oxygen (compound 7) or chlorine (compound 5), because it can donate electrons easier than the more electronegative species, oxygen and chlorine. It is also a "softer" atom than oxygen and chlorine. Thus, electron density is shifted to the titanium and causes greater shielding of the Cp-protons, resulting in the upfield shift on the NMR spectrum of the resonances for the Cp-protons of compound 6.

In the ^1H NMR spectra of compounds 6, 8 and 9, $^4J_{\text{H-H}}$ couplings are observed. The origin of these long-range couplings is the coupling of H4 with H6, affording a doublet. The magnitude of the respective coupling constants is $^4J_{\text{H-H}} = 1.29$ Hz for compound 6, $^4J_{\text{H-H}} = 1.52$ Hz for compound 8 and $^4J_{\text{H-H}} = 1.68$ Hz for compound 9. For compound 5 a $^4J_{\text{H-H}}$ coupling is observed for H3. This is probably the result of the coupling to H4, although this coupling is not observed in the splitting

pattern of H4 due to poor resolution. The magnitude of this coupling constant is 1.0 Hz.

The chemical shift pattern for H5 and H6 is observed as the overlap of two doublet of doublets on the ^1H NMR spectra of compounds **8** and **9**. The coupling constants for the coupling of H5 with H6 were calculated to be 5.9 Hz and 4.3 Hz for the two compounds respectively. A value close to 6.1 Hz was expected, since the values ought to be similar to that of the starting compound. The reason for this deviation is that these spectra were analysed according to the rules for a first order spectrum, while the spectra are actually of higher order. First order spectra^[16] are to be expected where the frequency interval, $\Delta\nu$, between the coupled nuclei is large compared to the coupling constants, *i.e.* $\Delta\nu \gg J$. If this requirement is not fulfilled, the intensity ratios as well as the coupling constants of the signals may alter and additional lines may appear. These spectra are said to be of higher order. The higher order effects are clearly observed in the spectra of compounds **8** and **9**, especially for H5 and H6. The frequency intervals are $\Delta\nu = 0.01$ for H5 and H6 for both compounds. Figure 3.17 illustrates this splitting pattern of compound **9** and the second order effects are visible.

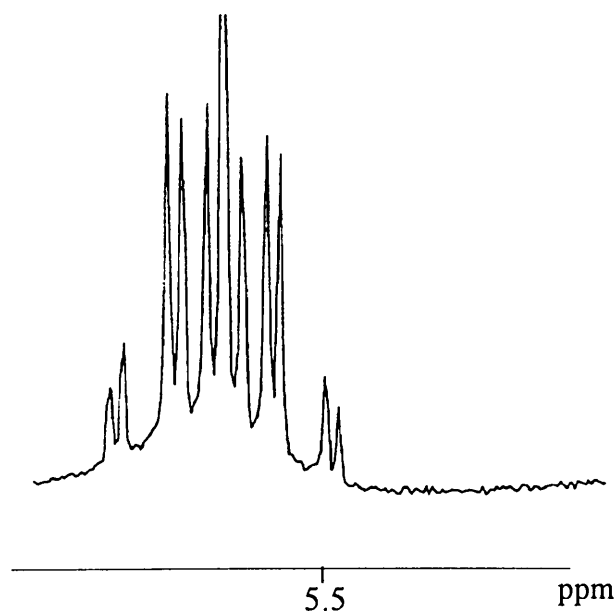


Figure 3.17 Second order splitting pattern observed for protons H5 and H6 of compound **9**

On the spectrum of **5** a doublet of doublets splitting pattern is observed for H4 instead of the

expected doublet. Furthermore, the observed doublet of doublets pattern for H5 is distorted. The reason for these results is unclear. It seems plausible to assume that the structure of **5** is such that the orientations of the Cp rings perturb the electronic environment around these protons.

The trend that a downfield chemical shift of the arene protons is encountered for the bimetallic compounds when the solvent is changed from d-chloroform to d⁶-acetone, has also been observed by Mangini and Taddei^[17]. This difference varies from 0.12-0.45 ppm.

Figure 3.18 represents the ¹H spectrum of compound **6**.

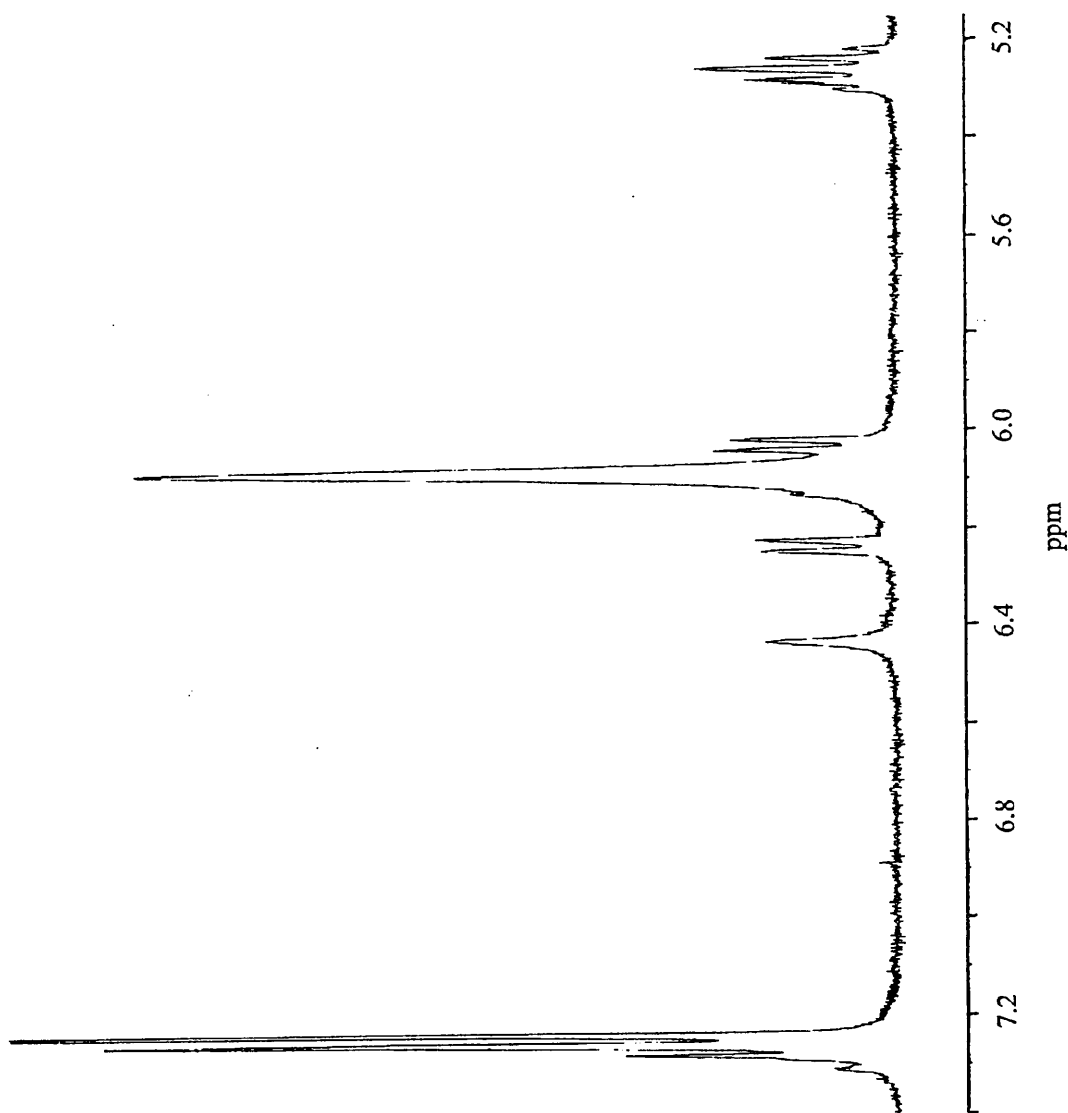


Figure 3.18 ¹H NMR spectrum of complex **6**

^{13}C NMR Spectroscopy**Table 3.4** ^{13}C NMR data of $(\eta^6\text{-BT})\text{Cr}(\text{CO})_3$ complexes **5**, **6**, **8** and **9**

Assignment	Complexes				
	Chemical shifts (δ , ppm)				
	$(\eta^6\text{-BT})\text{-Cr}(\text{CO})_3$	5	6	8	9^a
Carbon	δ	δ	δ	δ	δ
C2	131.3	n.o.	149.8	150.2	150.9
C3	123.4	123.5	128.4	126.6	138.3
C4	88.6	86.8	87.7	87.5	89.7
C5	89.7	89.0	89.4	89.1	90.9
C6	90.6	90.4	90.5	90.3	92.5
C7	86.9	85.5	87.6	87.3	89.3
C8	115.5	n.o.	n.o.	103.1	105.3
C9	110.3	n.o.	n.o.	98.8	n.o.
C11	-	-	-	150.2	173.7
C12	-	-	-	126.6	168.4
C13	-	-	-	87.5	127.6
C14	-	-	-	89.1	128.9
C15	-	-	-	90.3	129.6
C16	-	-	-	87.3	126.0
C17	-	-	-	103.1	n.o.
C18	-	-	-	98.8	132.5
Cp	-	116.7 116.9	113.4	116.0 116.3	119.1 119.3
CO	232.7	234.0	234.8	234.5	236.0

^a Recorded in deuterated acetone as solvent

The ^{13}C NMR data of complexes **5**, **6**, **8** and **9** as well as the data of the starting compound, (η^6 -benzo[*b*]thiophene)tricarbonylchromium, are summarized in Table 3.4. The data for compound **7** is not given because the product decomposed during the recording of the spectrum.

Notable differences are observed when comparing the ^{13}C NMR chemical shift values of the uncoordinated benzo[*b*]thiophene with those of the π -coordinated benzo[*b*]thiophene. The chemical shift values (ppm) of the uncoordinated benzo[*b*]thiophene are: 126.4 (C2), 124.0 (C3), 123.8 (C4), 124.3 (C5), 124.4 (C6), 122.6 (C7), 139.9 (C8), 139.8 (C9)^[18]. It is clear that the benzene ring, where the π -coordination occurs, is more affected than the thiophene ring fragment.

The two diastereomeric groups of Cp-rings can also be distinguished on the ^{13}C NMR spectra of compounds **5**, **8** and **9**. The anisotropic effect of the metal carbonyl fragment deshields the Cp-ring closer to it and affords a downfield chemical shift, while the other Cp-ring is more shielded by the electron density on the arene ring and thus an upfield chemical shift is observed. The difference in chemical shifts of the two Cp-rings, however, is only 0.3 ppm.

The tendency of the two carbon atoms C2 and C3 to shift downfield on σ -coordination to a titanium moiety, as seen for complex **5**, is repeated for the carbon atoms C11 and C12 of complex **9**.

The carbonyls of the $\text{Cr}(\text{CO})_3$ moiety are observed as a singlet on the ^{13}C NMR spectra of all the compounds studied. This suggests that the carbonyl groups are equivalent and indicates free rotation of the tricarbonylchromium fragment around the arene ring. The resonances lie in the narrow range 232.7-236.0 which indicates that the carbonyls are fairly insensitive to small changes on the arene ligand.

The ^{13}C spectrum of compound **9** is illustrated in figure 3.19. The uncoordinated ligand is clearly distinguished from the π -coordinated one, in that the π -coordination to a metal fragment shifts the signals to a higher field. The signals of the uncoordinated ligand are visible at 125-130 ppm on the spectrum, while the signals of the the π -coordinated one are observed at 90-95 ppm.

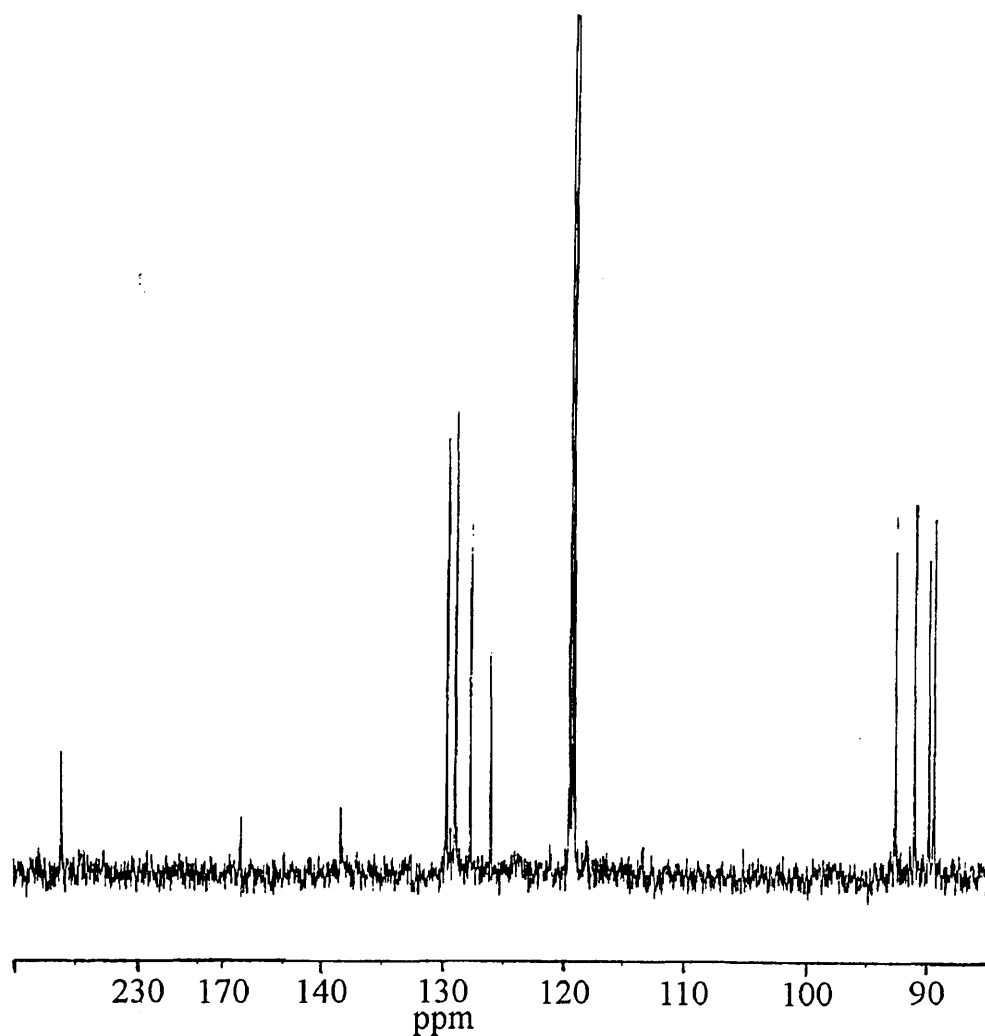


Figure 3.19 ^{13}C NMR spectrum of compound **9**

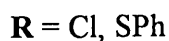
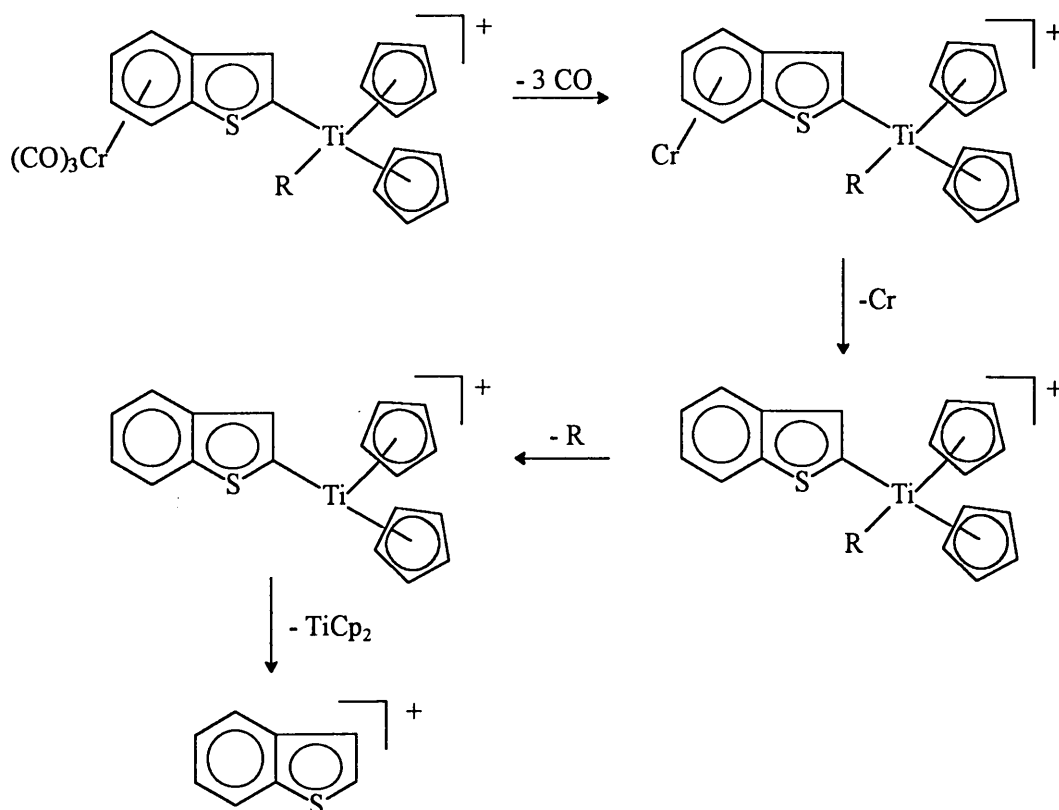
3.4.3 Mass Spectrometry

The m/z -values of the molecular ion peak and the most important fragment ions in the mass spectra of compounds **5** and **6** are shown in Table 3.5. The molecular ion peak was observed for compound **5** only.

Table 3.5 Fragmentation in the mass spectra of compounds **5** and **6**.

Complex	Mass peaks, m/z (I, %)
5	482 (1) [M ⁺], 398 (4) [M ⁺ -3CO], 346 (2) [M ⁺ -3CO-Cr], 310 (10) [Cp ₂ TiBT ⁺], 213 (59) [TiCp ₂ Cl ⁺], 148 (100) [TiCpCl ⁺], 134 (15) [BT]
6	500 (0) [M ⁺ -2CO], 472 (1) [M ⁺ -3CO], 420 (2) [M ⁺ -3CO-Cr], 312 (1) [Cp ₂ TiBT ⁺], 287 (12) [TiCp ₂ SPh ⁺], 178 (78) [TiCp ₂ ⁺], 134 (83) [BT]

Initial fragmentation of the carbonyl ligands as well as the successive loss of the Cr-atom is observed for both complexes. This is followed by the loss of the Cl in compound **5**, while in compound **6** the SPh-group is to follow the metal atom. Consecutive loss of the Ti-fragment eventually leaves only the uncoordinated ligand, BT.

**Figure 3.20** Fragmentation pattern for compounds **5** and **6**

3.5 References

- (1) M.T. Reetz, *Organotitanium Reagents in Organic Synthesis*, Springer Verlag, Berlin, 1986.
- (2) a. H. Sinn, W. Kaminsky, *Adv. Organomet. Chem.*, 1980, 18, 99.
b. P. Pino, R. Mülhaupt, *Angew. Chem. Int. Ed. Engl.*, 1980, 19, 857.
- (3) C. Beerman, H. Bestian, *Angew. Chem.*, 1959, 71, 618.
- (4) Gmelin Handbuch, "Titan-Organische Verbindungen", Part 1 (1977), Part 2 (1980), Part 3 (1984), Part 4 (1984), Springer Verlag, Berlin.
- (5) H.H. Brintzinger, D. Fischer, R. Mülhaupt, B. Rieger, R.M. Waymouth, *Angew. Chem. Int. Ed. Engl.*, 1995, 34, 1143.
- (6) a. M. Schindehutte, S. Lotz, P.H. van Rooyen, *Organometallics*, 1992, 11, 1104.
b. R. Meyer, S. Lotz, P.H. van Rooyen, *Adv. Organomet. Chem.*, 1995, 37, 219.
c. T. Waldbach, S. Lotz, P.H. van Rooyen, *Organometallics*, 1993, 12, 4250.
- (7) M. Novi, G. Guanti, *J. Heterocycl. Chem.*, 1975, 12, 1055.
- (8) C. Elschenbroich, *J. Organomet. Chem.*, 1968, 14, 157.
- (9) M.D. Rausch, *Pure Appl. Chem.*, 1972, 30, 523.
- (10) a. H.J. Beck, E.O. Fischer, G.C. Kreiter, *J. Organomet. Chem.*, 1971, 26, C41.
b. E.O. Fischer, P. Stückler, H.J. Beck, F.R. Kreisel, *Chem. Ber.*, 1976, 109, 3089.
- (11) J. Davidson, H. Patel, P. Preston, *J. Organomet. Chem.*, 1987, 336, C44.
- (12) M.L.H. Green, *J. Organomet. Chem.*, 1995, 500, 127.
- (13) M.A. Chaudhari, P.M. Treichel, F.G.A. Stone, *J. Organomet. Chem.*, 1964, 2, 206.
- (14) C. Elsenbroich, A. Salzer, *Organometallics: A Concise Introduction*, VCH Verlagsgeellschaft, Weinheim, Germany, 1992.
- (15) E.O. Fischer, H.A. Goodwin, C.G. Kreiter, D.D. Simmons Jr., K. Sonogashira, S.B. Wild, *J. Organomet. Chem.*, 1968, 14, 359.
- (16) H. Friebolin, *Basic One- and Two-Dimensional NMR Spectroscopy*, VCH Verlagsgesellschaft, Weinheim, Germany, 1991.

- (17) A. Mangini, F. Taddei, *Inorg. Chim. Acta*, **1968**, *2*, 8.
- (18) B. Iddon, R.M. Scrowton, *Adv. Heterocycl. Chem.*, **1970**, *11*, 178.

4 σ, π -Heteroarene Bimetallic complexes of Manganese, Rhenium and Chromium

4.1 Introduction

Bimetallic complexes of rhenium and chromium containing σ, π -bridged thienyl ligands have already been synthesized^[1] in our laboratories. Recently, Angelici^[2] reported the synthesis of the bimetallic compound ($\eta^2:\eta^6-\mu_2$ -benzo[*b*]thienyl-Re(CO)₂Cp)tricarbonylchromium, in which the chromium remains coordinated to the benzene ring and rhenium is bound to the C(2) = C(3) double bond. The structure of this compound was confirmed by X-ray diffraction studies. This structure contrasts with structures of benzo[*b*]thienyl-Re(CO)₂Cp, where the complexes exist as mixtures of isomers in which the benzo[*b*]thiophene is coordinated to the rhenium through either the sulphur or through the double bond (2,3- η^2). In these complexes the sulphur atom of the benzo[*b*]thiophene can act as an electron donor to the metal centre (η^1), or the olefin can act as a π -ligand (2,3- η^2). It was experimentally determined that the η^1 -coordination mode is favoured in these complexes.

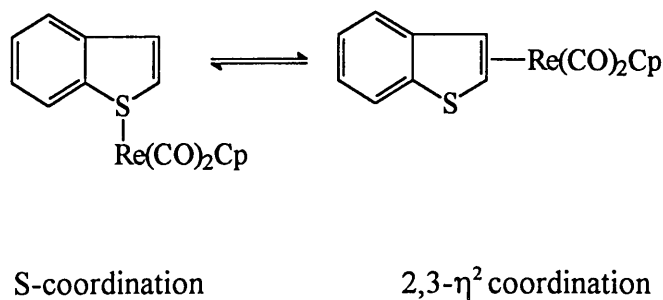


Figure 4.1 Different coordination modes of benzo[*b*]thienyl-Re(CO)₂Cp

Bimetallic complexes are known where both coordination modes are observed, for instance

$\eta^2:\eta^1(\text{S})-\mu_2$ -benzo[*b*]thienyl-(Re(CO)₂Cp)₂^[3]. One Re fragment is bonded to the sulphur and the other one is coordinated to the 2,3-olefin bond of the benzo[*b*]thiophene.

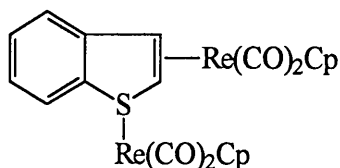


Figure 4.2 $\eta^2:\eta^1(\text{S})-\mu_2$ -benzo[*b*]thienyl-(Re(CO)₂Cp)₂.

In $(\eta^6$ -benzo[*b*]thiophene)Cr(CO)₃ the same two active sites are available for coordination to rhenium. The Cr(CO)₃ moiety could influence the coordination mode of the benzo[*b*]thiophene in either of two ways. The electron withdrawing effect of this moiety could reduce the ability of the sulphur of the benzo[*b*]thiophene to donate electrons and increase the π -accepting ability of the C(2)=C(3) moiety, thus favouring the coordination of the rhenium fragment to the olefinic bond. On the other hand, coordination of the Cr(CO)₃ fragment to the benzene ring of benzo[*b*]thiophene disrupts the aromaticity of the thiophene ring therefore sulphur has the ability to act as an electron donor. This argument suggests that the sulphur donor ability may be greater than in the uncoordinated aromatic benzo[*b*]thiophene. Valid reasons exist for expecting both the $\eta^1(\text{S})$ coordination and the 2,3- η^2 coordination of rhenium to $(\eta^6$ -benzo[*b*]thiophene)Cr(CO)₃; however, only the 2,3- η^2 isomer is observed^[2].

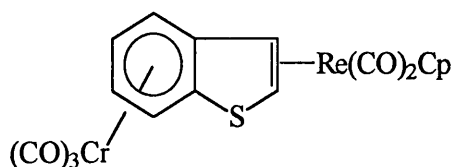


Figure 4.3 $(\eta^2:\eta^6-\mu_2$ -benzo[*b*]thienyl-Re(CO)₂Cp)tricarbonylchromium

Bimetallic and trimetallic complexes of manganese and chromium are known, where the manganese fragment is σ -bonded to the arene while the chromium moiety is π -coordinated to the

arene ring (arene = benzene^[4], thiophene^[5]). Metal exchange reactions between manganese and chromium have been observed^[6]. The complex $(\eta^1:\eta^5\text{-thienyl-Mn(CO)}_5)\text{tricarboylchromium}$ was found to be thermally unstable and irreversibly converted to an isomeric form in which the transition metals had exchanged coordination sites to afford the stable bimetallic complex $(\eta^1:\eta^5\text{-thienyl-Cr(CO)}_5)\text{tricarboylmanganese}$. This metal exchange reaction was studied when the complex was dissolved in acetone.

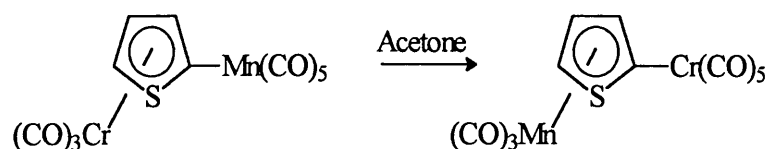


Figure 4.4 Metal exchange reaction

Treatment of $(\eta^6\text{-phenyl-Li})\text{tricarboylchromium}$ with $\text{Mn(CO)}_5\text{Br}$ could afford the σ, π -bimetallic complex $(\eta^1:\eta^6\text{-phenyl-Mn(CO)}_5)\text{tricarboylchromium}$ (path **a**), as well as a carbonyl inserted σ, π -bimetallic complex^{[4],[7]} (path **b**), since two active sites are present on the Mn compound. Nucleophilic attack can occur at the manganese metal centre or at a carbonyl moiety, affording the two respective products. However, the carbonyl inserted product was formed (route **b**) exclusively which could also have been achieved by the migration of the σ -bonded arene ring to an adjacent carbonyl ligand.

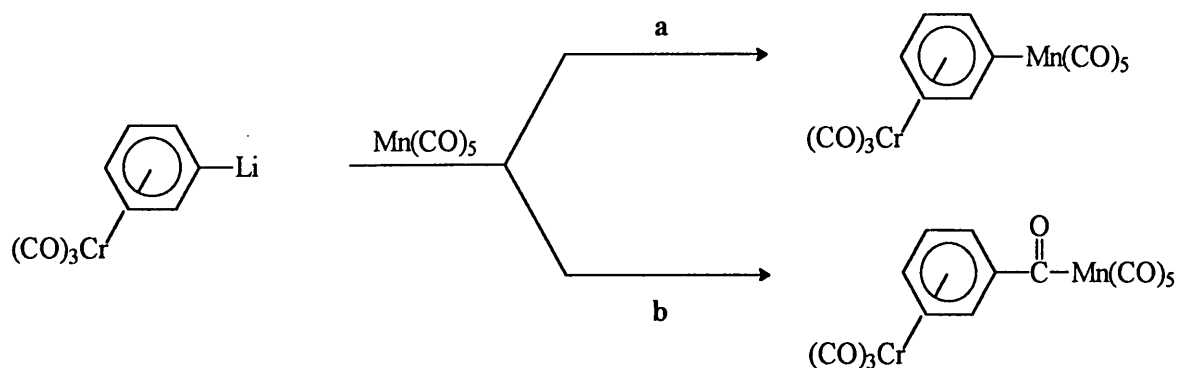


Figure 4.5 Treatment of lithiated $(\eta^6\text{-benzene})\text{tricarboylchromium}$ with $\text{Mn(CO)}_5\text{Br}$

4.2 Metallation

The (π -arene)tricarbonylchromium(0) complexes that were used in the syntheses, were prepared according to known literature methods^[8], (arene = benzo[*b*]thiophene, dibenzothiophene). Lithiation of the complexes were achieved by the use of the strong base, *n*-butyllithium. The addition of the transition metal compounds $M(\text{CO})_5\text{X}$, with $M = \text{Mn}$ or Re and $\text{X} = \text{Cl}$ or Br , afforded the σ, π -bimetallic complexes, unfortunately in poor yields.

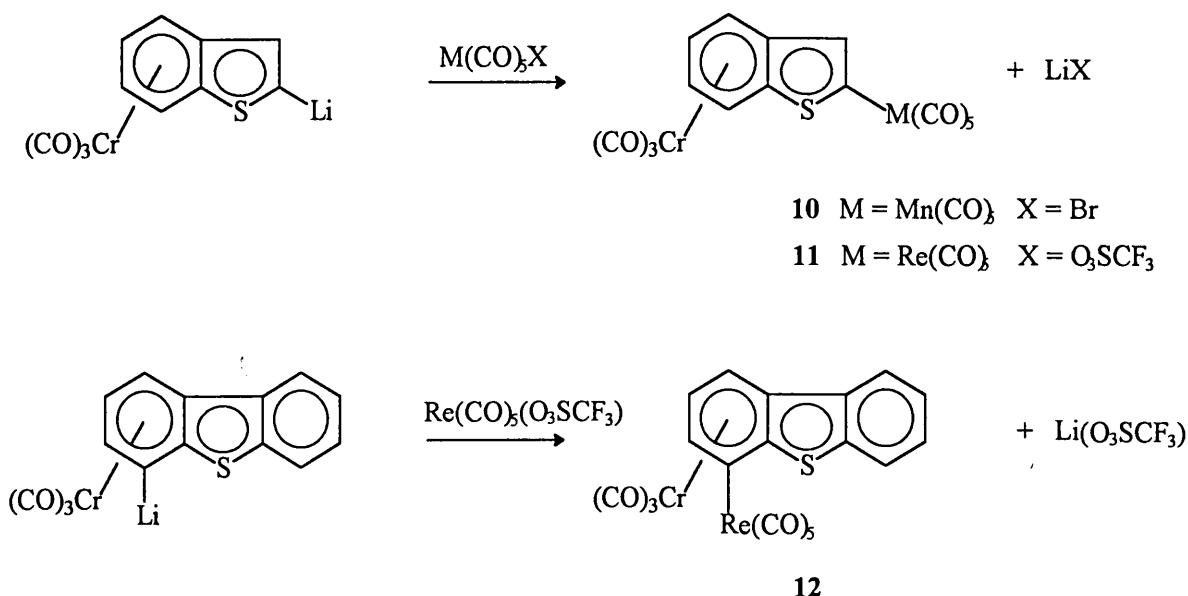


Figure 4.6 Synthesis of compounds **10**, **11** and **12**

$\text{Re}(\text{I})$ and $\text{Mn}(\text{I})$ in $M(\text{CO})_5\text{X}$ are both d^6 -species, and thus more electron-rich than for instance $\text{Ti}(\text{IV})$, a d^0 -species. The compound $\text{Re}(\text{CO})_5\text{Br}$ was reacted with silver triflate to yield $\text{Re}(\text{CO})_5(\text{O}_3\text{SCF}_3)$. This substitution was necessary since triflate is a better leaving group than the bromine. It was found that, on reacting the lithiated (π -thiophene) $\text{Cr}(\text{CO})_3$ complex with $\text{Re}(\text{CO})_5\text{Br}$, only a carbene complex could be isolated after subsequent alkylation (figure 4.7). Nucleophilic attack occurred at a carbonyl and not, as expected, at the metal centre^[1].

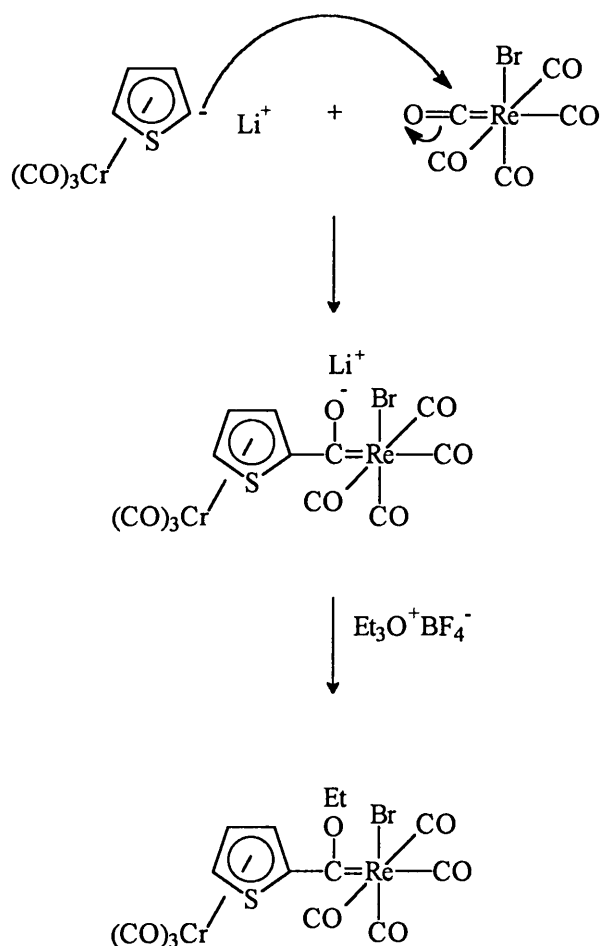


Figure 4.7 Reaction of lithiated $(\pi\text{-thiophene})\text{Cr}(\text{CO})_3$ with $\text{Re}(\text{CO})_5\text{Br}$

Bond strengths are known to increase in a group from top to bottom. It is therefore clear that the Re-Br bond is stronger than the Mn-Br bond. J.A. Connor *et al*^[9] found the dissociation energy of $\text{D}(\text{CH}_3\text{-Mn})$ to be $116.8 \text{ kJ.mole}^{-1}$, while the dissociation energy of $\text{D}(\text{CH}_3\text{-Re})$ was found to be $222.7 \text{ kJ.mole}^{-1}$. This result corresponds well with the experimental conclusions.

The effort to synthesize the dibenzothiophene analogue of compound 11, proved to be rather disappointing. On the ^1H NMR spectrum of this compound, it was clear that the compound was formed during the reaction, but decomposition occurred rapidly and these noise signals interfered with the signals of the product. It was thus impossible to unambiguously assign a specific chemical shift to a specific signal. The recording of a ^{13}C NMR spectrum was not even attempted due to the low yield of the compound and the rate of decomposition. However, spectroscopic evidence

seems to indicate migration of the $\text{Cr}(\text{CO})_3$ -moiety between the two benzene ring fragments (figure 4.8). The lability of this fragment is probably the reason why the isolation of this product proved to be difficult.



Figure 4.8 Migration of the $\text{Cr}(\text{CO})_3$ -moiety

Since the bimetallic complexes were obtained in low yield, a second synthetic route was decided on. It had been found that the insertion of electron-donor substituents into an aromatic ring raises the electron density of the latter and facilitates the formation of π -complexes with group VI metals^[10]. Kolobova and Goncharenko^[11] investigated the effect of $\text{Fe}(\text{CO})_2\text{Cp}$, a strong π -electron-donor substituent, on the ability of thiophene to form complexes with chromium. The σ -complexes thienyl- $\text{Fe}(\text{CO})_2\text{Cp}$ and benzofuran- $\text{Fe}(\text{CO})_2\text{Cp}$ were treated with $\text{Cr}(\text{CO})_6$ in refluxing dibutyl ether to afford the σ, π -bimetallic complexes in a relatively high yield. These reactions prompted the synthesis of compound **13**. Yet, the attempt to π -coordinate this compound to a $\text{Cr}(\text{CO})_3$ moiety, failed. Carbonyl ligands are far better π -acceptors than Cp ligands, resulting in the transfer of more electron density to the thienyl ring by the Fe-fragment.

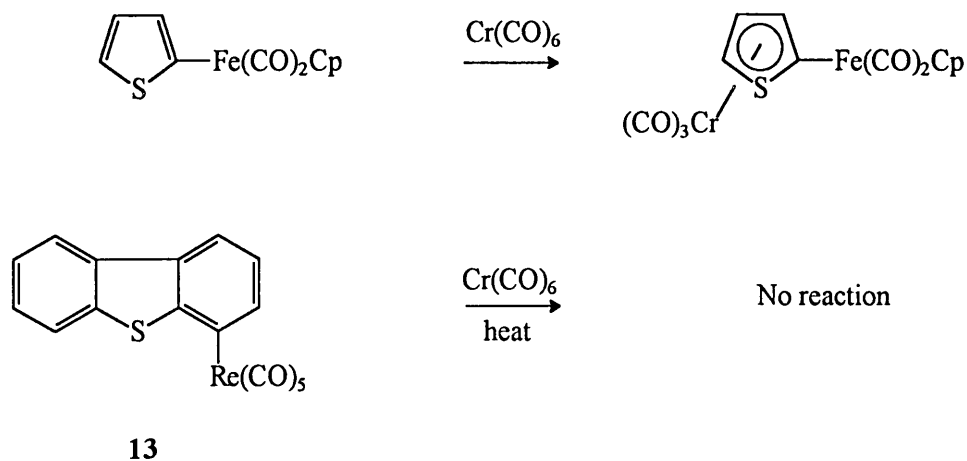


Figure 4.9 σ -Complexes as precursors of σ, π -bimetallic complexes

4.3 Spectroscopic characterization

4.3.1 Infrared Spectroscopy

Distinct patterns are observed for the bands of the different metal carbonyl fragments. The number, intensities and region of the bands aid in the characterization of the products. The individual vibrational modes are assigned to specific bands by taking the local symmetry of the carbonyls into consideration. According to the method of local symmetry^[12] a pentacarbonyl complex, e.g. $\text{Mn}(\text{CO})_5\text{L}$, belongs to the symmetry group C_{4v} , which has two vibrational bands that are IR active, the $\text{A}_1^{(2)}$ band, the B_1 band and the E band. The $\text{A}_1^{(1)}$ band becomes active due to coupling with the vibrational modes of the $\text{A}_1^{(2)}$ band vibrations. Since the bimetallic complexes do not exhibit absolute C_{4v} symmetry, distortions in the carbonyl plane are possible, resulting in an IR-active B_1 band.

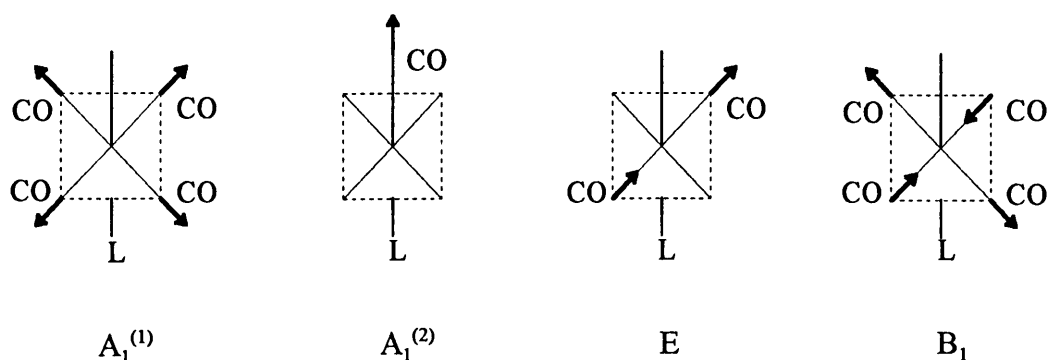


Figure 4.10 Stretching vibration modes of $\text{M}(\text{CO})_5\text{L}$

It is clear from figure 4.10 that the $\text{A}_1^{(2)}$ and the E bands will display the highest intensities on the IR spectrum. The $\text{A}_1^{(2)}$ band is often observed as a “shoulder” on the spectrum, at a lower frequency than the E band when the unique ligand is a poor π -acceptor ligand.

All the IR spectra were recorded in dichloromethane. Figure 4.11 represents the infrared spectrum of **10**. The pentacarbonyl vibrational bands as well as the tricarbonyl bands are present and can be distinguished on the spectrum.

Table 4.1 IR-data of $\text{Re}(\text{CO})_5(\text{O}_3\text{SCF}_3)^{[13]}$ and $\text{Mn}(\text{CO})_5\text{Br}^{[14]}$

Vibrational band	Complexes	
	Carbonyl vibrating frequencies (cm^{-1})	
	$\text{Re}(\text{CO})_5(\text{O}_3\text{SCF}_3)$	$\text{Mn}(\text{CO})_5\text{Br}$
$A_1^{(1)}$	2166 m	2138 m
B_2	2059 w	2064 w
E	2031 vs	2052 vs
$A_1^{(2)}$	2004 s	2008 s

Table 4.2 IR-data of 10, 11, 12 and 13

Vibrational band	Complexes			
	10	11	12	13
$\nu_{\text{CO}} (\text{cm}^{-1})$ of $\text{Cr}(\text{CO})_3$				
A_1	1966 s	1968 s	1964 s	-
E	1889 s	1893 s	1893 s	-
$\nu_{\text{CO}} (\text{cm}^{-1})$ of $\text{M}(\text{CO})_5$				
$A_1^{(1)}$	2139 m	2123 m	2139 m	2091 m
B_2	2072 w	2052 w	2074 w	n.o.
E	2025 vs	2028 vs	2025 vs	1993 vs
$A_1^{(2)}$	2020 s	2028 ^a	2008 s	1961 s

^a Observed as a shoulder on the spectrum

Due to overlap of the tricarbonyl-moiety and the pentacarbonyl moiety, the $A_1^{(2)}$ vibrational band was observed as a “shoulder” on the spectra.

The vibrational frequencies of the carbonyl ligands of the tricarbonylchromium fragment are slightly lower for the rhenium complex than for the manganese complexes. This suggests that the more electron rich $\text{Re}(\text{CO})_5$ substituent increases the electron density on the arene more than the $\text{Mn}(\text{CO})_5$ fragment.

Table 4.2 indicates that the IR data in the carbonyl region of compound **13** is considerably lower than the IR data of the starting compound $\text{Re}(\text{CO})_5(\text{O}_3\text{SCF}_3)$. This is also observed when comparing the carbonyl stretching frequencies of compounds **10** and **12** with those of compound **13**. A possible explanation for this difference in wavenumbers for the different compounds is that the $\text{Cr}(\text{CO})_3$ -moiety withdraws electron density from the arene ring, leaving the ring electron deficient. This enhances π -interaction with the σ -bonded metal fragments, reducing the demand for backbonding to the carbonyl ligands and resulting in carbonyl stretching frequencies that are higher in the spectra of **10** and **12**, than in the spectrum of **13**, for which the π -coordinated $\text{Cr}(\text{CO})_3$ -fragment is absent. Without the π -bonded $\text{Cr}(\text{CO})_3$ -moiety, the arene ring is electron-rich and the π -interaction between the arene carbon and the rhenium fragment less important. Therefore the M-CO bond order is increased, while the C-O bond order decreases accordingly, lowering the wavenumber of the carbonyl stretching frequencies in compound **13**.

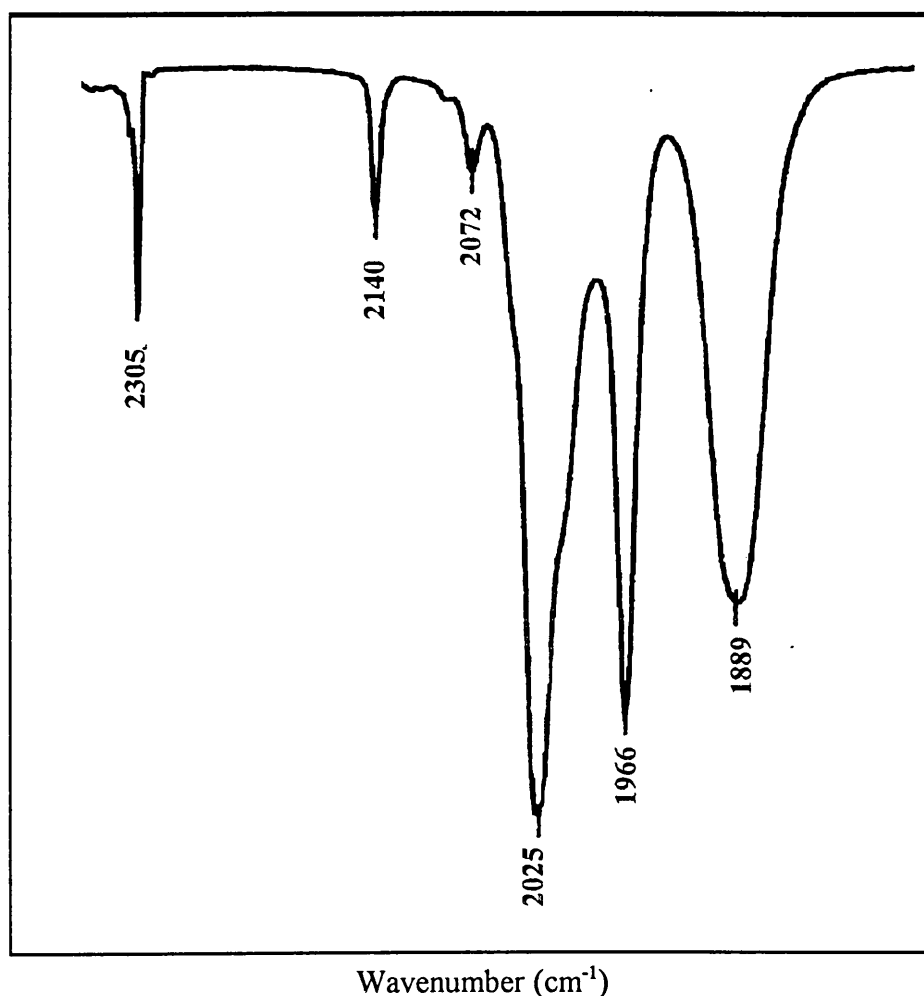


Figure 4.11 Carbonyl region on the infrared spectrum of **10**

4.3.2 NMR Spectroscopy

All NMR spectra were recorded in CDCl_3 unless indicated otherwise. The ^{13}C NMR spectra were recorded at -20°C in order to try and improve the resolution and to delay decomposition of the complexes. The following system of numbering the carbon and corresponding proton atoms of dibenzothiophene will be used throughout the whole discussion.

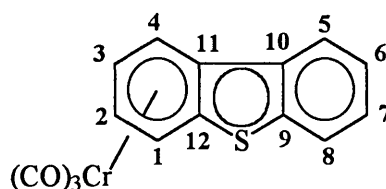


Figure 4.12 Numbering in dibenzothiophene complexes

^1H NMR Spectroscopy

The ^1H NMR data of the starting compound, $(\eta^6\text{-benzo}[b]\text{thiophene})\text{tricarboonylchromium}$ as well as the data of complexes **10** and **11** are summarized in table 4.3, while the ^1H NMR data of complexes **12** and **13** are reported in table 4.4. Figure 4.13 illustrates the ^1H NMR spectrum of **10**, while the ^1H NMR spectrum of **12** is depicted in figure 4.14.

Table 4.3 ^1H NMR data of $(\eta^6\text{-benzo}[b]\text{thiophene})\text{Cr}(\text{CO})_3$ and complexes **10** and **11**

Assignment	Complexes					
	Chemical shifts (δ , ppm) and coupling constants (J, Hz)					
	$(\eta^6\text{-BT})\text{Cr}(\text{CO})_3$		10		11	
	δ	$^3J_{\text{H-H}}$	δ	$^3J_{\text{H-H}}$	δ	$^3J_{\text{H-H}}$
H2	7.42 (d)	5.6	-	-	-	-
H3	7.07 (d)	5.7	7.39 (s)	-	7.52 (s)	-
H4	6.19 (d)	6.5	6.16 (d)	6.7	6.15 (d)	6.1
H5	5.24 (dd)	6.5 6.1	5.24 (dd)	6.7 6.1	5.25 (dd)	6.1 6.4
H6	5.41 (dd)	6.5 6.1	5.50 (dd)	6.1 5.7	5.51 (dd)	6.4 6.2
H7	6.26 (d)	6.5	6.21 (d)	5.7	6.23 (d)	6.2

The chemical shifts (ppm) of the protons of uncoordinated benzo[*b*]thiophene are: 7.40 (H2), 7.18 (H3), 7.67-7.92 (H4, H7) and 7.30 (H5, H6)^[15]. Rhenium has an electronegativity of 1.9 compared to manganese which has a value of 1.6. This affects the electron density at H3, thus causing a difference in the chemical shift as reflected in table 4.3. The metal fragment withdraws electron density from the arene ring, deshielding proton H3 and inducing a downfield shift. It can be deduced from the data in table 4.3 that the π -interaction between the arene ring and the second metal is insignificant and plays a negligible role in influencing the electron distribution of the arene ring. The remote protons H4-H7 are less affected by the coordination of the second metal. The chemical shift values of these protons of both products are similar to that of the starting compound. Figure 4.13 illustrates the proton NMR spectrum of compound **10**, which was recorded in acetone.

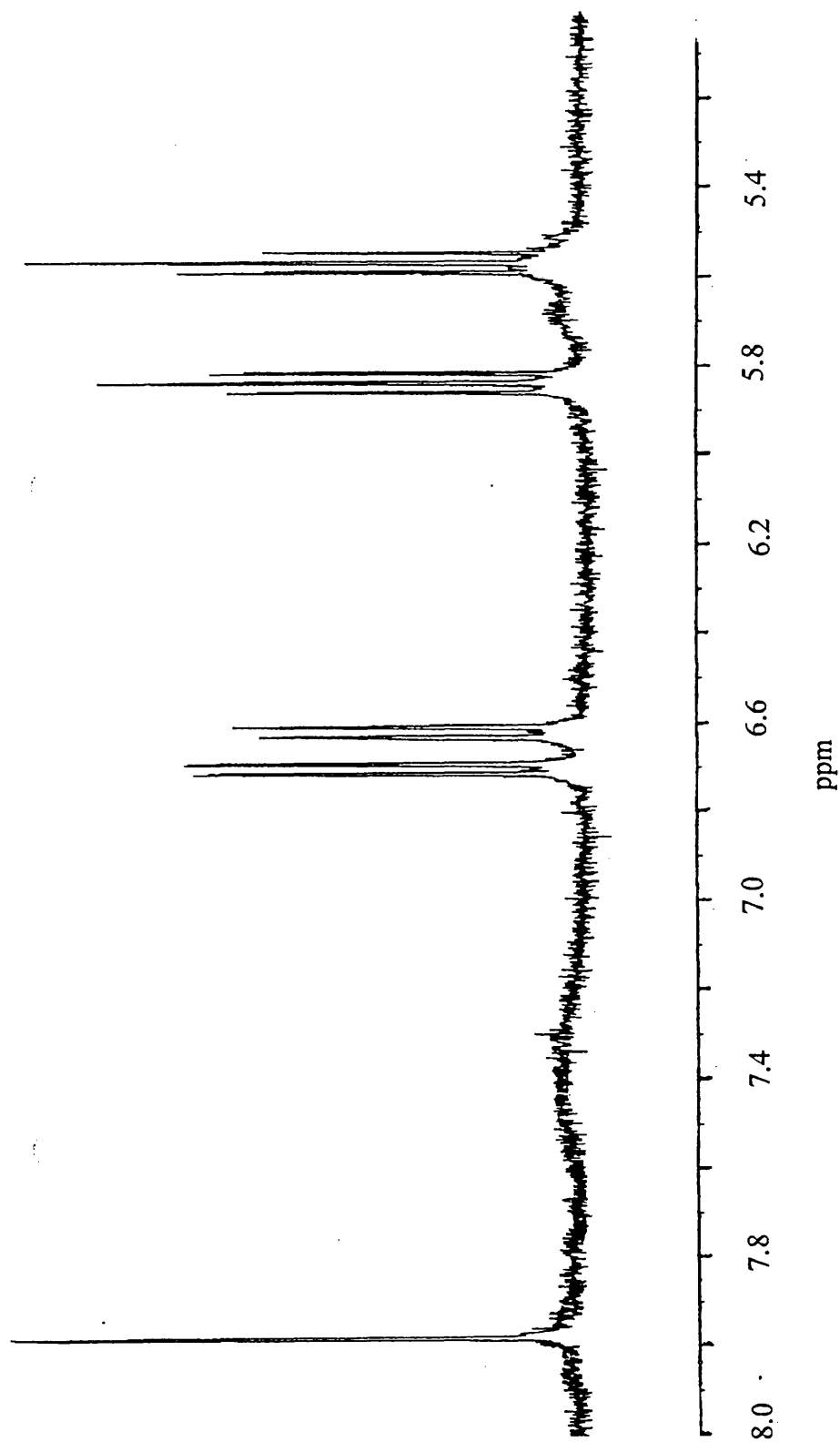


Figure 4.13 ^1H NMR spectrum of 10

Table 4.4 ^1H NMR data of complexes 12 and 13

Assignment	Complexes					
	Chemical shifts (δ , ppm) and coupling constants (J, Hz)					
	$(\eta^6\text{-DBT})\text{Cr}(\text{CO})_3$		12 ^a		13	
Proton	δ	$^3J_{\text{H-H}}$	δ	$^3J_{\text{H-H}}$	δ	$^3J_{\text{H-H}}$
H1	6.13 (dd)	6.7	-	-	-	-
H2	5.53 (ddd)	6.7 6.0	6.81 (d)	6.3	8.52 (d)	7.4
H3	5.28 (ddd)	6.6 6.8	5.86 (dd) ^b	6.5	7.75 (dd)	7.7
H4	6.38 (dd)	6.5	7.06 (d)	6.5	8.21 (d)	8.9
H5	7.95 (ddd)	8.3	8.39 (d)	7.8	7.96 (d)	8.9
H6	7.46 (dd)	8.3 7.6	8.29 (dd) ^b	4.6	7.51 (dd) ^b	5.5
H7	7.46 (dd)	8.3 7.6	8.30 (dd) ^b	5.0	7.50 (dd) ^b	7.2
H8	7.72 (ddd)	8.3	8.58 (d)	7.5	8.45 (d)	7.6

^a Recorded in deuterated acetone as solvent^b Seems like a triplet on the spectrum

The chemical shift values (ppm) of uncoordinated dibenzothiophene are: 8.00 (H1, H8), 7.75 (H4, H5) and 7.40 (H2, H3, H6, H7)^[16]. For compound 13, the electropositive rhenium metal, compared to a hydrogen, removes electron density from the arene ring, resulting in the significant downfield shift of H2 (~1.1 ppm). All the protons on the arene ring are affected, some more deshielded than others, by the σ -coordination to the metal fragment when compared to the chemical shift values of the uncoordinated ligand (DBT).

In compound **12** this same trend is observed, but the π -coordination of the $\text{Cr}(\text{CO})_3$ -moiety to the same ring fragment as where the σ -coordination occurred, “softened” the effect caused by this σ -bond. An increase of electron density on this ring fragment ensued, leaving the uncoordinated benzene ring fragment even more electron deficient. This explains the definite downfield shift of the uncoordinated benzene ring protons, when compared to both the uncoordinated ligand (DBT) as well as the starting compound $(\eta^6\text{-DBT})\text{Cr}(\text{CO})_3$. However, the π -coordination of the $\text{Cr}(\text{CO})_3$ caused an upfield shift of the protons H2, H3 and H4 compared to the chemical shifts of the same protons on the spectrum of compound **13**.

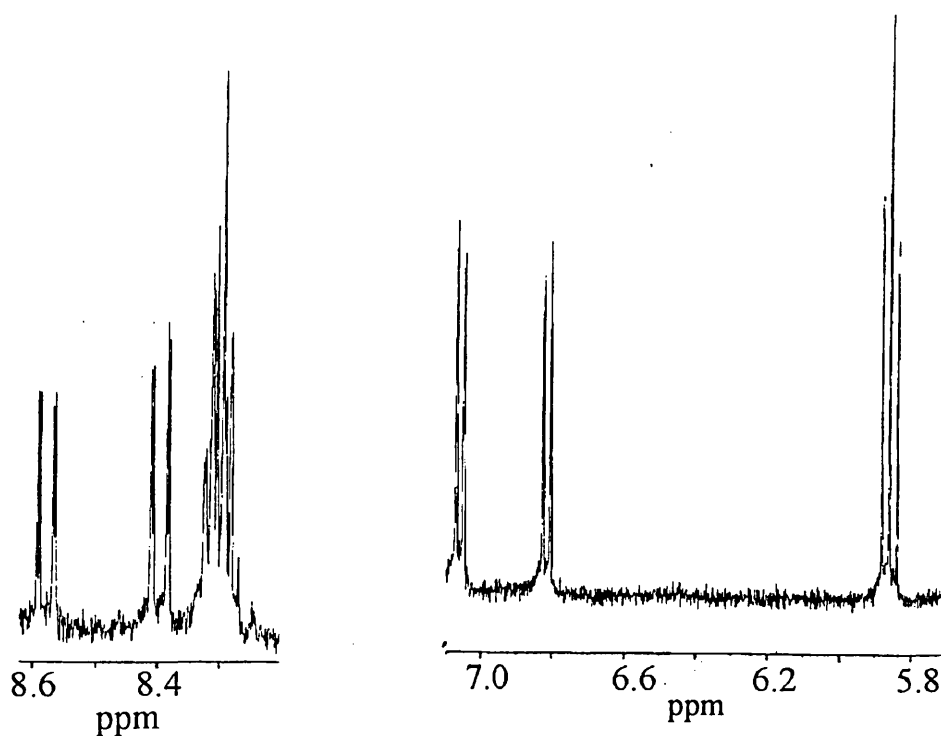


Figure 4.14 ^1H NMR spectrum of **12**

^{13}C NMR Spectroscopy

The ^{13}C NMR data of complexes **10** and **11** as well as the data of the starting compound, $(\eta^6\text{-benzo}[b]\text{thiophene})\text{tricarboonylchromium}$, are summarized in table 4.5.

Table 4.5 ^{13}C NMR data^a of complexes 10 and 11

Assignment	Complexes		
	Chemical shifts (δ , ppm)		
	$(\eta^6\text{-BT})\text{-Cr}(\text{CO})_3$	10	11
Carbon	δ	δ	δ
C2	131.3	150.3	150.2
C3	123.4	128.0	128.4
C4	88.6	89.1	89.2
C5	89.7	91.3	89.5
C6	90.6	93.5	91.7
C7	86.9	86.1	85.6
C8	115.5	n.o.	n.o.
C9	110.3	n.o.	n.o.
$\text{M}(\text{CO})_3$	232.7	n.o.	231.8
$\text{M}(\text{CO})_5$	-	207.6	206.6

^a Assignments were based on those for the free benzo[*b*]thiophene

The chemical shift values (ppm) of the uncoordinated benzo[*b*]thiophene are: 126.4 (C2), 124.0 (C3), 123.8 (C4), 124.3 (C5), 124.4 (C6), 122.6 (C7), 139.9 (C8), 139.8 (C9)^[17]. The trend in the ^1H NMR spectra is repeated in the ^{13}C NMR spectra. The arene ring fragment bonded to the second metal is affected by this coordination, whereas the values for the remote carbon atoms differ only slightly from the values of the starting compound. The chemical shift values (ppm) for uncoordinated dibenzothiophene are: 122.6 (C1, C8), 127.8 (C2, C7), 125.4 (C3, C6), 123.6 (C4, C5), 134.9 (C9, C12), 138.5 (C10, C11). The chemical shift values (ppm) for compound 13 are: 206.0 (C1), 137.5 (C2), 126.5 (C3), 125.6 (C4), 122.7 (C5), 124.2 (C6), 124.8 (C7), 121.4 (C8), 133.6 (C9), 141.7 (C10), 143.6 (C11), 137.5 (C12), 187.5 ($\text{Re}(\text{CO})_5$).

Spectroscopic evidence seems to indicate that a carbonyl inserted product formed from compound 13. While recording the ^{13}C NMR spectrum, it was observed that an equilibrium mixture was formed after a while (figure 4.15). The data originating from this compound is clearly visible on

the spectrum. The inserted carbonyl ligand generates a signal at 281 ppm, while the signal for the pentacarbonyl fragment is detected at 190 ppm. The chemical shift value of C1 is observed at 210 ppm. Comparing these values with those acquired for compound **13**, the electron withdrawing effect of the carbonyl is evident. The carbon atoms are deshielded and experience a downfield shift.

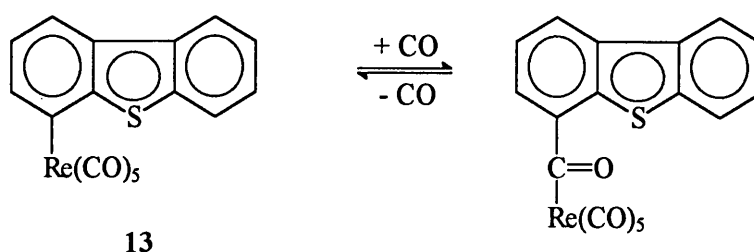


Figure 4.15 Carbonyl insertion reaction of **13**

4.3.3 Mass Spectrometry

The m/z -values of the molecular ion as well as the fragment ions in the mass spectra of compounds **10**, **11** and **13** are shown in table 4.6. The molecular ion peak was observed for all three compounds.

Table 4.6 Fragment ions in the mass spectra of compounds **10**, **11** and **13**

Complex	Mass peaks, m/z (I, %)
10	597 (10) [M^+], 429 (22) [$M^+ - 6 CO$], 320 (2) [$BTRe^+$], 134 (12) [BT^+]
11	463 (12) [M^+], 435 (5) [$M^+ - CO$], 407 (17) [$M^+ - 2CO$], 379 (10) [$M^+ - 3CO$], 351 (12) [$M^+ - 4CO$], 323 (38) [$M^+ - 5CO$], 296 (5) [$M^+ - 6CO$], 268 (39) [$M^+ - 7CO$], 240 (100) [$M^+ - 8CO$], 185 (32) [$BTCr^+$], 134 (45) [BT^+]
13	510 (41) [M^+], 482 (16) [$M^+ - CO$], 454 (54) [$M^+ - 2 CO$], 426 (42) [$M^+ - 3CO$], 398 (22) [$M^+ - 4CO$], 370 (77) [$M^+ - 5CO$], 184 (53) [DBT^+]

A general pattern in the fragmentation of all three compounds can be recognized. Initially the loss of all the carbonyl ligands ensues. For compounds **10** and **13** this is followed by the loss of the Cr-atom before the second metal, Re. Re succeeds the loss of the first metal to leave the uncoordinated fragment ions, BT^+ or DBT^+ . The opposite is observed for compound **11**, where the Mn-atom is first to go, followed by the Cr-atom. This result again confirms the observation that the Re-C bond is stronger than the Mn-C bond in organometallic compounds. Figure 4.16 depicts the mass spectrum of compound **13**.

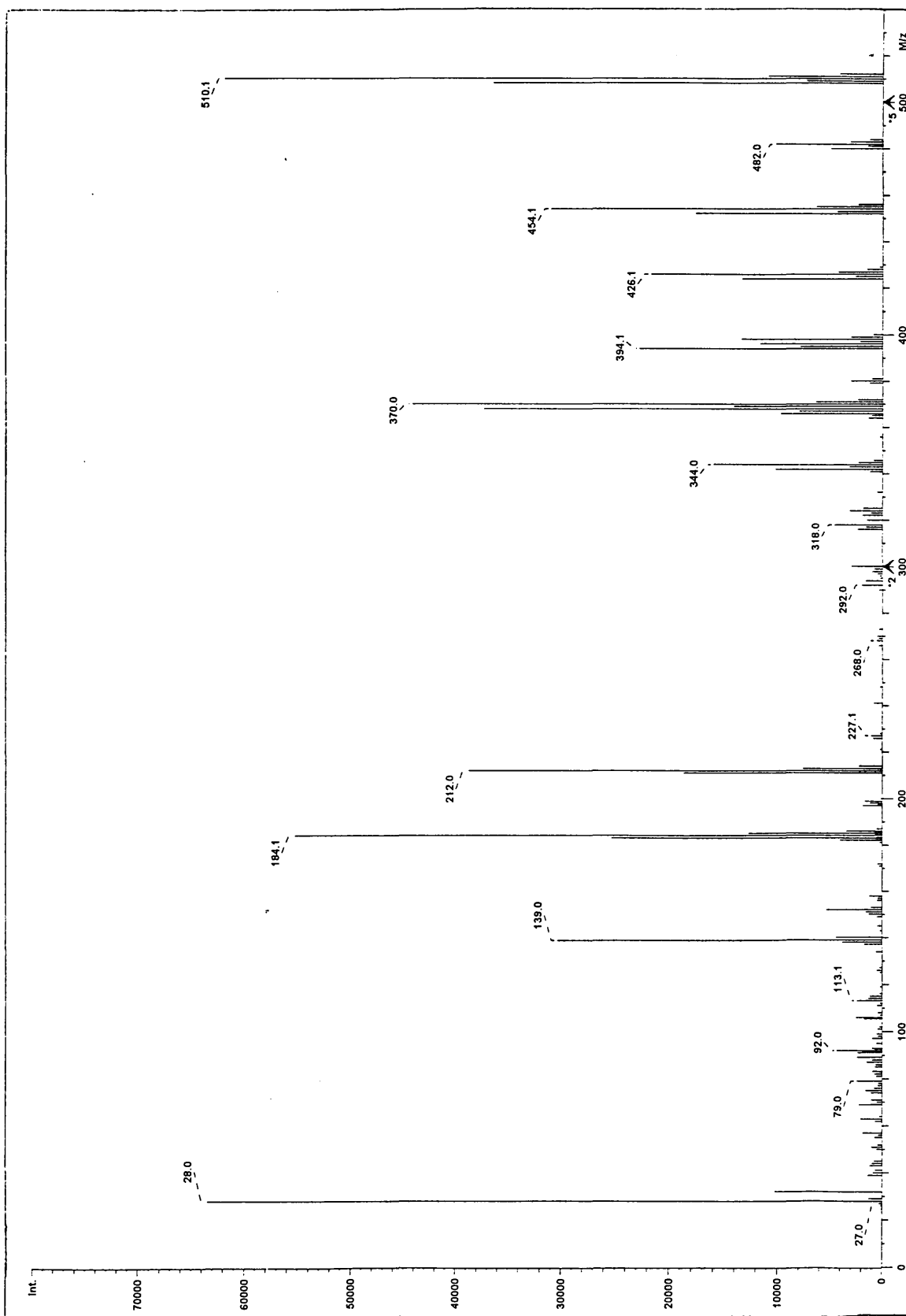


Figure 4.16 Mass spectrum of compound 13

4.4 References

- (1) T. Waldbach, *Heterobimetallic Complexes of Chromium, Manganese, Titanium and Rhenium with σ, π -bridging Thiophene, Selenophene and Substituted Thiophene*, Ph.D. Thesis, University of Pretoria, Pretoria, 1994.
- (2) R.J. Angelici, J.A. Rudd, *Inorg. Chim. Acta*, **1995**, *240*, 393.
- (3) M.J. Robertson, C.L. Day, R.A. Jacobson, R.J. Angelici, *Organometallics*, **1994**, *13*, 179.
- (4) S. Lotz, M. Schindehutte, P.H. van Rooyen, *Organometallics*, **1992**, *11*, 629.
- (5) T.A. Waldbach, P.H. van Rooyen, S. Lotz, *Organometallics*, **1993**, *12*, 4250.
- (6) T.A. Waldbach, P.H. van Rooyen, S. Lotz, *Angew. Chem. Int. Ed. Eng.*, **1993**, *32*, 710.
- (7) M. Schindehutte, S. Lotz, P.H. van Rooyen, *Organometallics*, **1992**, *11*, 629.
- (8) M. Novi, G. Guanti, C. Dell'Erba, *J. Heterocycl. Chem.*, **1975**, *12*, 1055.
- (9) J.A. Connor, D.L.S. Brown, H.A. Skinner, *J. Organomet. Chem.*, **1974**, *81*, 403.
- (10) A.N. Nesmeyanov, I.G. Polovyanyuk, L.G. Makarova, *Dokl. Akad. Nauk SSSR*, **1976**, *230*, 1351.
- (11) N.E. Kolobova, L.V. Goncharenko, *Izv. Akad. Nauk SSSR, Ser. Khim.*, **1979**, *4*, 900.
- (12) L.M. Haines, M.H.B. Stiddard, *Adv. Inorg. Chem. Radiochem.*, **1969**, *12*, 53.
- (13) S.P. Schmidt, J. Nitschke, W.C. Trogler, *Inorg. Synth.*, **1989**, *26*, 116.
- (14) M.H. Quick, R.J. Angelici, *Inorg. Synth.*, **1990**, *28*, 156.
- (15) E.O. Fischer, H.A. Goodwin, C.G. Kreiter, D.D. Simmons Jr., K. Sonogashira, S.B. Wild, *J. Organomet. Chem.*, **1968**, *14*, 359.
- (16) F. Balkau, M.L. Heffernan, *Aust. J. Chem.*, **1971**, *24*, 2305.
- (17) B. Iddon, R.M. Scrowton, *Adv. Heterocycl. Chem.*, **1970**, *11*, 178.

5 σ, π -Heteroarene Bimetallic complexes of Platinum and Chromium

5.1 Introduction

The chemistry of platinum-group metals is of current interest for several reasons:

- (i) Platinum group metals show the highest HDS activity^[1];
- (ii) Stereoregularity in conducting polymers (CP) may be improved by the synthesis of polymeric bimetallic complexes of platinum^[2];
- (iii) Platinum complexes show antitumour activity^[3].

Platinum has played a major role in the development of organometallic chemistry. The first organometallic compound containing an unsaturated hydrocarbon ligand was $[\text{Pt}(\text{C}_2\text{H}_4)\text{Cl}_2]_2$ and was discovered by W.C. Zeise in 1827. In 1831 he also reported the compound $\text{K}[\text{Pt}(\text{C}_2\text{H}_4)\text{Cl}_3] \cdot \text{H}_2\text{O}$, today known as Zeise's salt. In 1907 Pope prepared the platinum methyls, which were among the first-known transition metal alkyls.

Cis-diamminedichloroplatinum(II) ("cisplatin") has been known as Peyrone's chloride since 1845. It played an important role in Werner's elucidation of geometrical isomerism^[4] and enabled Chernyaev to postulate the "trans effect" theory. Nevertheless, it was not until 1969 that its anti-cancer properties were discovered by chance^[5]. Cisplatin, *cis*- $[\text{Pt}(\text{NH}_3)_2\text{Cl}_2]$, was found to have activity against ovarian, head, neck, bladder and lung cancers. Once the activity of cisplatin had been established, analogues were developed in the hope of reducing the dose and improving the spectrum of activity.

Relatively few π -coordinated platinum compounds are known. η^2 -arene complexes are rare and are mostly found among the later transition metals, e.g. platinum and palladium. The only known

η^2 -arene platinum complex, is the fluxional $[\eta^2-(C_6(CF_3)_6)Pt(PEt_3)_2]$ complex.

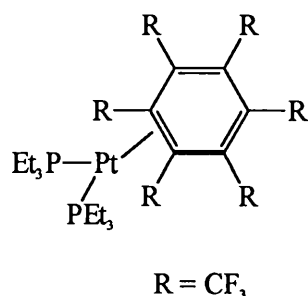


Figure 5.1 The complex $[\eta^2-(C_6(CF_3)_6)Pt(PEt_3)_2]$

The only known bimetallic η^5 -arene complexes containing Pt, are complexes where thiophene is the bridging arene ligand^[6]. The complexes were prepared by lithiation of $(\eta^5-C_4H_4S)Cr(CO)_3$ and the addition of a platinum(II) reagent. The platinum(II) reagents used were *cis*-PtCl₂(dppe) and *cis*-PtCl₂(PMe₃)₂. The resulting bimetallic complexes were obtained in relatively low yield.

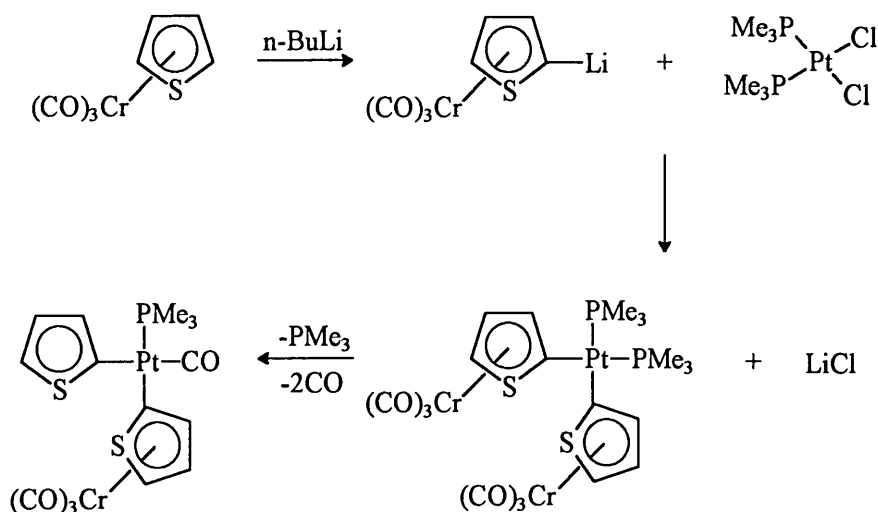


Figure 5.2 Synthesis of $[\eta^1:\eta^5-(C_4H_4S)\{Pt(CO)(C_4H_4S)(PMe_3)_2\}]Cr(CO)_3$

The expected product, $[\eta^1:\eta^5-(C_4H_4S)\{Pt(PMe_3)_2Cl\}]Cr(CO)_3$, was not obtained but instead the labile chlorine ligand was substituted by another $(\eta^5-C_4H_4S)Cr(CO)_3$ -moiety, which eventually lost the $Cr(CO)_3$ -fragment. One of the labile PMe_3 -ligands was displaced by a CO-ligand. The CO-ligand is a better π -acceptor than the phosphine ligand and not as labile. It can also accommodate

excess electron density on the platinum through π -backbonding.

In the attempt to stabilize a phosphine ligand on the Pt in the *cis*-position with respect to the ligand $(\eta^5\text{-C}_4\text{H}_4\text{S})\text{Cr}(\text{CO})_3$, the PMe_3 -ligands were replaced with the bidentate ligand bis(diphenylphosphino)ethane (dppe). Again the expected product, $[\eta^1:\eta^5\text{-}(\text{C}_4\text{H}_3\text{S})\{\text{Pt}(\text{dppe})\text{Cl}\}]\text{Cr}(\text{CO})_3$, was not yielded but instead $[\eta^1:\eta^5\text{-}(\text{C}_4\text{H}_3\text{S})\{\text{Pt}(\text{dppe})(\text{C}_4\text{H}_3\text{S})\}]\text{Cr}(\text{CO})_3$ was isolated. The remaining chlorine ligand is too labile and is substituted by a thienyl ligand. For both compounds it has been noticed that only one of the thiophene substituents is π -coordinated. It has been suggested that the main reason for this occurrence can be ascribed to steric reasons. Two *cis* π -coordinated thiophene substituents in a square planar complex are too bulky, and results in the loss of one $\text{Cr}(\text{CO})_3$ -fragment.

An alternative method could be followed to synthesize these bimetallic π -thiophene platinum complexes, in an attempt to improve the yield of the products. Eaborn *et al.*^[7] reported the employment of aryltin compounds for attaching aryl groups to platinum. Although RSnMe_3 (R = aryl) compounds do not react with bis(phosphine) complexes, they can be implemented to synthesize compounds of the form $[\text{Pt}(\text{COD})\text{RCl}]$ and $[\text{Pt}(\text{COD})\text{R}_2]$. Subsequent ligand replacement reactions are used to yield the analogous bis(phosphine) complexes. This preparation method is especially attractive since the by-product, SnMe_3Cl , is highly soluble in common non-polar solvents such as diethyl ether and pentane, and can be easily removed from the reaction mixture by thorough washing with one of these solvents.

Few examples of heterocyclic organotin(IV) compounds where the tin substituent is directly bonded to a carbon atom on the arene ring^[8] are known in literature, which can possibly be explained by the weakness of the Sn-C bond. The following bimetallic $(\pi\text{-thiophene})\text{Cr}(\text{CO})_3$ tin(IV) complexes (figure 5.3) were prepared and can be further explored for utilization as precursors in the syntheses of bimetallic $(\pi\text{-thiophene})\text{Cr}(\text{CO})_3$ platinum(II) complexes.

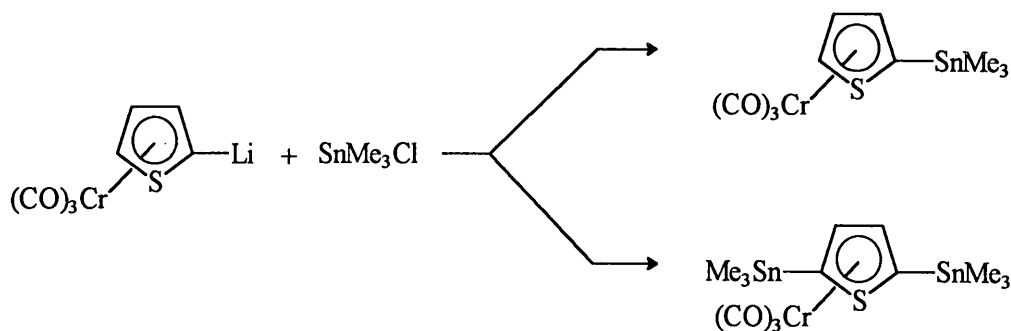


Figure 5.3 Synthesis of $[\eta^1:\eta^5\text{-}(\text{C}_4\text{H}_3\text{S})(\text{SnMe}_3)]\text{Cr}(\text{CO})_3$ and $[\eta^1:\eta^1:\eta^5\text{-}(\text{C}_4\text{H}_2\text{S})\{2,5\text{-}(\text{SnMe}_3)_2\}]\text{Cr}(\text{CO})_3$

The tin(IV) substituent can be easily replaced by a platinum(II) substituent. In this case the weakness of the Sn-C bond is used as an advantage.

5.2 Synthesis of $[\eta^1:\eta^6\text{-benzo}[b]\text{thienyl}(\text{Cr}(\text{CO})_3)_2\text{Pt}(\text{dppe})]$

The approach to the synthesis of the $(\pi\text{-benzo}[b]\text{thiophene})\text{Cr}(\text{CO})_3$ platinum(II) complex was *via* the lithiation of $(\eta^6\text{-BT})\text{Cr}(\text{CO})_3$ followed by the addition of $\text{Pt}(\text{dppe})\text{Cl}_2$, and not by applying the aryltin method described by Eaborn *et al*^[7].

The deprotonation of $(\eta^6\text{-BT})\text{Cr}(\text{CO})_3$ to yield the metallated complex, was readily achieved by reacting one equivalent of the complex with 1.1 equivalents of *n*-butyllithium in THF at -40°C . The $\text{Pt}(\text{dppe})\text{Cl}_2$ complex was added and, after purification, afforded the bimetallic complex $[\eta^1:\eta^6\text{-BT}(\text{Cr}(\text{CO})_3)_2\text{Pt}(\text{dppe})]$ (**14**). It is interesting to note that, as reported in literature^[6], the product containing one remaining Cl-ligand on the Pt could not be isolated; instead the product contained two BT-ligands, both coordinated to a $\text{Cr}(\text{CO})_3$ -moiety. The suggestion that σ -coordination of $\text{Pt}(\text{dppe})\text{Cl}_2$ to $(\eta^6\text{-BT})\text{Cr}(\text{CO})_3$ labilizes the remaining chlorine ligand on the platinum, is confirmed by this result. Figure 5.4 presents a schematic outline for the synthesis.

5.3 Spectroscopic characterization

5.3.1 Infrared Spectroscopy

On the IR spectrum of compound **14** only a $\text{Cr}(\text{CO})_3$ -moiety was visible and the two vibrational bands characteristic to $\text{M}(\text{CO})_3$ species, the A_1 and the E bands, could be clearly distinguished. The IR spectra were recorded in dichloromethane. In figure 5.6 the IR spectrum of **14** is illustrated. The two vibrational bands are present on this spectrum.

Table 5.1 IR-data of the starting compound $(\eta^6\text{-BT})\text{Cr}(\text{CO})_3$ and **14**

Vibrational band	Complexes	
	ν_{CO} (cm^{-1})	
	$(\eta^6\text{-BT})\text{Cr}(\text{CO})_3$	14
A_1	1964 s	1949 s
E	1885 vs	1866 vs

Comparing the values of the vibrational bands of the starting complex and compound **14**, it is observed that the wavenumbers for the $\text{Cr}(\text{CO})_3$ bands in the spectrum of **14** is lower than in the spectrum of the starting compound, $(\eta^6\text{-BT})\text{Cr}(\text{CO})_3$. This decrease signifies an increase in the bond order of the Cr-CO bond and a concurrent decrease in the bond order of the C-O bond. Two reasons can be put forward to explain this phenomenon:

- (i) Since platinum(II) is a d^8 -species, it qualifies as electron-rich as a result of its filled d-orbitals. It is probable that π -interaction plays an important role, since backbonding can occur from the filled t_{2g} orbitals of platinum into π^* -orbitals of the arene ligand, placing electron density on the ring.
- (ii) The σ -coordination of the electron-rich platinum ligand to the arene ring, can also enhance the electron density on the ring. Polarization of the σ -bond in the direction of the arene ring can occur due to the electron donating ability of the platinum. Since the electronegativity of platinum (1.4) is less than that of hydrogen

(2.2), it supports the argument that the replacement of a proton by a Pt-fragment will lead to a more polarized bond.

Both these arguments promote the increase of electron density on the arene ring and the subsequent effect this has on the $\text{Cr}(\text{CO})_3$ -moiety. The electron rich ring donates electron density to the Cr-nucleus, thus augmenting the strength of the Cr-C bond.

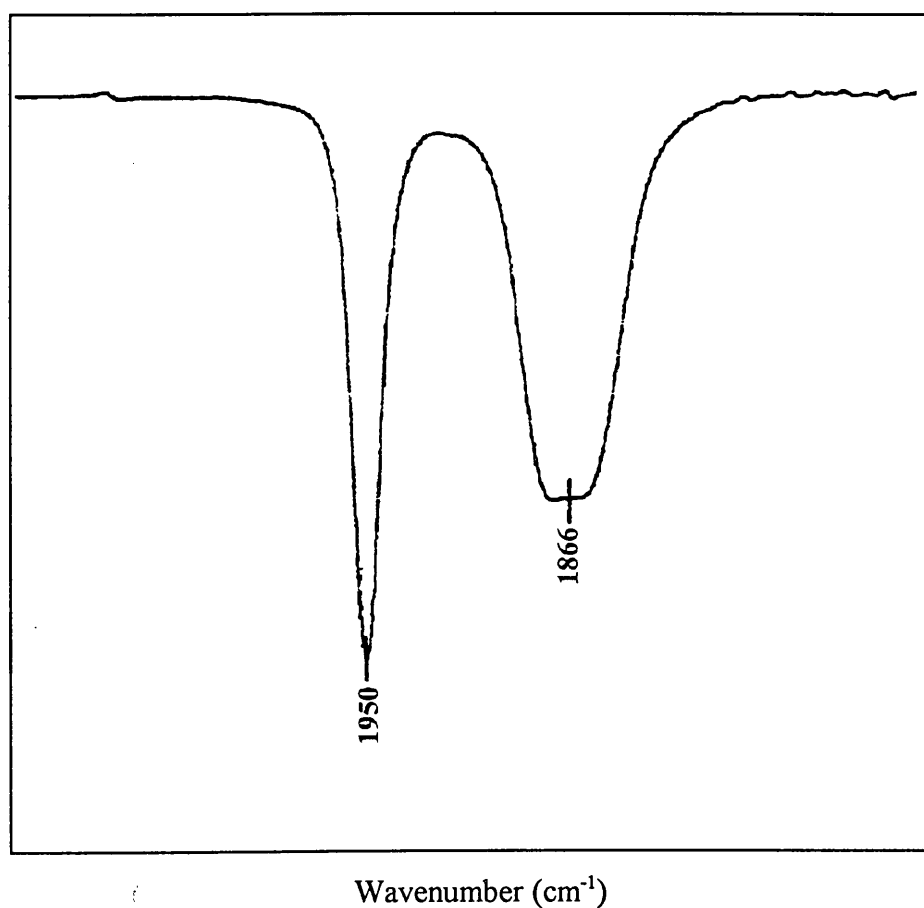


Figure 5.6 Carbonyl region on the infrared spectrum of **14**

5.3.2 NMR Spectroscopy

The system of numbering the carbon atoms and the associated protons will be as follows:

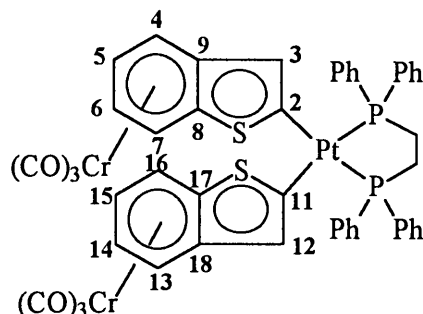


Figure 5.7 Atom numbering of compound **14**

The ^1H NMR spectrum was recorded in CDCl_3 as deuterated solvent. Due to the low solubility of the product in CDCl_3 , another solvent was tested. The ^{13}C NMR spectrum was recorded in deuterated acetone at -20°C in order to try and improve the resolution and to delay decomposition of the complex.

^1H NMR Spectroscopy

The ^1H NMR data of the starting compound, $(\eta^6\text{-benzo}[b]\text{thiophene})\text{tricarbonylchromium}$ as well as that of complex **14**, are summarized in Table 5.2.

The expected singlet, H2, was not observed on this spectrum of compound **14**. It is suggested that this signal overlaps with the multiplet signal obtained, representing the phenyl protons. The well-known trend is again perceived in that the π -coordination causes an upfield shift of the relevant protons.

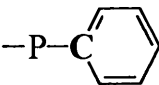
Table 5.2 ^1H NMR data of complex 14

Assignment	Complexes			
	Chemical shifts (δ , ppm) and coupling constants (J, Hz)			
	$(\eta^6\text{-BT})\text{Cr}(\text{CO})_3$		14	
	δ	$^3J_{\text{H-H}}$	δ	$^3J_{\text{H-H}}$
H2	7.42 (d)	5.6	-	-
H3	7.07 (d)	5.7	n.o.	-
H4	6.19 (d)	6.5	5.78 (d)	6.5
H5	5.24 (dd)	6.5 6.1	5.04 (dd)	6.5 6.0
H6	5.41 (dd)	6.5 6.1	5.12 (dd)	6.5 6.0
H7	6.26 (d)	6.5	6.02 (d)	6.2
$-\text{CH}_2$	-	-	2.33 (s)	-
Ph	-	-	7.40-7.50 (m)	-

 ^{13}C NMR Spectroscopy

The ^{13}C NMR data of the starting compound, $(\eta^6\text{-benzo}[b]\text{thiophene})\text{tricarboxylchromium}$, as well as that of complex 14, are summarized in Table 5.3.

Table 5.3 ^{13}C NMR data^a of complex 14

Assignment	Complexes	
	Chemical shifts (δ , ppm)	
	$(\eta^6\text{-BT})\text{Cr}(\text{CO})_3$	14
Carbon	δ	δ
C2, C11	131.3	151.1
C3, C12	123.4	125.0
C4, C13	88.6	89.4
C5, C14	89.7	90.3
C6, C15	90.6	91.1
C7, C16	86.9	n.o.
C8, C17	115.5	n.o.
C9, C18	110.3	105.8
M(CO) ₃	232.7	235.6
-CH ₂	-	30.6
	-	134.2
C ₆ H ₅ (<i>ortho</i>)	-	134.2
C ₆ H ₅ (<i>meta</i>)	-	129.8
C ₆ H ₅ (<i>para</i>)	-	132.2

^a Assignments were based on those for the free benzo[*b*]thiophene

The ^{13}C NMR spectrum of compound 14 is represented in figure 5.8. On the spectrum of compound 14 it is obvious that both benzo[*b*]thiophene ligands are π -coordinated to a $\text{Cr}(\text{CO})_3$ -moiety, since the characteristic uncoordinated benzene signals are absent. While both carbon and phosphorus have a spin quantum number of $\frac{1}{2}$, the two nuclei couple to one another. This coupling is clearly visible at the phenyl signals. The magnitude of the coupling of the phosphorus to the *ortho* carbons is 20.5 Hz, while the coupling to the *meta* carbons has a value of 10.9 Hz. Coupling to the *para* carbon was not observed. Also, coupling of Pt with C(2) of the benzothienyl

ligands was not observed.

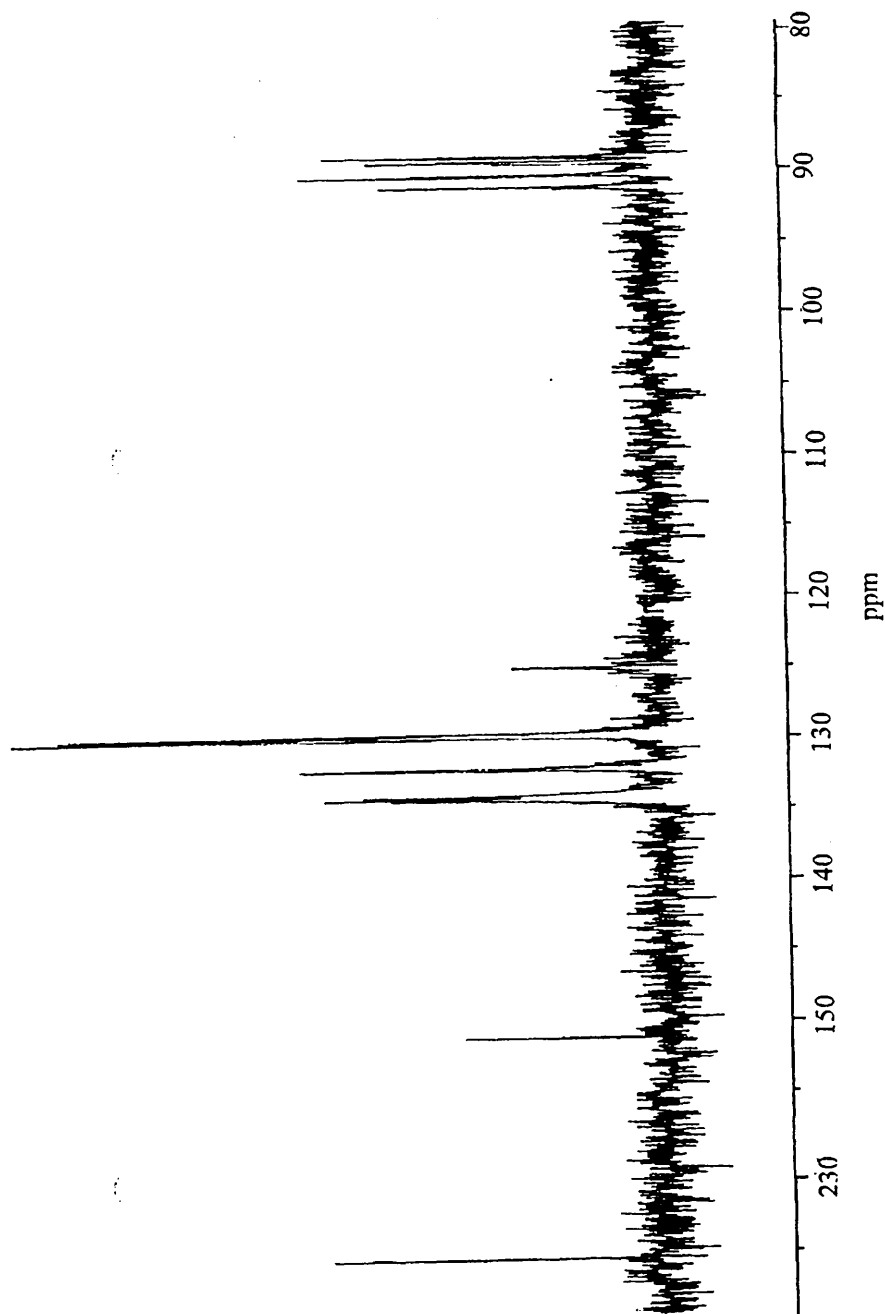


Figure 5.8 Part of the ^{13}C spectrum of compound 14

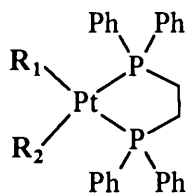
^{31}P NMR Spectroscopy

A phosphorus program using H_3PO_4 as internal standard was used to obtain the chemical shifts of this spectrum. The spectrum was recorded in deuterated acetone as solvent. The ^{31}P data of the reagent $\text{Pt}(\text{dppe})\text{Cl}_2$ as well as that of compound **14** are compared in table 5.4.

Table 5.4 ^{31}P data of compound **14**

Assignments	Chemical shifts (δ , ppm) and coupling constants (J, Hz)	
	δ	$^1J_{\text{P-Pt}}$
Complexes		
$\text{Pt}(\text{dppe})\text{Cl}_2$	47.0	3618
14	44.5	2072

From the ^{31}P spectrum of compound **14** it is apparent that the compound contains two identical substituents, since only one signal was observed. The coupling constant differs considerably when the substituents on the platinum is varied. This difference is evident in table 5.5, where literature values^[9] are reported for the various substituents on complex **A**.

Table 5.5 $^1J_{\text{P-Pt}}$ coupling constants of compound **A****A**

Sustituents		$^1J_{\text{P-Pt}}$ (Hz)	
R_1	R_2	<i>trans</i> (to R_2)	<i>cis</i> (to R_2)
Thienyl	Cl	3929	1973
Furanyl	Cl	3986	1875
Phenyl	Cl	4165	1663
CH_3	CH_3	1783	1783
$(\eta^6\text{-T})\text{-Cr}(\text{CO})_3$	Thienyl	2233	2117

The presumption^[10] was made that the difference in coupling constants of the various trialkylphosphine complexes of platinum(II) arises due to deviation in the covalency (s-character) of the Pt-P bond. The magnitude of the coupling constant decreases with decreasing covalent character of the Pt-P bond. The nature of the *trans* ligand affects the coupling constant, since the covalency of the Pt-P bond is influenced. *Trans* influence is defined as the tendency of a ligand to weaken the bond *trans* to itself. It results in the increase of the σ -donor ability of the ligand, ensuing in the increase in s-character of the ligand-Pt bond. This increase is concurrent with a decrease in s-character of the Pt-P bond of the phosphine ligand. A lower value for $^1J_{\text{P-Pt}}$ is obtained. Explanations for *trans* influence seem to involve both π - and σ effects. The ligands exerting the strongest *trans* influence are those whose bonding to a metal is thought to exhibit the most π -character and are able to remove π -electron density from the metal. This reduces the electron density at the *trans* coordination site, weakening the bond. On the other hand, a strong σ -donor ligand can produce polarization of the metal, since its lone pair induces a positive charge on the near side of the metal and a negative charge on the far side. The *trans* bond will be weakened. The approximate order of increasing *trans* influence, comparing tables 5.4 and 5.5, is:



This sequence implies that the π -coordination of a $\text{Cr}(\text{CO})_3$ -fragment to a ligand, improves the π -acceptor ability of that ligand. This assumption is consistent with previous arguments that the formation of a $(\eta^6\text{-arene})\text{Cr}(\text{CO})_3$ complex reduces the electron density on the arene ring and promotes backbonding from the metal.

In conclusion: For both early (Ti) and late (Pt) transition metal substituents in σ, π -bimetallic complexes the benzo[*b*]thiophene ligand activates the remaining chloro ligand to such an extent that a second lithiated benzothiophene unit displaces this chloro ligand. This effect is greater for PtL_2Cl_2 (L = diphos) than for TiL_2Cl_2 (L = Cp).

5.4 References

- (1) E. Viola, C. Lo Sterzo, R. Crescenzi, G. Frachey, *J. Organomet. Chem.*, **1995**, 493, C9.
- (2) S. Kotani, K. Shiina, K. Sonogashira, *J. Organomet. Chem.*, **1992**, 429, 403.
- (3) B. Rosenberg, L. van Camp, T. Krigas, *Nature*, **1965**, 205, 698.
- (4) A. Werner, *J. Chem. Ed.*, **1966**, 43, 155.
- (5) B. Rosenberg, L. van Camp, J.E. Trasko, V.H. Mansour, *Nature*, **1969**, 222, 385.
- (6) A. du Toit, *Applications of transition metals in thiophene activation*, M.Sc Thesis, University of Pretoria, Pretoria, **1995**.
- (7) C. Eaborn, A. Pidcock, R.R. Steele, *J. Chem. Soc. Chem. Comm.*, **1968**, 1051.
- (8) V.G. Kumar Das, Lo Kong Mun, *J. Organomet. Chem.*, **1987**, 334, 307.
- (9) S. Berger, S. Braun, H. Otto, *NMR-Spektroskopie von Nichtmetallen*, **1993**, 3; Georg Thieme Verlag, Stuttgart.
- (10) F. H. Allen, A. Pidcock, *J. Chem. Soc. A*, **1968**, 2700.

6

Experimental

6.1 Standard Operational Procedure

The synthesis and characterization of the compounds were performed in an inert atmosphere of nitrogen or argon gas. Solvents were dried in an inert atmosphere according to conventional laboratory methods. All chemicals were used without prior purification, unless stated otherwise elsewhere. Column chromatography, using Kieselgel 60 (particle size 0.0063-0.200 mm), was used for all separations. The column was cooled by circulating cold isopropanol (-30°C) through the column jacket.

6.2 Characterization techniques

6.2.1 Infrared Spectroscopy

Infrared spectra were recorded on a Bomem Michelson-100 FT spectrophotometer. All spectra were recorded using either dichloromethane or hexane as solvent. Vibrational bands in the carbonyl stretching region (ca. 1500-2200 cm^{-1}) are reported only.

6.2.2 Nuclear Magnetic Resonance Spectroscopy

NMR spectra were recorded on a Bruker AC-300 spectrometer. ^1H NMR spectra were recorded at 300.135 MHz and ^{13}C NMR spectra at 75.469 MHz. The signal of the deuterated solvent was used as reference, e.g. ^1H CDCl_3 7.24 ppm and ^{13}C CDCl_3 77.0 ppm.

6.2.3 Mass Spectrometry

The mass spectra were recorded on a Perkin-Elmer RMU-6H instrument operating at 70 eV.

6.2.4 X-ray Crystallography

The Röntgen structure analysis was done using a Enraf-Nonius CAD 4 diffractometer with graphite monochromatized Mo-K α radiation. The data was processed and the structures solved with the aid of the Patterson method employing the SHELX 76 and SHELX 86 programmes.

6.3 Preparation of Starting Compounds

The following compounds were prepared according to known literature methods:

Trisammine(tricarbonyl)chromium^[1], [1,2-Bis(diphenylphosphino)ethane]platinum(II)chloride ^[2], Rheniumpentacarbonyltriflate^{[3],[4]}, Manganesepentacarbonylbromide^[5] and 3,6-Dimethylthieno-[3,2-*b*]thiophene^[6].

6.4 Synthesis of Organometallic Compounds

6.4.1 Preparation of π -heteroarene complexes

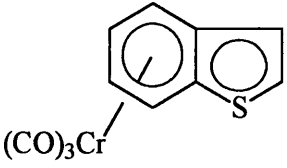
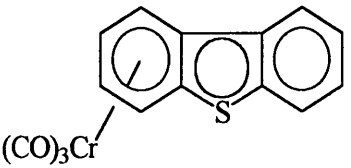
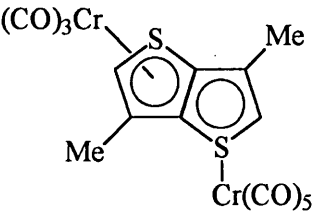
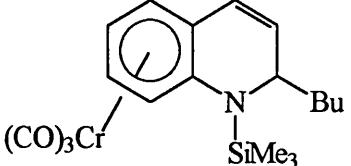
The π -heteroarene complexes were synthesized according to various known literature methods.

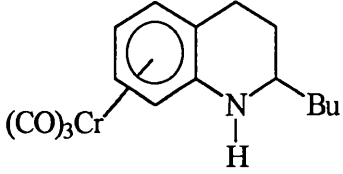
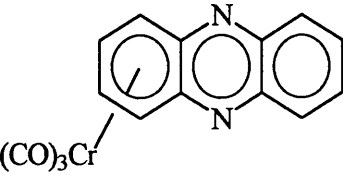
The general synthetic methods of preparation were as follows:

A: Ligand + Cr(NH₃)₃(CO)₃

B: Ligand + Cr(CO)₆ (refluxing in dibutyl ether)

Table 6.1 Preparation of π -complexes

Complex	Synthesis Method	Reference
 <chem>(Co)3Cr</chem>	A	7
 <chem>(Co)3Cr</chem>	A	7
 <chem>(Co)3Cr</chem> , <chem>Me</chem> , <chem>Cr(CO)5</chem>	A	7
 <chem>(Co)3Cr</chem> , <chem>Bu</chem> , <chem>SiMe3</chem>	B	8

Complex	Synthesis Method	Reference
	B	8
	B	8

6.4.2 Sulphur-containing π -heteroarene complexes

These compounds were synthesized in part according to the method described by Novi and Guanti^[7].

(a) (η^6 -benzo[*b*]thiophene)tricarbonylchromium

Trisamine(tricarbonyl)chromium (2.00 g, 10.7 mmol) was dissolved in diethyl ether (~ 95 ml). Freshly distilled boron trifluoride diethyl etherate (3.95 ml, 33 mmol) was added to the solution, followed by 2.82 g (21 mmol) of benzo[*b*]thiophene. The reaction mixture was stirred for 12 h. Diethyl ether (100 ml) was added and the solution was cooled to 0°C after which 100 ml air-free water was added. The mixture was repeatedly extracted with diethyl ether until the extracts were virtually colourless. The ether extracts were combined and dried over anhydrous sodium sulphate. The solvent was removed under reduced pressure. The product was purified with column chromatography which afforded the starting compounds and the orange product. The crude product was recrystallized from dichloromethane and hexane. The orange crystals were

washed with hexane and dried under reduced pressure. Yield: 0.93 g (32%)

(b) (η^6 -dibenzothiophene)tricarbonylchromium

The reaction was performed as described for the analogous benzo[*b*]thiophene reaction in (a). Trisammine(tricarbonyl)chromium (2.00 g, 10.7 mmoles) was dissolved in diethyl ether (~ 95 ml). Freshly distilled boron trifluoride diethyl etherate (3.95 ml, 33 mmoles) was added to the solution, followed by 3.30 g (21 mmoles) of dibenzothiophene. The crude product was recrystallized from dichloromethane and hexane. The orange crystals were washed with hexane and dried under reduced pressure. Yield: 1.40 g (41%)

(c) (η^1 (S): η^6 -3,6-dimethylthieno[3,2-*b*]thiophene-Cr(CO)₃)tricarbonylchromium

The reaction was performed as described for the analogous benzo[*b*]thiophene reaction in (a). Trisammine(tricarbonyl)chromium (0.56 g, 3.00 mmoles) was dissolved in 95 ml of diethyl ether. Freshly distilled boron trifluoride diethyl etherate (1.10 ml, 9.00 mmoles) was added to the solution, followed by 0.75 g (4.50 mmoles) of 3,6-dimethylthieno[3,2-*b*]thiophene. The product was purified with column chromatography, starting with hexane as eluent and gradually increasing the polarity by adding dichloromethane. Since the product is very sensitive to temperature and air, the compound was collected at -50°C in a nitrogen atmosphere. The starting compounds and the yellow product **1** were eluted from the column. Yield: 0.13 g (25%)

6.4.3 Nitrogen-containing π -heteroarene complexes

The following compounds were synthesized in part according to the method described by Mahaffy and Pauson^[8].

(a) (η^6 -N-trimethylsilyl-2-butyl-1,2-dihydroquinoline)tricarbonylchromium

Quinoline (1.20 ml, 10.0 mmoles) was dissolved in THF (~ 15 ml). The solution was cooled to -35°C and 6.8 ml (11.0 mmoles) of butyllithium was added to the stirred solution. Stirring was

maintained for 1 h at this temperature during which time the colour of the solution changed from light yellow to orange. A solution of 1.40 ml (11.0 mmoles) of chlorotrimethylsilane in 20 ml of THF was added. The mixture was stirred for 1 h. The cooling bath was removed and the temperature allowed to rise to room temperature. The light yellow solution was concentrated to a volume of ~30 ml and washed with two 50 ml portions of air-free water. The organic layer as well as one ether extract were dried over anhydrous potassium carbonate. The solvents and unreacted TMS-Cl were removed by distillation (~70°C).

Chromium hexacarbonyl (1.1 g, 10 mmoles) was added to a solution of the silylated quinoline product in 10 ml of THF and 100 ml of dibutyl ether. The mixture was heated at reflux for 30 h. The orange solution was cooled on ice and filtered through silica gel. The solvent was distilled off on a rotary evaporator. The resulting brown-yellow oil afforded three bands on purification with column chromatography (eluent: petroleum ether/dichloromethane 1/1). The first product was a yellow compound and was identified as (η^6 -N-trimethylsilyl-2-butyl-1,2-dihydroquinoline)-tricarbonylchromium (**2**), yield: 0.45 g (11%). The second yellow-orange band was characterized as (η^6 -2-butyl-1,2,3,4-tetrahydroquinoline)tricarbonylchromium (**3**), yield: 1.99 g (62%). The third orange band was not characterized because of the low yield. This third product could only be eluted from the column using pure dichloromethane as eluent.

(b) (η^6 -phenazine)tricarbonylchromium

Phenazine (1.80 g, 10.0 mmoles) was dissolved in 100 ml of dibutyl ether. Chromium hexacarbonyl (2.60 g, 12.0 mmoles) was dissolved in 10 ml of THF and added to this solution. The mixture was heated at reflux for 18 h. The solution was cooled on ice and filtered through silica gel. After the solvent had been removed on a rotary evaporator, the crude product was purified with column chromatography (eluent: dichloromethane/petroleum ether 2/1). This afforded the starting compounds and the yellow product (**4**), yield: 0.46 g (15%)

6.4.4 Bimetallic sulphur-containing π -heteroarene complexes

An excess of 10% of butyllithium was used in the syntheses.

(a) ($\eta^1:\eta^6$ -benzo[*b*]thienyl-TiCp₂Cl)tricarbonylchromium

(η^6 -Benzo[*b*]thiophene)tricarbonylchromium (0.55 g, 2.04 mmoles) was dissolved in THF (~15 ml). The solution was cooled to -40°C and 1.4 ml (2.24 mmoles) of butyllithium was added to the stirred solution. Stirring was maintained for 1 h at this temperature during which time the colour of the solution changed from orange-yellow to dark brown. 0.50 g (2.04 mmoles) of titanocene dichloride was gradually added to the cooled reaction mixture, after which stirring was maintained for a further 30 min. The mixture was heated to room temperature and stirred for 30 min. The mixture was filtered through silica gel, using dichloromethane as eluent. The solvent was removed under reduced pressure.

Two bands were separated by means of column chromatography (eluent: petroleum ether/dichloromethane 1/2). The first band removed from the column was characterized as the orange starting compound, yield: 0.20 g (37%). The second green band was a mixture of two compounds. They were identified as ($\eta^1:\eta^6$ -benzo[*b*]thienyl-TiCp₂Cl)tricarbonylchromium (**5**) and [($\eta^1:\eta^6$ -benzo[*b*]thienyl)₂TiCp₂]tricarbonylchromium (**8**), yield: 0.54 g (55%).

(b) ($\eta^1:\eta^6$ -benzo[*b*]thienyl-TiCp₂(SPh))tricarbonylchromium

Thiophenol (0.92 ml, 7.46 mmoles) was added to 0.40 g (0.82 mmoles) of ($\eta^1:\eta^6$ -benzo[*b*]thienyl-TiCp₂Cl)tricarbonylchromium. Dichloromethane (10 ml) and 0.62 ml (4.10 mmoles) of TMEDA were added and the mixture was stirred for 1 h at room temperature. The colour changed from green to orange-red. The solvent was removed under reduced pressure.

Three bands were separated with column chromatography (eluent petroleum ether/dichloromethane 1/2). The first yellow band was identified as the starting compound, (η^6 -benzo[*b*]thiophene)tricarbonylchromium(0), yield: 0.06 g (28%). The second orange-red band was characterized as ($\eta^1:\eta^6$ -benzo[*b*]thienyl-TiCp₂(SPh))tricarbonylchromium (**6**), yield: 0.11 g (24%). The third purple band was characterized as TiCp₂(SPh)₂, yield: 0.13 g (41%).

(c) ($\eta^1:\eta^6$ -benzo[*b*]thienyl-TiCp₂OH)tricarbonylchromium

($\eta^1:\eta^6$ -Benzo[*b*]thienyl-TiCp₂Cl)tricarbonylchromium (0.48 g, 1.00 mmole) was dissolved in dichloromethane (~50 ml). Water (~20 ml) was added and the mixture was stirred for 12 h, during which time the colour of the solution changed from green to orange. The organic and water layers were separated and the organic layer was dried over sodium sulphate. The solvent was removed under reduced pressure. The orange-brown product (7) was washed with hexane and dried *in vacuo*. Yield: 0.28 g (65%)

(d) ($\eta^1:\eta^6$ -benzo[*b*]thienyl-Re(CO)₅)tricarbonylchromium

(η^6 -Benzo[*b*]thiophene)tricarbonylchromium (0.55 g, 2.04 mmoles) was dissolved in THF (~15 ml). The solution was cooled to -40°C and 1.4 ml (2.24 mmoles) of butyllithium was added to the stirred solution. Stirring was maintained for 1 h at this temperature during which time the colour of the solution changed from orange-yellow to dark brown. Rheniumpentacarbonyl triflate (0.97 g, 2.04 mmoles) was gradually added to the cooled reaction mixture, after which stirring was maintained for a further 30 min. The mixture was heated to room temperature and stirred for 30 min. The mixture was filtered through silica gel, using dichloromethane as eluent. The solvent was removed under reduced pressure.

Two bands were separated by means of column chromatography (eluent: petroleum ether/dichloromethane 1/1). The first band removed from the column was characterized as the orange starting compound, (η^6 -benzo[*b*]thiophene)tricarbonylchromium, yield: 0.36 g (66%). The second orange-red band was identified as ($\eta^1:\eta^6$ -benzo[*b*]thienyl-Re(CO)₅)tricarbonylchromium (10), yield: 0.21 g (17%) .

(e) ($\eta^1:\eta^6$ -benzo[*b*]thienyl-Mn(CO)₅)tricarbonylchromium

(η^6 -Benzo[*b*]thiophene)tricarbonylchromium (0.75 g, 2.80 mmoles) was dissolved in THF (~30 ml). The solution was cooled to -40°C and 2.1 ml (3.3 mmoles) of butyllithium was added to the

stirred solution. Stirring was maintained for 1 h at this temperature during which time the colour of the solution changed from orange-yellow to dark brown. Manganese-pentacarbonyl bromide (0.92 g, 3.3 mmol) was gradually added to the cooled reaction mixture, after which stirring was maintained for a further 30 min. The mixture was heated to room temperature and stirred for 30 min. The mixture was filtered through silica gel, using dichloromethane as eluent. The solvent was removed under reduced pressure.

Two bands were separated with column chromatography (eluent: petroleum ether/dichloromethane 1/1). The first band removed from the column was characterized as the orange starting compound, (η^6 -benzo[*b*]thiophene)tricarbonylchromium. The second red band was identified as (η^1 : η^6 -benzo[*b*]thienyl-Mn(CO)₅)tricarbonylchromium (**11**), yield: 0.12 g (9%).

(f) (η^1 : η^6 -dibenzothieryl-Re(CO)₅)tricarbonylchromium

A solution of 0.64 g (2.00 mmol) of (η^6 -dibenzothiophene)tricarbonylchromium in THF (15 ml) was cooled to -20°C. Butyllithium (1.35 ml, 2.20 mmol) was added to the stirred solution. Stirring was maintained for 1 h at this temperature. The colour of the solution changed from orange to dark brown. Rheniumpentacarbonyltriflate (0.96 g, 2.00 mmol) was gradually added to the cooled reaction mixture, after which stirring was maintained for a further 30 min. The temperature was allowed to rise to room temperature and stirred for 30 min. The mixture was filtered through silica gel, using dichloromethane as eluent. The solvent was removed under reduced pressure.

The product was purified using column chromatography (eluent: petroleum ether/dichloromethane 1/2). Three bands were eluted from the column. The first yellow band was identified as the starting compound. The third orange band was characterized as (η^1 : η^6 -dibenzothieryl-Re(CO)₅)tricarbonylchromium (**12**), yield: 0.15g (12%).

(g) $[\eta^1:\eta^6\text{-benzo}[b]\text{thienyl}(\text{tricarbonylchromium})_2\text{Pt}(\text{dppe})$

0.55 g (2.04 mmoles) of (η^6 -benzo[*b*]thiophene)tricarbonylchromium was dissolved in THF (~15 ml). The solution was cooled to -40°C and 1.4 ml (2.24 mmoles) of butyllithium was added to the stirred solution. Stirring was maintained for 1 h at this temperature during which time the colour of the solution changed from orange-yellow to dark brown. 1.30 g (2.04 mmoles) of [1,2-bis(diphenylphosphino)ethane]platinum(II)chloride was gradually added to the cooled reaction mixture, after which stirring was maintained for a further 30 min. The mixture was heated to room temperature and stirred for 30 min. The mixture was filtered through silica gel, using dichloromethane as eluent. The solvent was removed under reduced pressure. Two bands were separated with column chromatography (eluent: petroleum ether/dichloromethane 1/1). The first band removed from the column was characterized as the orange starting compound, (η^6 -benzo[*b*]thiophene)tricarbonylchromium, yield: 0.30 g (57%). The second yellow band was identified as compound **14**, $[\eta^1:\eta^6\text{-benzo}[b]\text{thienyl}(\text{tricarbonylchromium})_2\text{Pt}(\text{dppe})$, yield: 0.63 g (34%) .

6.4.5 Sulphur-containing σ -heteroarene complexes**(a) η^1 -dibenzothieryl-Re(CO)₅**

Dibenzothiophene (0.46 g, 2.50 mmoles) was dissolved in THF (~40 ml). The solution was cooled to 0°C . A solution of 1.38 ml (3.00 mmoles) of butyllithium in diethyl ether (~20 ml) was added. The mixture was stirred for 6 h at 0°C . The colour of the solution changed from colourless to light green.

A solution of 1.18 g (2.50 mmoles) of rheniumpentacarbonyl triflate in 30 ml of THF was gradually added at 0°C . The colour changed to yellow-orange. Stirring was maintained for a further 30 minutes after which time the temperature was allowed to rise to room temperature. The mixture was stirred for 30 minutes at this temperature. The solvent was removed under reduced pressure. The product was purified with column chromatography. The pure product (**13**) had a yellow colour and yield of 0.87 g (68%).

6.5. References

- (1) M.D. Rausch, G.A. Moser, E.J. Zaiko, A.L. Lipman Jr., *J. Organomet. Chem.*, **1970**, *23*, 185.
- (2) G.K. Anderson, H.C. Clark, J.A. Davies, *Inorg. Chem.*, **1981**, *20*, 3607.
- (3) S.P. Schmidt, W.C. Trogler, F. Basolo, *Inorg. Synth.*, **1985**, *23*, 41.
- (4) S.P. Schmidt, J. Nitschke, W.C. Trogler, *Inorg. Synth.*, **1989**, *26*, 115.
- (5) M.H. Quick, R.J. Angelici, *Inorg. Synth.*, **1979**, *19*, 160.
- (6) K.S. Choi, K. Sawada, H. Dong, M. Hoshino, J. Nakayama, *Heterocycles*, **1994**, *38* nr. 1, 143.
- (7) M. Novi, G. Guanti, *J. Heterocycl. Chem.*, **1975**, *12*, 1055.
- (8) C.A.L. Mahaffy, P.L. Pauson, *Inorg. Synth.*, **1990**, *28*, 137.

Appendix 1

Crystallographic Data of (η^6 -N-trimethylsilyl-2-butyl-1,2-dihydroquinoline)Cr(CO)₃

Table 1 . Crystallographic data acquisition and refinement details of compound 2.

Empirical formula	C ₁₉ H ₂₅ NO ₃ CrSi
Molecular weight	395.49
Crystal dimension, mm	0.18 x 0.24 x 0.27
Space group	P $\bar{1}$
Cell dimensions	
a, Å	9.129(2)
b, Å	9.153(1)
c, Å	13.304(2)
α , °	85.66(1)
β , °	80.89(2)
γ , °	70.03(2)
Z	2
Volume, Å ³	1031(1)
D(calc), g·cm ⁻³	1.26
μ , cm ⁻¹	0.58
Radiation (λ , Å)	Mo-K α (0.7107)
T, °C	22
F(000)	416.0
Scan type (ω :2 θ)	1:1
Scan Range (θ °)	3 \leq θ \leq 30
Zone collected:	
<i>h</i>	-12, +12
<i>k</i>	-12, +12
<i>l</i>	0, +18

Max. scan speed (deg.min ⁻¹)	5.49
Max. scan time, sec.	60
Scan angle ($\omega + 0.34 \tan \theta$)°	0.50
Aperture size (mm)	1.3 x 4.0
Reflections collected	6100
Decay, %	-2.6 (uncorrected)
EAC correction factor:	
Maximum	1.000
Minimum	0.990
Average	0.995
Unique reflections used (> 3 $\sigma(I)$)	4538
R_{int}	0.013
Parameters refined	239
Max. positional shift/esd	< 0.1
Residual electron density (eÅ ³):	
Maximum	+0.42
Minimum	-0.50
$U_{\text{iso}}(\text{H}), \text{Å}^2$	0.143(3)
R	0.051
R_w	0.039

Table 2 Fractional atomic coordinates ($\times 10^4$) and Equivalent thermal factors ($\times 10^3 \text{ \AA}^2$)

Atom	x/a	y/b	z/c	U_{eq}
N(1)	2513(2)	784(2)	2403(2)	55(1)
C(2)	3454(4)	819(3)	3213(2)	70(1)
C(3)	5153(4)	553(3)	2780(3)	81(1)
C(4)	5587(3)	909(3)	1838(3)	68(1)
C(5)	4835(3)	2013(3)	147(2)	61(1)
C(6)	3742(4)	2491(3)	-546(2)	66(1)
C(7)	2205(3)	2477(3)	-231(2)	61(1)
C(8)	1773(3)	2004(3)	769(2)	51(1)
C(9)	2891(3)	1412(3)	1459(2)	47(1)
C(10)	4431(3)	1485(3)	1140(2)	51(1)
C(11)	2729(4)	2293(4)	3815(2)	83(1)
C(12)	3553(5)	2352(4)	4710(3)	106(1)
C(13)	2824(4)	3841(5)	5282(3)	114(1)
C(14)	3682(5)	3926(5)	6125(3)	146(2)
C(15)	2255(3)	5636(3)	10(2)	55(1)
O(16)	1970(2)	6746(2)	-518(2)	73(1)
C(17)	3863(3)	4738(3)	1517(2)	60(1)
O(18)	4514(3)	5261(3)	1981(2)	90(1)
C(19)	1032(3)	4869(3)	1740(2)	63(1)
O(20)	-64(3)	5483(2)	2325(2)	95(1)
Cr	2737(1)	3907(1)	835(1)	50(1)
Si	909(1)	94(1)	2708(1)	61(1)
C(21)	696(4)	-898(3)	1600(2)	80(1)
C(22)	1358(4)	-1374(4)	3762(3)	97(1)
C(23)	-951(3)	1695(3)	3113(3)	82(1)
H(2)	3436(4)	-132(3)	3742(2)	143(3)*

H(3)	6045(4)	48(3)	3269(3)	143(3)*
H(4)	6807(3)	775(3)	1577(3)	143(3)*
H(5)	6010(3)	2051(3)	-85(2)	143(3)*
H(6)	4079(4)	2864(3)	-1311(2)	143(3)*
H(7)	1354(3)	2829(3)	-757(2)	143(3)*
H(8)	562(3)	2092(3)	1019(2)	143(3)*
H(11A)	2755(4)	3263(4)	3305(2)	143(3)*
H(11B)	1522(4)	2405(4)	4103(2)	143(3)*
H(12A)	4766(5)	2222(4)	4427(3)	143(3)*
H(12B)	3507(5)	1398(4)	5230(3)	143(3)*
H(13A)	1630(4)	3943(5)	5598(3)	143(3)*
H(13B)	2816(4)	4800(5)	4754(3)	143(3)*
H(14A)	3192(5)	4970(5)	6565(3)	143(3)*
H(14B)	4828(5)	3862(5)	5727(3)	143(3)*
H(14C)	3793(5)	2922(5)	6628(3)	143(3)*
H(21A)	-148(4)	-1482(3)	1853(2)	143(3)*
H(21B)	1832(4)	-1748(3)	1356(2)	143(3)*
H(21C)	316(4)	-112(3)	972(2)	143(3)*
H(22A)	447(4)	-1896(4)	3926(3)	143(3)*
H(22B)	1446(4)	-851(4)	4441(3)	143(3)*
H(22C)	2469(4)	-2257(4)	3512(3)	143(3)*
H(23A)	-1878(3)	1201(3)	3320(3)	143(3)*
H(23B)	-1243(3)	2538(3)	2499(3)	143(3)*
H(23C)	-823(3)	2257(3)	3763(3)	143(3)*

* Isotropic temperature factor

$$U_{eq} = \frac{1}{3} \sum_i \sum_j U_{ij} a_i^* a_j^* (a_i \cdot a_j)$$

Table 3 Bond lengths (Å)

N(1)-C(2)	1.489(3)	N(1)-C(9)	1.383(3)
N(1)-Si	1.764(2)	C(2)-C(3)	1.509(4)
C(2)-C(11)	1.512(4)	C(3)-C(4)	1.305(4)
C(4)-C(10)	1.453(4)	C(5)-C(6)	1.403(4)
C(5)-C(10)	1.409(3)	C(5)-Cr	2.220(3)
C(6)-C(7)	1.404(3)	C(6)-Cr	2.216(3)
C(7)-C(8)	1.405(3)	C(7)-Cr	2.213(3)
C(8)-C(9)	1.422(3)	C(8)-Cr	2.217(2)
C(9)-C(10)	1.426(3)	C(9)-Cr	2.336(2)
C(10)-Cr	2.278(2)	C(11)-C(12)	1.519(4)
C(12)-C(13)	1.503(4)	C(13)-C(14)	1.486(4)
C(15)-O(16)	1.167(3)	C(15)-Cr	1.822(3)
C(17)-O(18)	1.149(3)	C(17)-Cr	1.841(3)
C(19)-O(20)	1.165(3)	C(19)-Cr	1.811(3)
Si-C(21)	1.857(3)	Si-C(22)	1.860(3)
Si-C(23)	1.858(3)		

Table 4 Valence angles (°)

C(2)-N(1)-C(9)	117.0(2)	C(2)-N(1)-Si	119.3(2)
C(9)-N(1)-Si	123.5(2)	N(1)-C(2)-C(3)	111.3(2)
N(1)-C(2)-C(11)	111.7(2)	C(3)-C(2)-C(11)	112.2(3)
C(2)-C(3)-C(4)	122.6(3)	C(3)-C(4)-C(10)	120.1(3)
C(6)-C(5)-C(10)	121.4(3)	C(6)-C(5)-Cr	71.4(2)
C(10)-C(5)-Cr	74.0(1)	C(5)-C(6)-C(7)	119.0(3)
C(5)-C(6)-Cr	71.7(2)	C(7)-C(6)-Cr	71.4(2)
C(6)-C(7)-C(8)	120.1(3)	C(6)-C(7)-Cr	71.7(2)
C(8)-C(7)-Cr	71.7(1)	C(7)-C(8)-C(9)	121.6(2)
C(7)-C(8)-Cr	71.3(1)	C(9)-C(8)-Cr	76.4(1)
N(1)-C(9)-C(8)	121.8(2)	N(1)-C(9)-C(10)	120.9(2)
C(8)-C(9)-C(10)	117.3(2)	N(1)-C(9)-Cr	134.8(2)
C(8)-C(9)-Cr	67.3(1)	C(10)-C(9)-Cr	69.8(1)
C(4)-C(10)-C(5)	121.3(3)	C(4)-C(10)-C(9)	118.3(3)
C(5)-C(10)-C(9)	120.2(2)	C(4)-C(10)-Cr	132.2(2)
C(5)-C(10)-Cr	69.5(1)	C(9)-C(10)-Cr	74.2(1)
C(2)-C(11)-C(12)	114.7(3)	C(11)-C(12)-C(13)	113.5(3)
C(12)-C(13)-C(14)	113.3(3)	O(16)-C(15)-Cr	178.9(2)
O(18)-C(17)-Cr	176.8(3)	O(20)-C(19)-Cr	179.8(1)
C(5)-Cr-C(6)	36.9(1)	C(5)-Cr-C(7)	66.1(1)
C(6)-Cr-C(7)	37.0(1)	C(5)-Cr-C(8)	77.9(1)
C(6)-Cr-C(8)	66.6(1)	C(7)-Cr-C(8)	37.0(1)
C(5)-Cr-C(9)	65.2(1)	C(6)-Cr-C(9)	77.7(1)
C(7)-Cr-C(9)	65.7(1)	C(8)-Cr-C(9)	36.3(1)
C(5)-Cr-C(10)	36.5(1)	C(6)-Cr-C(10)	66.1(1)
C(7)-Cr-C(10)	77.7(1)	C(8)-Cr-C(10)	65.5(1)
C(9)-Cr-C(10)	36.0(1)	C(5)-Cr-C(15)	112.1(1)

C(6)-Cr-C(15)	88.5(1)	C(7)-Cr-C(15)	93.5(1)
C(8)-Cr-C(15)	122.9(1)	C(9)-Cr-C(15)	158.6(1)
C(10)-Cr-C(15)	148.3(1)	C(5)-Cr-C(17)	94.7(1)
C(6)-Cr-C(17)	124.1(1)	C(7)-Cr-C(17)	160.4(1)
C(8)-Cr-C(17)	146.8(1)	C(9)-Cr-C(17)	111.3(1)
C(10)-Cr-C(17)	89.3(1)	C(15)-Cr-C(17)	90.0(1)
C(5)-Cr-C(19)	158.5(1)	C(6)-Cr-C(19)	148.7(1)
C(7)-Cr-C(19)	112.1(1)	C(8)-Cr-C(19)	88.8(1)
C(9)-Cr-C(19)	94.1(1)	C(10)-Cr-C(19)	122.3(1)
C(15)-Cr-C(19)	89.3(1)	C(17)-Cr-C(19)	87.1(1)
N(1)-Si-C(21)	110.1(1)	N(1)-Si-C(22)	107.7(1)
C(21)-Si-C(22)	107.7(2)	N(1)-Si-C(23)	111.4(1)
C(21)-Si-C(23)	110.1(1)	C(22)-Si-C(23)	109.7(2)

Table 5 Anisotropic thermal factors ($\times 10^3 \text{ \AA}^2$)

Atom	U(11)	U(22)	U(33)	U(23)	U(13)	U(12)
N(1)	59(1)	57(1)	57(1)	9(1)	-17(1)	-27(1)
C(2)	83(2)	78(2)	57(2)	12(2)	-24(2)	-33(2)
C(3)	64(2)	84(2)	99(3)	7(2)	-40(2)	-19(2)
C(4)	53(2)	62(2)	87(2)	-8(2)	-15(2)	-15(1)
C(5)	62(2)	51(2)	69(2)	-17(1)	10(2)	-24(1)
C(6)	90(2)	59(2)	56(2)	-11(1)	1(2)	-36(2)
C(7)	81(2)	53(2)	58(2)	-3(1)	-18(2)	-30(2)
C(8)	58(2)	47(1)	58(2)	1(1)	-16(1)	-26(1)
C(9)	53(2)	39(1)	53(2)	-2(1)	-10(1)	-19(1)
C(10)	48(2)	40(1)	66(2)	-9(1)	-9(1)	-13(1)
C(11)	90(2)	85(2)	79(2)	-8(2)	-35(2)	-24(2)
C(12)	130(3)	106(3)	86(3)	-10(2)	-45(2)	-31(3)
C(13)	103(3)	134(4)	106(3)	-53(3)	-31(2)	-22(3)
C(14)	139(4)	140(4)	153(5)	-56(3)	-41(3)	-20(3)
C(15)	55(2)	57(2)	59(2)	0(1)	-10(1)	-24(1)
O(16)	74(1)	67(1)	80(1)	20(1)	-21(1)	-26(1)
C(17)	73(2)	54(2)	58(2)	-2(1)	-10(2)	-26(1)
O(18)	109(2)	99(2)	87(2)	-12(1)	-26(1)	-62(1)
C(19)	76(2)	51(2)	65(2)	1(1)	-3(2)	-28(2)
O(20)	92(2)	76(2)	97(2)	-8(1)	26(1)	-18(1)
Cr	56(1)	44(1)	53(1)	-1(1)	-7(1)	-22(1)
Si	64(1)	56(1)	65(1)	3(1)	-3(1)	-29(1)
C(21)	90(2)	69(2)	91(3)	-15(2)	1(2)	-45(2)
C(22)	104(3)	98(3)	96(3)	34(2)	-11(2)	-52(2)
C(23)	66(2)	89(2)	88(2)	-17(2)	-4(2)	-23(2)

Appendix 2

Crystallographic Data of (η^6 -2-butyl-1,2,3,4-tetrahydroquinoline)Cr(CO)₃

Table 1 . Crystallographic data acquisition and refinement details of compound 3.

Empirical formula	C ₁₆ H ₁₉ NO ₃ Cr
Molecular weight	325.33
Crystal dimension, mm	0.06 x 0.26 x 0.51
Space group	P2 ₁ /c
Cell dimensions	
a, Å	15.961(4)
b, Å	8.097(2)
c, Å	12.571(6)
α , °	90
β , °	107.08(3)
γ , °	90
Z	4
Volume, Å ³	1552(1)
D(calc), g·cm ⁻³	1.37
μ , cm ⁻¹	0.69
Radiation (λ , Å)	Mo-K α (0.7107)
T, °C	22
F(000)	680.0
Scan type (ω :2 θ)	1:1
Scan Range (θ °)	3 \leq θ \leq 30
Zone collected:	
<i>h</i>	0, +22
<i>k</i>	0, +11
<i>l</i>	-17, +17

Max. scan speed (deg.min ⁻¹)	4.12
Max. scan time, sec.	60
Scan angle ($\omega + 0.34 \tan \theta$)°	0.50
Aperture size (mm)	1.3 x 4.0
Reflections collected	4960
Decay, %	+1.6 (uncorrected)
EAC correction factor:	
Maximum	1.000
Minimum	0.593
Average	0.781
Unique reflections used (> 3 $\sigma(I)$)	2083
R_{int}	0.016
Parameters refined	194
Max. positional shift/esd	< 0.1
Residual electron density (eÅ ³):	
Maximum	+1.23
Minimum	-1.32
$U_{\text{iso}}(\text{H}), \text{Å}^2$	0.258(23)
R	0.099
R_g	0.107

$$\text{Weight} = 0.2126 / ((\sigma^2(F_o) + 0.068551(F_o^2)))$$

Table 2 Fractional atomic coordinates ($\times 10^4$) and Equivalent thermal factors ($\times 10^3 \text{ \AA}^2$)

Atom	x/a	y/b	z/c	U_{eq}
N(1)	2197(5)	5771(9)	4901(6)	76(2)
C(2)	2910(7)	6598(15)	4586(8)	97(3)
C(3)	3071(8)	5770(18)	3632(10)	114(4)
C(4)	2366(6)	5165(12)	2764(7)	83(2)
C(5)	943(6)	3612(11)	2388(6)	73(2)
C(6)	225(5)	2969(11)	2706(8)	79(2)
C(7)	237(6)	3218(13)	3817(10)	93(3)
C(8)	916(5)	4085(11)	4574(7)	69(2)
C(9)	1590(5)	4827(9)	4200(6)	64(2)
C(10)	1634(5)	4476(9)	3105(5)	60(1)
C(11)	3638(8)	6688(20)	5703(11)	154(5)
C(12)	4436(9)	7733(21)	5668(12)	154(5)
C(13)	5014(11)	7869(27)	6884(12)	180(7)
C(14)	5800(12)	8802(30)	6697(14)	180(7)
C(15)	1808(5)	546(10)	2931(6)	65(2)
O(16)	2006(5)	-381(9)	2343(5)	97(2)
C(17)	1135(5)	167(9)	4472(5)	59(1)
O(18)	940(4)	-1001(8)	4877(5)	83(2)
C(19)	2549(5)	1855(10)	4870(6)	65(2)
O(20)	3215(5)	1758(9)	5528(6)	101(2)
Cr	1473(1)	1976(1)	3836(1)	52(1)
H(1)	2161(5)	5931(9)	5739(6)	258(23)*
H(2)	2795(7)	7836(15)	4253(8)	258(23)*
H(3A)	3491(8)	4728(18)	3958(10)	258(23)*
H(3B)	3418(8)	6640(18)	3264(10)	258(23)*
H(4A)	2116(6)	6171(12)	2195(7)	258(23)*

H(4B)	2613(6)	4206(12)	2341(7)	258(23)*
H(5)	954(6)	3419(11)	1541(6)	258(23)*
H(6)	-305(5)	2319(11)	2124(8)	258(23)*
H(7)	-292(6)	2728(13)	4095(10)	258(23)*
H(8)	928(5)	4190(11)	5435(7)	258(23)*
H(11A)	3860(8)	5448(20)	5952(11)	258(23)*
H(11B)	3364(8)	7223(20)	6314(11)	258(23)*
H(12A)	4790(9)	4129(21)	5166(12)	258(23)*
H(12B)	4230(9)	8944(21)	5332(12)	258(23)*
H(13A)	5201(11)	6671(27)	7256(12)	258(23)*
H(13B)	4699(11)	8569(27)	7389(12)	258(23)*
H(14A)	6105(12)	8848(30)	7586(14)	258(23)*
H(14B)	5496(12)	9977(30)	6414(14)	258(23)*
H(14C)	6291(12)	8541(30)	6285(14)	258(23)*

* Isotropic temperature factor

$$U_{eq} = \frac{1}{3} \sum_i \sum_j U_{ij} a_i^* a_j^* (a_i \cdot a_j)$$

Table 3 Bond lengths (Å)

N(1)-C(2)	1.471(13)	N(1)-C(9)	1.340(9)
C(2)-C(3)	1.460(14)	C(2)-C(11)	1.540(1)
C(3)-C(4)	1.406(13)	C(4)-C(10)	1.468(11)
C(5)-C(6)	1.419(12)	C(5)-C(10)	1.391(11)
C(5)-Cr	2.209(7)	C(6)-C(7)	1.405(14)
C(6)-Cr	2.229(7)	C(7)-C(8)	1.402(13)
C(7)-Cr	2.207(8)	C(8)-C(9)	1.429(11)
C(8)-Cr	2.248(7)	C(9)-C(10)	1.427(9)
C(9)-Cr	2.351(7)	C(10)-Cr	2.269(7)
C(11)-C(12)	1.540(1)	C(12)-C(13)	1.540(1)
C(13)-C(14)	1.540(1)	C(15)-O(16)	1.161(9)
C(15)-Cr	1.811(7)	C(17)-O(18)	1.159(9)
C(17)-Cr	1.824(7)	C(19)-O(20)	1.142(9)
C(19)-Cr	1.827(7)		

Table 4 Valence angles (°)

C(2)-N(1)-C(9)	123.3(7)	N(1)-C(2)-C(3)	110.4(8)
N(1)-C(2)-C(11)	102.2(8)	C(3)-C(2)-C(11)	120.2(12)
C(2)-C(3)-C(4)	120.2(9)	C(3)-C(4)-C(10)	115.5(7)
C(6)-C(5)-C(10)	123.6(7)	C(6)-C(5)-Cr	72.1(4)
C(10)-C(5)-Cr	74.3(4)	C(5)-C(6)-C(7)	116.8(8)
C(5)-C(6)-Cr	70.6(4)	C(7)-C(6)-Cr	70.7(4)
C(6)-C(7)-C(8)	121.9(8)	C(6)-C(7)-Cr	72.4(5)
C(8)-C(7)-Cr	73.2(4)	C(7)-C(8)-C(9)	119.5(7)
C(7)-C(8)-Cr	70.1(5)	C(9)-C(8)-Cr	75.9(4)
N(1)-C(9)-C(8)	119.5(7)	N(1)-C(9)-C(10)	121.1(7)
C(8)-C(9)-C(10)	119.3(7)	N(1)-C(9)-Cr	133.5(5)
C(8)-C(9)-Cr	68.0(4)	C(10)-C(9)-Cr	68.9(4)
C(4)-C(10)-C(5)	123.3(7)	C(4)-C(10)-C(9)	118.3(7)
C(5)-C(10)-C(9)	118.2(7)	C(4)-C(10)-Cr	130.7(5)
C(5)-C(10)-Cr	69.6(4)	C(9)-C(10)-Cr	75.1(4)
C(2)-C(11)-C(12)	114.1(10)	C(11)-C(12)-C(13)	105.7(10)
C(12)-C(13)-C(14)	99.3(11)	O(16)-C(15)-Cr	178.7(7)
O(18)-C(17)-Cr	178.3(6)	O(20)-C(19)-Cr	178.7(7)
C(5)-Cr-C(6)	37.3(3)	C(5)-Cr-C(7)	66.0(3)
C(6)-Cr-C(7)	36.9(4)	C(5)-Cr-C(8)	77.5(3)
C(6)-Cr-C(8)	66.5(3)	C(7)-Cr-C(8)	36.7(3)
C(5)-Cr-C(9)	63.9(3)	C(6)-Cr-C(9)	77.0(3)
C(7)-Cr-C(9)	64.8(3)	C(8)-Cr-C(9)	36.1(3)
C(5)-Cr-C(10)	36.2(3)	C(6)-Cr-C(10)	66.8(3)
C(7)-Cr-C(10)	78.2(3)	C(8)-Cr-C(10)	66.1(3)
C(9)-Cr-C(10)	35.9(2)	C(5)-Cr-C(15)	88.7(3)
C(6)-Cr-C(15)	101.8(3)	C(7)-Cr-C(15)	135.4(4)

C(8)-Cr-C(15)	166.1(3)	C(9)-Cr-C(15)	136.8(3)
C(10)-Cr-C(15)	103.1(3)	C(5)-Cr-C(17)	138.8(3)
C(6)-Cr-C(17)	104.2(3)	C(7)-Cr-C(17)	89.6(3)
C(8)-Cr-C(17)	103.0(3)	C(9)-Cr-C(17)	136.1(3)
C(10)-Cr-C(17)	167.7(3)	C(15)-Cr-C(17)	86.7(3)
C(5)-Cr-C(19)	132.1(3)	C(6)-Cr-C(19)	161.8(3)
C(7)-Cr-C(19)	133.0(4)	C(8)-Cr-C(19)	98.6(3)
C(9)-Cr-C(19)	84.8(3)	C(10)-Cr-C(19)	98.1(3)
C(15)-Cr-C(19)	91.3(3)	C(17)-Cr-C(19)	89.0(3)

Table 5 Anisotropic thermal factors ($\times 10^3 \text{ \AA}^2$)

Atom	U(11)	U(22)	U(33)	U(23)	U(13)	U(12)
N(1)	108(4)	56(4)	64(4)	-4(3)	26(3)	-4(4)
C(2)	118(7)	84(7)	81(6)	-2(6)	15(6)	-14(5)
C(3)	130(8)	112(10)	115(9)	-28(8)	61(7)	-34(8)
C(4)	126(7)	65(5)	69(5)	2(4)	48(5)	-6(5)
C(5)	98(5)	58(4)	57(4)	11(4)	11(4)	14(4)
C(6)	85(5)	62(5)	80(6)	19(5)	8(4)	8(4)
C(7)	79(5)	81(7)	126(9)	31(6)	40(5)	25(5)
C(8)	95(5)	52(4)	72(5)	7(4)	42(4)	18(4)
C(9)	101(5)	40(4)	50(3)	3(3)	20(3)	18(4)
C(10)	94(4)	42(4)	44(3)	10(3)	18(3)	10(3)
C(11)	145(11)	131(14)	156(13)	4(11)	-1(10)	-30(10)
C(12)	144(11)	102(11)	182(17)	1(11)	-6(11)	-6(9)
C(13)	170(14)	187(21)	163(17)	-52(16)	20(13)	-52(15)
C(14)	181(16)	209(21)	148(15)	-60(16)	46(12)	-23(16)
C(15)	102(5)	50(4)	50(3)	4(3)	32(3)	5(4)
O(16)	154(5)	76(4)	70(4)	-6(3)	46(4)	24(4)
C(17)	84(4)	49(4)	47(3)	7(3)	25(3)	8(3)
O(18)	113(4)	65(4)	78(4)	11(3)	38(3)	-4(3)
C(19)	78(4)	57(4)	59(4)	3(3)	17(3)	14(3)
O(20)	95(4)	100(6)	89(4)	-3(4)	-4(4)	12(4)
Cr	72(1)	41(1)	44(1)	6(1)	17(1)	7(1)